

CARBON STOCKS AND CYCLING IN THE AMAZON BASIN:
MEASUREMENT AND MODELING OF NATURAL DISTURBANCE AND
RECOVERY USING AIRBORNE LIDAR

BY

MARIA O'HEALY HUNTER

BA Physics, Mount Holyoke College, 2004

DISSERTATION

Submitted to the University of New Hampshire
in Partial Fulfillment of
the Requirements for the Degree of

Doctor of Philosophy

in

Natural Resources and Earth Systems Science

September, 2014

UMI Number: 3581824

All rights reserved

INFORMATION TO ALL USERS

The quality of this reproduction is dependent upon the quality of the copy submitted.

In the unlikely event that the author did not send a complete manuscript and there are missing pages, these will be noted. Also, if material had to be removed, a note will indicate the deletion.



UMI 3581824

Published by ProQuest LLC 2014. Copyright in the Dissertation held by the Author.

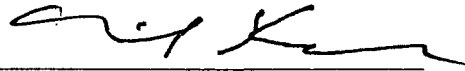
Microform Edition © ProQuest LLC.

All rights reserved. This work is protected against unauthorized copying under Title 17, United States Code.



ProQuest LLC
789 East Eisenhower Parkway
P.O. Box 1346
Ann Arbor, MI 48106-1346

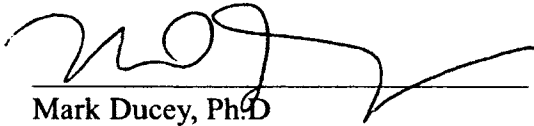
This dissertation has been examined and approved.



Advisor, Michael M. Keller, Ph.D
Affiliate Professor
Department of Natural Resources and Earth Systems Science



Bobby Braswell, Ph.D
Affiliate Research Associate Professor
Department of Natural Resources and Earth Systems Science



Mark Ducey, Ph.D
Professor
Department of Natural Resources and the Environment



Michael Lefsky, Ph.D
Associate Professor
Department of Ecosystem Science and Sustainability
Colorado State University



Mary E. Martin, Ph.D
Research Assistant Professor
Earth Systems Research Center

8/1/2014

Date

ACKNOWLEDGEMENTS

This research was supported by NASA Earth and Space Science Fellowship NNX09AO46H in addition to NASA grants NNG06GE11A, NNX09AI33G, NNG04G073G and NNX06AH36G, NSF grant DEB0721140 and USAID Sustainable Landscapes.

TABLE OF CONTENTS

ACKNOWLEDGEMENTS	iii
LIST OF TABLES	ix
LIST OF FIGURES	xi
ABSTRACT	xiv

CHAPTER	PAGE
I. INTRODUCTION	1
Gap phase patterns and carbon-cycling in tropical forests	1
Problem Description	5
Data Exploration and Uncertainty Analysis	6
Gap Dynamics	8
Relating Light Conditions to Regrowth within Gaps	10
Summary	11
II. PENETRATION OF WAVEFORM LIDAR INTO TROPICAL FOREST CANOPIES	12
Abstract	12
Introduction	13
Objectives	19
Methods	19
Airborne Lidar Data	19
GLAS Lidar Data	22
Synthetic Waveforms	23

Canopy Penetration	25
Results	28
Synthetic Waveforms	28
Defining the Outer-Canopy-Surface	29
Discussion	37
Synthetic Waveforms	37
Lidar Penetration	41
Conclusions	45
III. MEASUREMENT OF TREE HEIGHT AND TROPICAL FOREST BIOMASS ESTIMATION	48
Abstract	48
Introduction	49
Methods	54
Site Descriptions	54
Field Inventory Measurement	59
Airborne Lidar Data	62
Lidar Estimation of Tree Heights	64
Statistical Analysis and Simulation	66
Results	68
Precision of Ground Based Height Measurements	68
Accuracy of Field Measurements of Height Compared to Lidar	69
Effect of Height Error on Plot Level Biomass	70
Height Prediction via Allometry	72
Optimization of Height Measurements for Biomass Prediction	75
Discussion	75

Height Measurement Precision	76
Height Measurement Accuracy	79
Biomass Precision	82
Height Allometries	85
Height Allometric Optimization	86
Conclusions	87
Acknowledgements	88
Author Contributions	89
IV. STRUCTURAL DYNAMICS OF TROPICAL MOIST FOREST GAPS	90
Abstract	90
Introduction	91
Methods	97
Site Descriptions	97
Airborne Lidar Data	98
Field Surveys	100
Height Structure	101
Gap Definitions	101
Distribution of Gap Area	102
Gap Creation and Lifetimes	103
Gap Contagiousness	105
Results	106
Variability of Forest Structure	106
Height Change	107
Dynamic Gap Definition and Minimum Gap Size	108

Gap Area	110
Gap Creation and Lifetimes	111
Gap Contagiousness	114
Discussion	117
Gap Definition	117
Gap Area	119
Gap Creation and Forest Turnover	120
Gap Contagiousness	122
Conclusions	123
Author Contributions	124
V. EFFECT OF LIGHT AVAILABILITY ON HEIGHT GROWTH IN TROPICAL FORESTS	125
Introduction	125
Methods	128
Site Description	128
Field Surveys	129
Airborne Lidar Data	129
Incoming Radiation	130
Modeled Annual Solar Radiation	131
Analysis	135
Results	136
Field Surveys	136
Estimates of Incoming Radiation	138
Modeled Annual Solar Radiation	140
Effects of Light Availability on Growth	142

Discussion	145
Field Surveys	145
Modeled Annual Solar Radiation	146
Effects of Light Availability on Growth	148
Conclusions	152
VI. CONCLUSION	154
Primary Results	154
Next Steps	157
REFERENCES	160

LIST OF TABLES

I. INTRODUCTION	1
II. PENETRATION OF WAVEFORM LIDAR INTO TROPICAL FOREST CANOPIES	12
Table 2.1 Summary of airborne lidar survey plots	20
Table 2.2 Height offset with varying outer-canopy-surface depth and canopy surface model scale	32
III. MEASUREMENT OF TREE HEIGHT AND TROPICAL FOREST BIOMASS ESTIMATION	48
Table 3.1 Data used to address each of the five questions posed by this research	55
Table 3.2 Site locations and climatic characteristics	55
Table 3.3 Details of field and lidar data collection	56
Table 3.4 Transect live biomass and 95% confidence interval due to height uncertainty based on 1000 repetitions	71
Table 3.5 Site average biomass based on multiple biomass allometries (Chave 2005 and Chambers 2001) and height allometries (Feldpausch 2011 Regional and Pan-Tropical)	84
IV. STRUCTURAL DYNAMICS OF TROPICAL MOIST FOREST GAPS	90
Table 4.1 Details of airborne lidar data collections	99
Table 4.2 Frequency of gap formation presented for both sites and gap definitions	111
Table 4.3 Gap recurrence frequencies based on persistence times calculated from the inter-sample period growth	113
Table 4.4 Estimates of annual mortality based on field and lidar samples	116

V. EFFECT OF LIGHT AVAILABILITY ON HEIGHT GROWTH IN TROPICAL FORESTS	125
Table 5.1 Input parameters to ArcGIS ‘Area Solar Radiation’ tool	133
Table 5.2 Model forms tested to predict height change using initial height and annual solar radiation	135
Table 5.3 Details of study areas including gap fraction, canopy height and estimated solar radiation	141
Table 5.4 Parameters of models fit to vertical growth data within six areas of interest within Tapajos National Forest	142
Table 5.5 Parameters of models fit to vertical growth data in gap areas (areas with less than 10 m initial height) within six areas of interest within Tapajos National Forest	144

LIST OF FIGURES

I. INTRODUCTION	1
Figure 1.1 Schematic diagram of data and topics	6
II. PENETRATION OF WAVEFORM LIDAR INTO TROPICAL FOREST CANOPIES	12
Figure 2.1 Potential issues with the definition of the outer-canopy-surface based on two spatial parameters: the scale of the horizontal window used to determine the "local" maximum value and the depth of the outer-canopy- surface zone considered	18
Figure 2.2 GLAS waveform locations overlaid on a canopy height map generated using airborne lidar data collected in June and July 2008	22
Figure 2.3 Example synthetic waveform (black) with gaussian decomposition (light grey) and cumulative summation of energy (dark grey)	24
Figure 2.4 Classification of lidar point returns within a 1 m by 50 m swath at Tapajos National Forest, Brazil (Area 14) into outer canopy (red), inner canopy (yellow) and ground (green) components	27
Figure 2.5 Percentage of returns in the outer canopy surface with depth of outer canopy surface for each of the six considered scales of the canopy surface model (CSM)	31
Figure 2.6 Comparison of horizontal and vertical scales used to define canopy layers	34
Figure 2.7 Relationship between mean height of returns within the outer- canopy-surface and the mean height of all returns	35
Figure 2.8 The percentage of returns within the outer canopy surface ranges from 37 - 65% when an outer-canopy-surface depth of 1 m is considered. It is also a strong indicator of the error in prediction of overall mean height from the outer-canopy-surface height	36
Figure 2.9 GLAS and synthetic waveforms compared for two waveforms within Site 15 (Tapajós National Forest)	39

Figure 2.10 Cumulative percentage of returns in the outer (blue) and inner (green) canopy regions by height for four waveforms with increasing mean height and varying percentage of returns in the outer canopy surface	43
III. MEASUREMENT OF TREE HEIGHT AND TROPICAL FOREST BIOMASS ESTIMATION	48
Figure 3.1 Crown Ellipses of canopy and emergent stems overlaid on the canopy height model	64
Figure 3.2 Comparison of field measured height to the height estimated using the Lidar Canopy Height Model (CHM) for emergent stems	65
Figure 3.3 Precision of repeated height measurement of 174 trees during the 2009 field campaign at Tapajos National Forest	69
Figure 3.4 Comparison of allometric scaling relationship. Regional, Pan-tropical and site-specific allometries based on field measurements at four sites: Tapajos, Reserva Ducke, Tanguro and Cauaxi	73
Figure 3.5 Effect of sample size on the resulting diameter to height allometric equation for Reserva Ducke	74
Figure 3.6 Comparison of site-specific Diameter: Height Allometries	83
IV. STRUCTURAL DYNAMICS OF TROPICAL MOIST FOREST GAPS	90
Figure 4.1 Distribution of canopy surface heights in 2008 airborne lidar data acquisitions	107
Figure 4.2 Mean and confidence interval of height change between initial and final lidar data acquisitions	108
Figure 4.3 Gap formation anomaly with distance from existing gaps	115
V. EFFECT OF LIGHT AVAILABILITY ON HEIGHT GROWTH IN TROPICAL FORESTS	125
Figure 5.1 Field measured growth by canopy class and light availability class ..	137
Figure 5.2 Incoming radiation in PAR wavelengths at Tapajos Tower and fraction of shady days	138

Figure 5.3 Area 6 canopy height and estimated total annual solar radiation composed of weighted sums of direct and diffuse radiation	139
Figure 5.4 Relationship between initial canopy height (m) and estimated annual solar radiation (kWh m^{-2})	140
Figure 5.5 Modeled canopy height difference based on initial canopy height and annual solar radiation	143
Figure 5.6 Correlation between incident solar radiation and height change for individual gap height bins of 2 m	150

ABSTRACT

CARBON STOCKS AND CYCLING IN THE AMAZON BASIN: MEASUREMENT AND MODELING OF NATURAL DISTURBANCE AND RECOVERY USING AIRBORNE LIDAR

by

Maria O’Healy Hunter

University of New Hampshire, September, 2014

Forest structure, the three dimensional distribution of living and dead plant material including live crowns, understory vegetation and coarse woody debris, is the concrete physical form of carbon storage, the framework for biodiversity, and the instantaneous manifestation of disturbance and recovery processes. The frequency of disturbance and rate of decomposition drives the fractions of living and dead biomass, and the size of and intensity of disturbance drives the rate and species composition of forest recovery; both are primary sinks and sources in the carbon cycle. To improve understanding of disturbance and recovery processes, high-resolution airborne LIDAR (light detection and ranging) data from the Amazon region is combined with field measurements to analyze forest structure. These measurements are incorporated into a simple model to estimate light availability and the associated changes in carbon stocks. This work improves the understanding of Amazon forest dynamics and its role in the carbon cycle.

CHAPTER ONE

INTRODUCTION

PATTERNS OF GAPS AND CARBON CYCLING IN TROPICAL FORESTS

Our understanding of carbon cycling and ecosystem dynamics in tropical ecosystems is limited by a lack of information about patterns of disturbance and recovery.

Measurements of forest structure advance knowledge of current forest form and also provide evidence of how a forest has changed through time. A primary driver of forest structure is the size and frequency of disturbance or gaps (Brokaw 1985). Gaps are a prominent feature on the tropical forest landscape and key to carbon cycle of tropical forests (Brokaw 1985, Denslow 1987, Molino and Sabatier 2001). Gap phase dynamics maintain high light environments within closed forest canopies and promote natural regeneration and turnover (Bormann and Likens 1979, Oliver and Larson 1996).

Oliver and Larson (1996) describe gap-phase regeneration with four stages: stand initiation, stem exclusion, understory re-initiation and old-growth. Although this work was focused on northern hardwood forests, processes described are similar in the tropics (Brokaw and Busing 2000). The period of time necessary to pass through stand initiation varies widely and is partly dependent on the gap formation process (fire, wind-throw,

landslide) and environmental controls such as drought. Stand establishment is typically most rapid when it is formed from advanced regeneration existing prior to the disturbance event (Franklin et al. 2002). This is generally the case in the Brazilian Amazon where disturbances that remove advanced generation are rare (Franklin et al. 2002, Cochrane 2003, Del Bom Espirito-Santo et al. 2010).

Despite the importance of forest structure, existing studies in tropical forests are most often at the plot-scale and non-randomly distributed (Phillips et al. 1998, Saatchi et al. 2007). Rare larger plots exist, but are infrequent across the tropics (Hubbell and Foster 1986, Lewis et al. 2009). Remote sensing provides a means for more objective and comprehensive sampling, but traditional optical instruments are limited in the amount of information they provide about structure (Gibbs et al. 2007). However, LIDAR (light detection and ranging) remote sensing provides a feasible method of studying forest structure at local and regional scales, especially when used in combination with other measurements and models.

Forest structure changes over time and space due to disturbance and recovery. Natural disturbances vary from small and frequent individual tree falls to large infrequent disturbances and lead to a mosaic of forest stands varying in size, age and species composition (Brokaw 1985, Steege et al. 2006). Variability in the species composition of recently disturbed areas is affected by increased nutrient and light availability within forest canopy openings (Denslow 1987, Tabarelli and Mantovani 2000); larger gaps are more likely to be colonized by faster growing pioneers such as *Cecropia* (Brokaw 1985).

Given that the size of a disturbance affects the degree to which light and nutrients are available, patterns in the scale and frequency of disturbance affect regional carbon dynamics.

Light availability is a primary controller of the rate at which forests recover from disturbance. However, it is difficult to measure light availability throughout complex forest ecosystems especially at the landscape scale. In temperate forests methods have been developed that take into account the stature and placement of surrounding vegetation, either directly or through the calculation of gap geometries (Monserud and Ek 1977, Hibbs 1982, Canham 1988). Canham (1988) reports general agreement between a light index based on gap geometry and the percent transmission of photosynthetically active radiation (PAR) compared to open conditions. Canham (1988) further showed that growth was significantly higher within the higher light conditions of gaps as compared to closed-canopy forests. In tropical forests, Denslow (1990) showed increased relative growth rates at gap centers as compared to gap edges. However, the extent to which light availability controls variation in tree growth in tropical ecosystems is still not well understood. As trees grow taller they are generally exposed to higher light environments (Metcalf et al. 2009), but few studies take into account tree size and light availability simultaneously.

Lidar (Light Detection And Ranging), an active remote sensing technique, provides a valuable tool to measure forest canopy structure that has been applied infrequently in

ecological studies (Lefsky et al. 2002). Lidar sensors on ground, airborne or space-based platforms emit short duration laser pulses that are reflected off of leaf, branch and ground matter. Round trip time of the reflected pulse is recorded and converted to distance to the reflected surface. Lidar sensors can record the temporal pattern of the returned energy (the waveform) or provide discrete returns that represent individual reflected surfaces within the laser-beam path. Discrete-return lidar systems automatically threshold the returned waveform to above a given energy level. These systems typically return between 1 and 4 points for each emitted pulse. Though lidar does not directly measure biomass, previous work has shown that both full waveform and single return discrete lidar correlate strongly with ground-based measurements of biomass on the plot level by correlation with height and fractional cover (Lefsky et al. 1999a, Drake et al. 2002b).

Lidar provides more information than just height and fractional cover. Based on height measurements alone, canopy surface light availability can be modeled in a simplified manner. However, airborne and terrestrial lidar provide a three-dimensional cloud of points representing individual reflective surfaces. With limited assumptions about occlusion and signal die-off, this cloud of points can be transformed to a matrix of vegetation presence / absence that quantifies vegetation structure (Stark et al. 2012). Theoretically, by using information about vegetation structure, light availability throughout the day, and throughout the year, can be modeled with more detail for any point in a forest. In turn, information on light availability can then be correlated with patterns of

growth measured in the field or through lidar remote sensing. This approach links forest disturbance size, light availability and regrowth rates across the landscape.

PROBLEM DESCRIPTION

Disturbances within tropical forests have been described over small areas using field data, and larger areas using optical remote sensing (Chambers et al. 2013, Espírito-Santo et al. 2014a). Studies have concentrated on changes in the light environment within gaps (Poulson and Platt 1989, Canham et al. 1990), nutrient availability (Denslow et al. 1998), and growth for a limited sub-set of species (Denslow 1987). While models have been used to study gap dynamics over broad regions (Huang et al. 2008), direct measurements have come from field-based studies that are limited in area. Lidar data, that can measure gaps at landscape scales, was previously not available within the Brazilian Amazon and has been used infrequently in ecological studies in tropical forests (Drake et al. 2002a, Clark et al. 2004, Thomas et al. 2008). With repeat measurements, lidar is capable of measuring gap dynamics over large areas. I propose using lidar data collected at 2008 and 2012 to investigate the dynamics of gaps and generalized growth within gap environments across two landscapes within the Brazilian Amazon. Multi-temporal lidar data can be used to test relations between light availability and growth at a landscape scale. However, detailed understanding of airborne lidar data and field estimates of carbon dynamics are necessary to inform functional analyses (Figure 1.1).

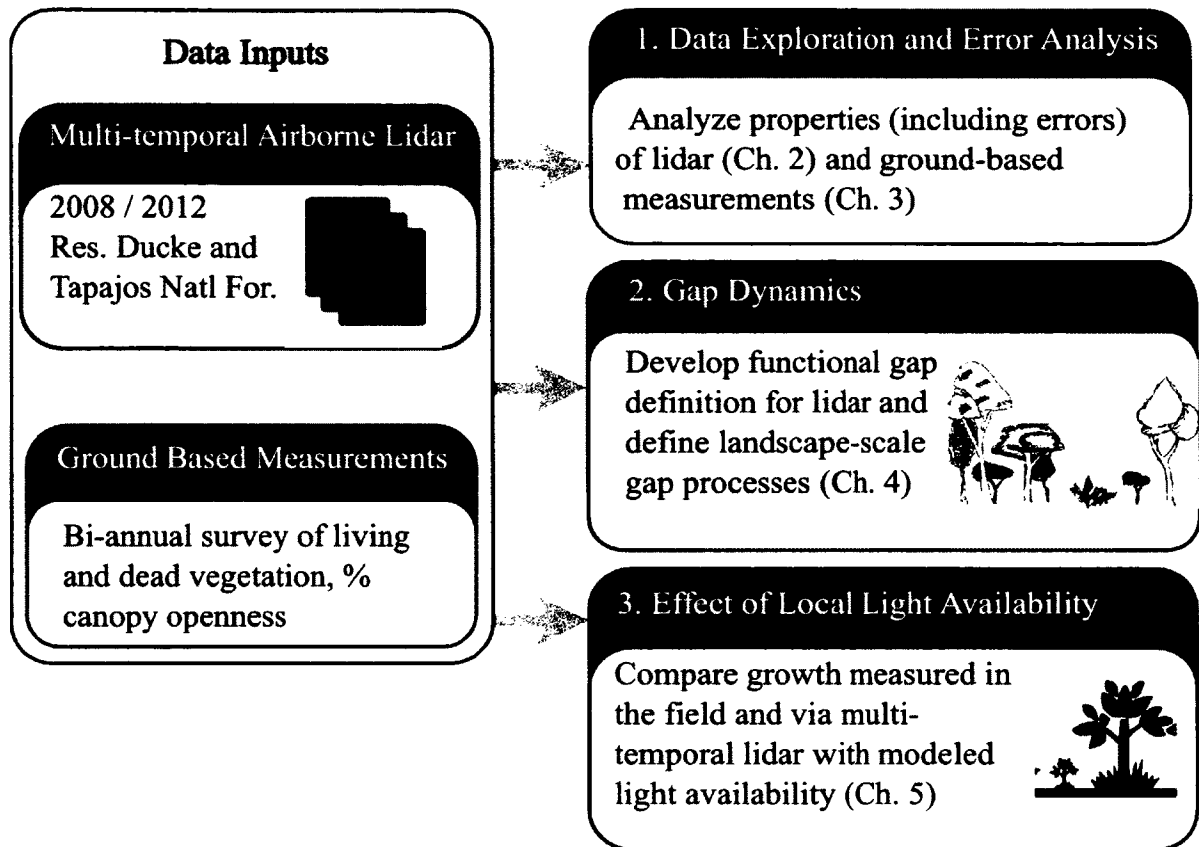


Figure 1.1 Schematic diagram of data and topics incorporated into the work presented here.

Data Exploration and Uncertainty Analysis

Following initial exploration of the data, I identified two key uncertainties. First, how effectively does discrete return lidar data penetrate into tropical forests and second, how important are accurate measurements of tree height for quantification of field biomass. When using multi-temporal data sets other issues are raised including the consistency between lidar data collections and repeatability of field measurements.

In Chapter 2, I specifically aim to improve understanding of where returns are located within forest canopies which will improve my ability to model forests measured. I also aim to determine practical scales for determining the outer canopy surface that can be used to develop Canopy Height Models that will be used throughout this thesis. I specifically aim to answer the following questions: What is the estimated error of geo-location of lidar returns? Can small footprint lidar data available to us be used to simulate GLAS waveforms? How can we best define the outer-canopy-surface zone? Is most energy returned from the outer-canopy-surface zone and, if not, what errors are introduced when we use a hypsometric interpretation of waveform power?

Lidar remote sensing data alone is not sufficient to estimate carbon stocks or changes within forests. Estimation of tropical forest biomass is ultimately linked to the estimation of biomass of individual trees (although see Clark and Kellner, 2012). Individual tree biomass estimates depend upon allometric equations that are developed using a finite number of individuals from a limited region or a broader combination of sites (Chambers et al., 2001, and others). Recently, regional or global allometries, based on significantly larger sample sizes have been used, and are assumed to be more robust for regions without site-specific equations (e.g. Chave et al. 2005).

The Chave et al. (2005) allometry uses stem diameter and wood density, and optionally total tree height. Chave et al. (2005) suggested that the inclusion of height in biomass allometries may not reduce overall precision, but removes typical biases. Therefore, the

accuracy of biomass estimation for individual trees and subsequently for plot scale biomass fundamentally depends on the accuracy of tree height measurements. Field-based measurement of tree height in tropical forests are error-prone because of dense understory vegetation, and tall and closed canopies conditions that limit the line of sight. In chapter 3, I aim to evaluate the effect of tree height accuracy on biomass estimation accuracy by answering the following questions: How precise and accurate are ground-based tree height measurements using a hand-held clinometer and metric tape? What is the effect of tree-level uncertainty in height on the estimation of plot biomass? Are global and/or regional height-diameter relations adequate for accurate biomass estimation? How can fieldwork be optimized to achieve acceptable accuracy in plot level biomass while limiting the number of tree height measurements used?

Gap Dynamics

Gaps are a prominent feature on the tropical forest landscape and key to the dynamics and species distribution of tropical forests (Brokaw 1985, Denslow 1987, Molino and Sabatier 2001). Gap phase dynamics maintain high light environments within closed forest canopies and promote natural regeneration and turnover (Bormann and Likens 1979, Oliver and Larson 1996). While the dynamic processes of regeneration and turnover of individuals and species are the ecological rationale for the study of gaps across the landscape, gaps are often treated as static environments defined in terms of light availability or vegetation height (Whitmore et al. 1993, van der Meer et al. 1994).

Lidar remote sensing has been used to successfully describe surface canopy roughness and forest structure at varying scales (Drake et al. 2002a, Lefsky et al. 2002, Frazer et al. 2005). Recently, lidar has been used for tropical gap studies, for example, to examine size frequency distributions over large areas (400 - 125000 ha) (Kellner et al. 2009, Asner et al. 2013, Lobo and Dalling 2014). These studies use traditional gap definitions, where height thresholds define gaps.

In chapter 4, I aim to use multi-temporal lidar data to define gaps in a way that takes into account the structural dynamics of the forest. Lidar is particularly well suited to this task because it measures height accurately, and can cover large areas (Vepakomma et al. 2011). The high resolution of airborne lidar allows for measurements of individual tree growth and mortality as well as generalized views of the forest structure. I intend to define the rate of gap formation, the size frequency, distribution and regrowth rates of gaps at two contrasting forest areas by asking the following questions: What is an ecologically appropriate definition for gaps at the two well-studied forest sites in the Brazilian Amazon? What is the distribution of gap area and gap size at these two sites? What is the frequency of gap creation and how long do gaps persist within a landscape? How does the frequency of gap creation compare to field estimates of mortality? And finally, are gaps contagious?

Relating Light Conditions to Regrowth within Gaps

Local ecosystem modeling allows for testing our current understanding of interactions between plants and environmental factors. While many environmental factors are difficult to determine without extensive field sampling, incoming light availability can be modeled based on canopy geometry and known atmospheric conditions. In chapter 5, light availability is modeled for six scenes within one of the focus sites within the Brazilian Amazon (Tapajos National Forest) following the equations of Rich et al. (Rich 1990, Rich et al. 1994, Fu and Rich 2002). A detailed canopy height model is used to generate a hemispherical viewshed for each pixel, identifying the portion of the sky visible for each portion of the scene. This is combined with the solar path specific to the scene location to determine incoming direct solar radiation. Diffuse radiation is calculated for each location based on the proportion of global solar radiation that is diffused and the portion of the sky visible. Local tower data was used to determine the fraction of direct and diffuse radiation by month. This model was implemented within ArcGIS 9.2.

I aim to determine the extent to which light availability effects growth within Tapajos National Forest. While similar studies have been conducted in the past, none have used high density lidar data that allow for the classification of light environments at the individual tree / pixel scale. I intend to investigate the effects of light availability by asking the following questions: What are the trends in field measured parameters of growth (including diameter, crown radius and height increment) with simplistic field

assessments of light availability? How does modeled incident solar radiation compare with assumed patterns based on gap size and gap fraction? To what extent does the light environment explain variability in height change as measured by multi-temporal lidar data?

SUMMARY

The primary objective of this research is to quantify the effect of disturbance size and frequency on the rate and pattern of carbon cycling. Each of the steps listed above, from determining data uncertainties to gap dynamics and investigation of local light environments lead to advances in the understanding of forest structure and light controls on growth within the humid tropics. This research will open many additional questions that will be taken briefly into consideration in the thesis conclusion, Chapter 6.

CHAPTER TWO

PENETRATION OF WAVEFORM LIDAR INTO TROPICAL FOREST CANOPIES

Dissertation chapter rejected from publication in Remote Sensing of Environment after submission in collaboration with H. Duong and M. Lefsky.

2.0 ABSTRACT

Forest ecologists, foresters and others are interested in the estimation of forest structure for varied reasons, from growth and yield models in commercial plantations, to biomass estimation for REDD+ projects, or predictions of plant and animal biodiversity important to ecosystem management. Lidar, a form of active remote sensing, has proven capable of distinguishing biomass and basal area of forests characteristic of later stages of development (Lefsky et al. 1999a, Drake et al. 2002a, 2002b, Lefsky et al. 2005b).

However, these metrics are strongly weighted by the largest (most likely to be the tallest) trees. As interest grows in estimates of structural characteristics of forests that are less heavily weighted by large trees (such as the overall size distribution), understanding the location of lidar returns within the canopy becomes increasingly important (Zimble et al. 2003, Chasmer et al. 2006, Palace et al. 2010). In this work an attempt is made to define the outer canopy surface to describe the locations of lidar returns within the canopy

surface. Direct comparison of synthetic waveforms based on airborne lidar data with GLAS waveforms collected over the Brazilian Amazon shows that GLAS waveforms are not significantly different from synthetic waveforms in terms of a commonly used index of canopy height (HOME - the height of median energy) or percentage of near ground returns. Further analysis of the airborne lidar data shows that 53% of lidar returns come from the outer canopy surface, with large variation between individual waveforms and high sensitivity to the scale used for identification of the outer canopy surface. This implies that a hypsometric approach to waveform analyses (which assumes that most returns are from the outer canopy) will introduce large errors.

2.1 INTRODUCTION

Structural characteristics of forest ecosystems such as height, crown size and position of vegetation are important for ecosystem studies at multiple scales. These measurements can be used to estimate stand-level biomass, basal area and size structure, and provide insights into growth and mortality (Gillespie et al. 1992, Keller et al. 2001). The presence and absence of vegetation in various height strata is also used to predict plant and animal biodiversity (Goetz et al. 2007). However, field measurement of forest structural characteristics is often limited to small areas due to limited access to the upper canopy and the time consuming nature of the measurements.

Passive remote sensing (i.e. Landsat and MODIS sensors) has been used to estimate aspects of forest structure such as average crown size and gap fraction (Asner and Keller 2002, Wang et al. 2005, Palace et al. 2010). However, these sensors are unable to measure canopy height that would allow them to distinguish between later stages of forest development (Saatchi et al. 2007). Lidar remote sensor is an active remote sensing technique that is capable of measuring components of forest structure including those necessary to distinguish later stages of forest development such as height and canopy rugosity (Parker and Russ 2004). This is of great importance for the study of primary tropical forests with dense canopy cover.

Lidar (light detection and ranging) estimates canopy structure by directly measuring the distance to reflected objects using a laser pulse. Lidar remote sensing techniques provide a method of rapidly estimating forest structural characteristics over large areas and have been shown to estimate dominant crown size (Forzieri et al. 2009, Palace et al. 2010), gap distribution (Weishampel et al. 2000, Gaulton and Malthus 2010), canopy height (Drake et al. 2002a, 2002b), tree height (Zimble et al. 2003) as well as biomass and basal area (Nelson et al. 1988, Lefsky et al. 2005a).

The area illuminated by the laser pulse (footprint) and the method of recording a returning pulse vary between instruments. Footprint size varies from 5 cm to 70 m, and sensors record single- or multiple- discrete returns or full-waveforms. In the case of a single-return system the sensor records the time to the first or last return only,

corresponding to the maximum canopy height or ground respectively. A return is determined as a peak of returned energy that exceeds a noise threshold. Multiple-return sensors typically record three to four returns. Full-return sensors record the amount of energy returned per time step for the entire light pulse. Most commercial sensors which are flown on aircraft are single or multiple-return sensors. Research-oriented and some commercial sensors record a full waveform from either aircraft or satellite platforms. Waveforms record the vertical distribution of surfaces that were illuminated by the laser, but there is no general understanding of how those surfaces are distributed in complex canopies (however see Chasmer et al. 2006, Neuenschwander et al. 2008). Some methods of waveform interpretation report metrics that only specify the heights at which various energy thresholds are met and do not require assumptions about the three-dimensional distribution of these surfaces. Metrics such as the Height Of Median Energy (HOME) have precise definitions within the context of waveform analysis but their meaning as related to the physical organization of canopies is unclear.

There are two general interpretations of the physical meaning of these metrics. One assumes that the majority of reflected light comes from a shallow zone near the outer canopy surface (the hypsometric approach of Parker et al. 2001, see also Lefsky et al. 1999a, 1999b, Næsset and Uklund 2002, Popescu et al. 2002). If this assumption holds true, the power of the waveforms is proportional to the area of tree crown surface at that height, which allows direct interpretations of tree size distributions. An alternate assumption posits that light penetrates into the canopy according to the approach of

MacArthur and Horn (1969) and that the rate of extinction is low enough to allow for substantial penetration into the interior of the canopy (Blair and Hofton 1999, Drake et al. 2002b, Pesonen et al. 2010). If this assumption is correct then this approach allows direct retrieval of the vertical distribution of all canopy surfaces (not just the illuminated sample of surfaces) via the MacArthur-Horn transformation.

A direct test of the validity of the MacArthur-Horn interpretation is extremely difficult as it requires that the actual three dimensional distribution of foliage and non-photosynthetic surfaces to be known. Indirect evaluation of the MacArthur-Horn interpretation relies on comparison of vegetation profiles created using lidar data from downward-looking airborne and upward-looking terrestrial sensors. If canopies are structured in accordance to the assumptions made by MacArthur and Horn, then their approach should be able to reconcile these two sets of disparate observations. Although these comparisons have found that observations from the upward- and downward- orientation will create generally similar vertical features (Lefsky et al. 1999b, 1999a, Harding et al. 2001, Lovell et al. 2003, Hilker et al. 2010) no definite comparison has yet been published.

Preliminary work presented by Leitold (2009) shows improved agreement between upward- and downward- oriented lidar systems by applying a Beer's Law correction.

In contrast, a direct test of the hypsometric approach is possible by estimating the fraction of energy returned from the outer-canopy-surface zone and testing the effect of observed departures from the underlying assumptions. While this test is not possible using

waveform lidar, it can be done using conventional discrete return lidar data to synthesize lidar waveforms. Data of this type has been shown to closely match coincidentally collected waveform data (Blair and Hofton 1999) if the discrete return data is collected at high spatial density with small footprints. However, the data presented here have a larger footprint size and lower spatial density than the data presented by Blair and Hofton. Their data were collected with a footprint size of approximately 5 cm but had only single returns while the data used in this study have a footprint size of 15 - 20 cm and include up to four returns. An additional complication is that the footprint size of the waveforms they used for comparison with the synthesized waveforms was 25 m, whereas the GLAS footprints used here were 60 m. As a consequence, we first test the agreement between synthesized and GLAS waveforms.

As the hypsometric approach assumes that most returned energy comes from the outer canopy surface, a primary methodological concern is the definition of the outer-canopy-surface zone. The optimal definition will be as shallow as possible while capturing the shape of individual crown surfaces, lower tree crowns in canopy openings and the ground surface (Figure 2.1). While this is easy to describe qualitatively, we performed a quantitative analysis of key parameters in the delineation of the outer-canopy-surface zone.

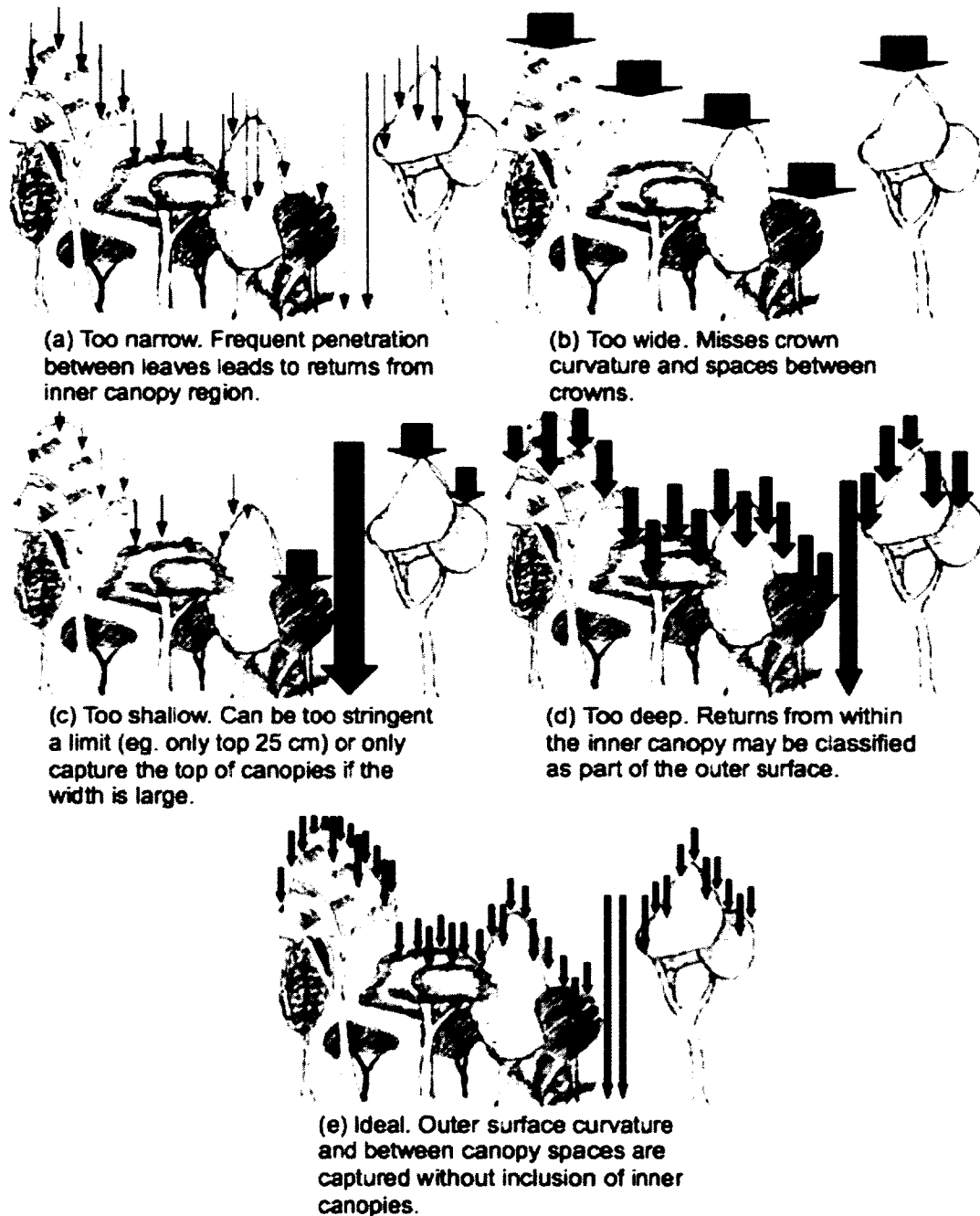


Figure 2.1 Definition of the outer-canopy-surface was examined on the basis of two spatial parameters: the scale of the horizontal window used to determine the "local" maximum value and the depth of the outer-canopy-surface zone considered. Potential issues with the scales of canopy surface identification are detailed here, with grey arrows representing returns from the inner canopy, and black arrows returns from the outer-canopy-surface.

2.2 OBJECTIVES

This research focuses on the following questions:

- Can small footprint lidar data available to us be used to simulate GLAS waveforms?
- How can we best define the outer-canopy-surface zone?
- Is most energy returned from the outer-canopy-surface zone and, if not, what errors are introduced when we use a hypsometric interpretation of waveform power?

2.3 METHODS

Airborne Lidar Data

Airborne lidar data was collected by Esteio Ltd. (Curitiba, Brazil) between June 7 and July 3 2008 in the Brazilian Amazon. Seventeen areas, a total of 4700 ha (Table 2.1), were flown in the regions of Manaus (Amazonas State) and Santarém (Pará State). The instrument was a Leica ALS-50, a discrete-return lidar capable of capturing four returns (1st, 2nd, 3rd and last). Flights were conducted between 700-900 m above ground level which resulted in a footprint size of 15-20 cm diameter (approximately 0.025 m²). The maximum two-sided scan angle was 30 degrees. Minimum return densities of 10 pts m⁻² were specified at Tapajós Km 67 and Reserva Ducke and 3 pts m⁻² at other sites. With up

to four returns for every shot, mean return densities of 12.1 for low density sites and 46.7 for high density sites were observed.

Table 2.1 Summary of plots surveyed with airborne lidar in June and July of 2008 by Esteio Ltd (Curitiba, Brazil). UTM center coordinates are UTM 20S for Manaus plots and UTM 21S for plots near Santarem. Sites 11-14 were flown with a return density over 10 returns per m².

Site	Region	Area Overflown (hectares)	Mean Return Density (SD)	Maximum Return Density	UTM E Center	UTM N Center
1	Manaus	516	10.6 (9.3)	198	822208	9741109
2	Manaus	42	8.2 (8.4)	143	842939	9734987
3	Manaus	229	9.4 (9.6)	189	847054	9733793
4	Manaus	244	13.1 (11.1)	188	849090	9735397
5	Manaus	139	12.0 (10.1)	194	850423	9731633
6	Manaus	145	15.0 (13.2)	232	857405	9729685
7	Manaus	3.3	10.6 (7.5)	112	859442	9729818
8	Manaus	3.4	16.2 (10.0)	141	859831	9729676
9	Manaus	3.9	23.0 (14.0)	159	859492	9729329
10	Manaus	593	10.4 (9.5)	193	811542	9711484
11	Manaus	469	38.3 (28.8)	470	841106	9674444
12	Manaus	485	39.7 (34.6)	421	841229	9673542
13	Manaus	486	52.4 (43.5)	487	841497	9672453
14	Santarem	400	53.4 (32.5)	555	727386	9684047
15	Santarem	810	13.4 (11.9)	282	726439	9666276
16	Santarem	53	13.0 (10.6)	162	726814	9664391
17	Santarem	87	10.6 (9.5)	139	728142	9662631

Point data was geo-referenced by Esteio Ltd and delivered in LAS format, including information on the position of the returned point, intensity of the return, and return number (1-4). Position errors were tested using areas of overlapping data from multiple flight lines. Features identifiable in both scenes were used to identify spatial offset

between overlapping ground returns. The mean differences did not exceed 70 cm vertical and 40 cm horizontal.

A “bare earth” digital elevation model (DEM) with 2 m horizontal spatial resolution was developed using the Tiffs program (Toolbox for Lidar Data Filtering and Forest Studies, Chen 2007) using both first and last return lidar data at each study site. Tiffs uses progressively larger window sizes for morphological operations (similar to Zhang et al. 2003), but without the assumption of a constant slope. Height within the canopy was calculated for each point by subtracting off the local elevation as estimated using the DEM. A canopy surface model was created by calculating the maximum canopy heights within 0.5 m resolution pixels.

The original 0.5 m resolution canopy surface model (CSM) was modified to create five additional surface models simulating the first return obtained at increasing footprint size. This was conducted using the morphological operator “dilate” that replaces every pixel value with the maximum pixel value within a given structural element. In this analysis, square structural elements with the following edge lengths were applied: 1 m, 2 m, 3 m, 4 m and 5 m.

GLAS Lidar Data

The Geoscience Laser Altimeter System (GLAS) onboard the Ice, Cloud and Elevation Satellite (ICESat) collected full waveform lidar data between 13 January 2003 and 11 October 2009. Individual footprints of between 40 m and 90 m diameter were recorded every 175 m along the satellite's path with between track distances of less than 10 km in the tropics. One hundred and sixty-three waveforms fell within six regions of airborne lidar data. Figure 2.2 shows the locations of GLAS footprints overlapping one airborne lidar region of 229 ha located near Manaus, Brazil (Site 3). Orientation and shape of the footprints show the effects of eccentricity and azimuth of variation of the GLAS data.

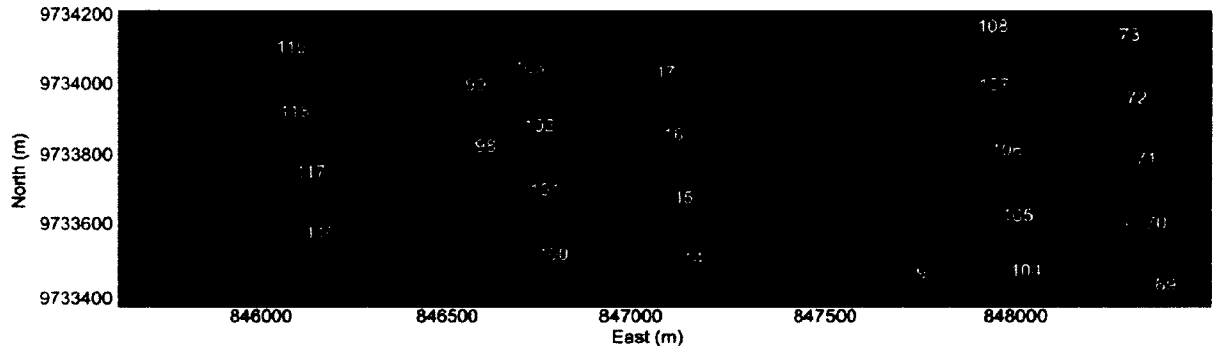


Figure 2.2 GLAS waveform locations overlaid on a canopy height map generated using airborne lidar data collected in June and July 2008. The area shown is a Biodiversity of Forest Fragments Project (BDFFP; Site 3) plot in the vicinity of Manaus, Amazonas state, Brazil. This is one of 17 areas flown, totaling over 4700 ha sampled.

Illumination intensity over lidar footprints has a two-dimensional Gaussian distribution; by convention, the footprint radius is defined as the distance where the relative intensity has decreased to e^{-2} (Blair and Hofton 1999). In the data considered here (observation periods from L2B to L3H), the footprint diameter of GLAS sensors varied between 51.2

m and 89.8 m (mean of 60.6 m and standard deviation of 14.0 m) (Attributes for ICESat Laser Operations Periods, http://nsidc.org/data/icesat/glas_laser_ops_attrib.pdf).

Synthetic Waveforms

GLAS waveforms were compared with waveforms synthesized from airborne lidar returns collected coincident with GLAS footprints. Each lidar return was weighted by the product of its intensity (as recorded by the sensor) and the relative power of laser illumination caused by the Gaussian distribution of energy within the laser beam (Blair and Hofton 1999, Pang et al. 2008, Duong et al. 2008). Vertical smoothing was performed to match the Gaussian distribution of energy within the laser pulse itself. This was done for two cases: using all lidar returns and using first returns only.

Fifty-six waveform pairs were used in the final analysis of synthetic waveforms. Other waveform pairs were removed due to problems with vertical referencing of the GLAS waveform and incomplete overlap. Three waveform-based metrics were calculated for each waveform and waveform pairs were compared (GLAS v. synthetic). The three metrics compared were: Maximum height, height of median energy (HOME) and percentage of power at less than two meters from the ground (Figure 2.3). All metrics were based on the gaussian decomposition of the waveform.

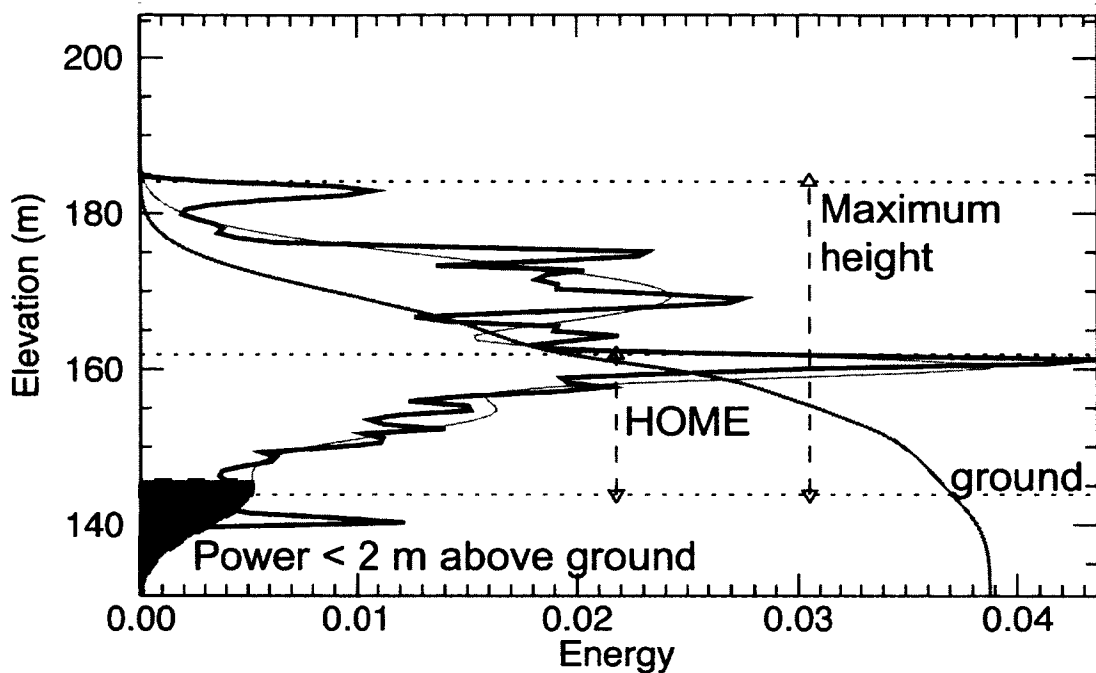


Figure 2.3 Example synthetic waveform (black) with gaussian decomposition (light grey) and cumulative summation of energy (dark grey). Vertical arrows display maximum height and height of median energy (HOME). The region shaded dark grey demonstrates the proportion of power at less than 2 m above ground. All metrics are calculated from the gaussian decomposition of the waveform with ground elevation determined as the peak of the lowest Gaussian. Each metric is calculated using the same methods for GLAS waveforms and synthetic waveforms based on all returns and 1st returns of airborne lidar data.

The metrics were defined as follows: Ground elevation was determined as the peak of the lowest Gaussian. Maximum height is the distance between the ground elevation and the start of the waveform signal. The start of the waveform signal is defined as the highest point at which the signal returned is above the background noise threshold (Harding and Carabajal 2005, Lefsky et al. 2005a). The height of median energy (HOME) is the distance from the ground elevation to the median of waveform power above a noise threshold (Drake et al. 2002a). Within this analysis, percentage of ground return of the

waveform is defined as the ratio of the total signal power less than two meters above the ground return to the total power of the waveform.

The effect of the large difference in collection times (spanning 239 - 1565 days between GLAS and airborne lidar data collection) was filtered for by applying a minimum correlation coefficient of 0.75. This serves to remove waveform pairs that present large changes in structure due to tree-falls or other events.

Canopy Penetration

Definition of the outer-canopy-surface zone was examined on the basis of two spatial parameters: the width of the horizontal window (scale) used to determine the local maximum value and the depth of the zone considered. Potential issues with the scale of canopy surface identification are detailed in Figure 2.1. If the horizontal scale considered is too narrow (Figure 2.1a) objects within the inner-canopy that reflect light back to the sensor due to small openings in the outer canopy may be classified as part of the outer-canopy-surface. This will yield an extremely rough outer canopy surface and runs counter to the common sense notion of an outer-canopy-surface defined by crown height, diameter and shape. If the horizontal scale considered is too wide (Figure 2.1b), crown curvature will not be captured, and crowns or terrain surfaces within gaps between crowns will also be missed.

Variation in the depth of the outer-canopy-surface zone is also important. The effects of a shallow depth vary depending on the horizontal scale used (Figure 2.1c). In the case of a narrow horizontal scale it is possible to use a depth that is too shallow. In this case, returns that are near the outer-canopy-surface will be erroneously classified as inner canopy. In the case of larger horizontal scales only the tops of canopies will be included, missing large portion of canopies with curved outer surfaces. If a deep zone is classified as outer canopy, it is likely that inner canopy regions will be included in the outer-canopy-surface zone (Figure 2.1d). An ideal definition of the outer-canopy-surface includes the upper surface of each crown (whether flat topped or curved), ignores spaces between leaves of individual crowns but captures small gaps between crowns and does not capture inner canopy regions (Figure 2.1e).

Scales were compared and canopy penetration evaluated based on multiple factors including percentage of returns within each canopy layer. For each set of ALS returns coincident with a single GLAS footprint, returns were classified by region: outer-canopy-surface, ground and inner-canopy (Figure 2.4, red, green and yellow points respectively).

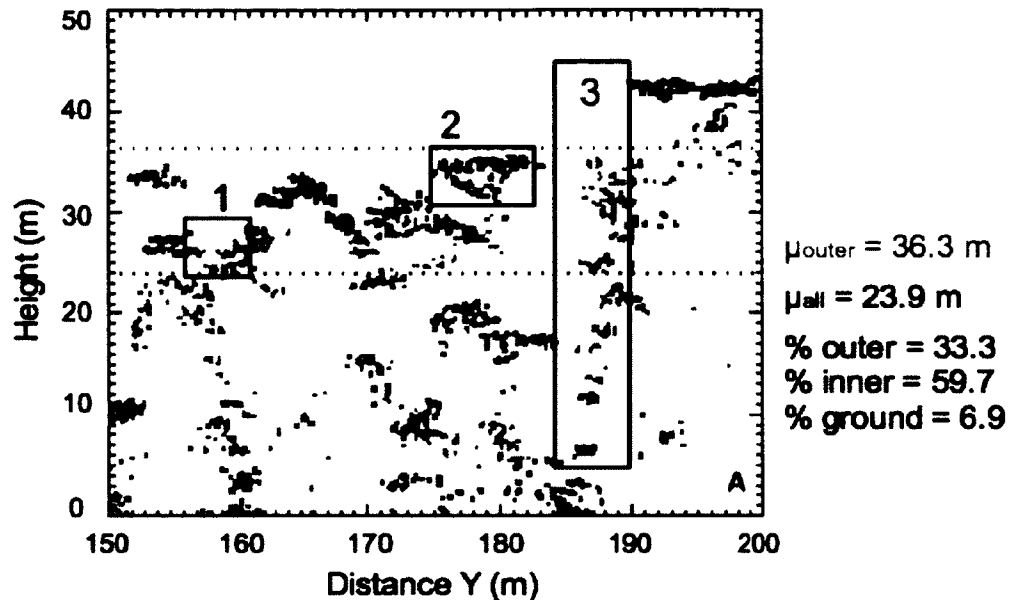


Figure 2.4 Classification of lidar point returns within a 1 m by 50 m swath at Tapajos National Forest, Brazil (Area 14) into outer canopy (red), inner canopy (yellow) and ground (green) components using a 5 m outer-canopy-surface depth and canopy surface model with 5 m horizontal scale. Percentage of returns from the outer-canopy-surface (%outer), percentage of returns from within the canopy (%inner), percentage of returns near the ground surface (%ground), outer canopy mean height (red dashed line; μ_{outer}), and overall mean height (black dashed line; μ_{all}) are reported. The height offset is the outer-canopy-surface mean height minus the overall mean height. Boxed regions show potential problems in outer canopy surface delineation due to the wide pixel size of the 5 m canopy surface model and the large depth considered. Boxes 1 and 3 show regions with no outer canopy surface points due to the wide pixel size of the 5m canopy surface model. Box 1 has a clear outer-canopy-surface layer that is 5 - 10 m below the surrounding canopies. Box 3 shows a region with a sharp drop-off in outer canopy height and penetration to the near ground surface. Box 2 shows a potential problem with an overly large depth considered to be the outer canopy surface. Here, a large number of returns are classified as outer canopy that appear to be within canopy points.

The classification of each point is determined by comparison with the CSM consisting of local maximum heights. Returns within a given distance of the CSM height are classified as outer-canopy-surface returns. Returns within the same distance of the DEM are classified as near ground returns. The balance is defined as within canopy. Six horizontal

scales (the original CSM at 0.5 m scale and the five degraded CSM's) and five vertical depths (1 m – 5 m) were considered.

In addition we use a new metric, the mean height of returns classified as outer canopy surface minus the mean height of all returns which we refer to as the height offset (Figure 2.4). The height offset quantifies a practical aspect of the hypsometric approach's applicability and is defined such that waveforms that fully support the hypsometric approach will show an offset of zero. This occurs under two conditions. The first is the most straight-forward case, where all returns are within the outer-canopy-surface. However, there is a second possibility where much of the energy in the waveform is from within the canopy but the vertical distribution of that energy closely follows the distribution of those we consider part of the outer canopy surface. If so, even though we cannot assume that most points come from the outer canopy, we could still use the vertical distribution of the waveform to estimate the vertical distribution of crown area.

2.4 RESULTS

Synthetic Waveforms

Synthetic waveforms generally under-estimated maximum height and HOME as compared to GLAS waveforms. This is true for synthetic waveforms constructed using both first and all returns. For first returns, the difference in maximum height (GLAS value – synthetic value) for the 56 waveform pairs used in this analysis is 5.90 m on

average with a standard deviation of 8.21 m, and for HOME the difference was 2.35 m (5.2 m standard deviation). When calculated for all returns the differences are less pronounced; the difference in maximum height was 4.25 m (9.3 m standard deviation), and HOME 1.35 m (6.0 m S.D.). Values of maximum height and HOME are all significantly different from zero in the case of 1st returns. When all returns are used, maximum height is significantly different from zero, but height of median energy is not. The standard deviation of each metric was greater than the difference between the mean and zero. Results did not change when a minimum correlation coefficient of 0.75 was applied.

The ratio of energy within 2 m meters of the ground surface to the total waveforms energy was higher for synthetic waveforms than for GLAS waveforms. Using first returns only the energy ratio of GLAS waveforms was 3 percentage points lower with a range of -37% - +31% and a standard deviation of 12 points. When all returns were included the energy ratio of GLAS waveforms had a mean 1.6 percentage points lower with the same range and a standard deviation of 13 points. In neither case was the mean significantly different from zero.

Defining the Outer-Canopy-Surface

In Figure 2.4, the effect of a 5 m horizontal width and 5 m outer-canopy-surface depth are shown. The CSM is degraded so that each pixel represents the maximum height within a

5 x 5 m window. Returns within 5 m of the CSM height are classified as outer canopy surface returns (Figure 2.4, red). Returns within 5 m of the DEM are classified as near ground returns (Figure 2.4, green). The remainder are classified as inner-canopy-returns (Figure 2.4, yellow). Percentage of returns within each layer is calculated as are the mean heights of all returns and returns within the outer-canopy-surface. Returns in the outer-canopy-surface account for 33.3% of all returns and have a mean height of 36.3 m. The internal canopy points are 59.7% of the total, and the near ground returns are 6.9% of the total. This area shows a large height offset of 12.4 m between all points and the outer canopy surface points.

Three regions within Figure 2.4 are boxed to display problems with the large pixel width (horizontal scale) of the CSM (5 m) and the large outer-canopy-surface depth (5 m). As shown in Figure 2.1, the use of a large pixel width causes low returns that are along-side higher canopies to be mis-classified as inner-canopy-surface elements. These lower returns may include a small gap between canopies, or be a wide canopy that is bordered by taller trees. Boxes 1 and 3 of Figure 2.3 show regions with no returns classified as outer-canopy-surface due to the large pixel width and taller surrounding trees. Box 1 highlights a region with clumped returns between 6 and 10 m below the surrounding canopies. In Box 3 the outer-canopy-surface height declines sharply from 43 m to 5 m over a 6 m span. A narrow horizontal scale is necessary to capture this rapid variation. The use of a deep outer-canopy-surface depth results in the inclusion of inner canopy space as seen in Box 2. This occurs independently of the CSM scale.

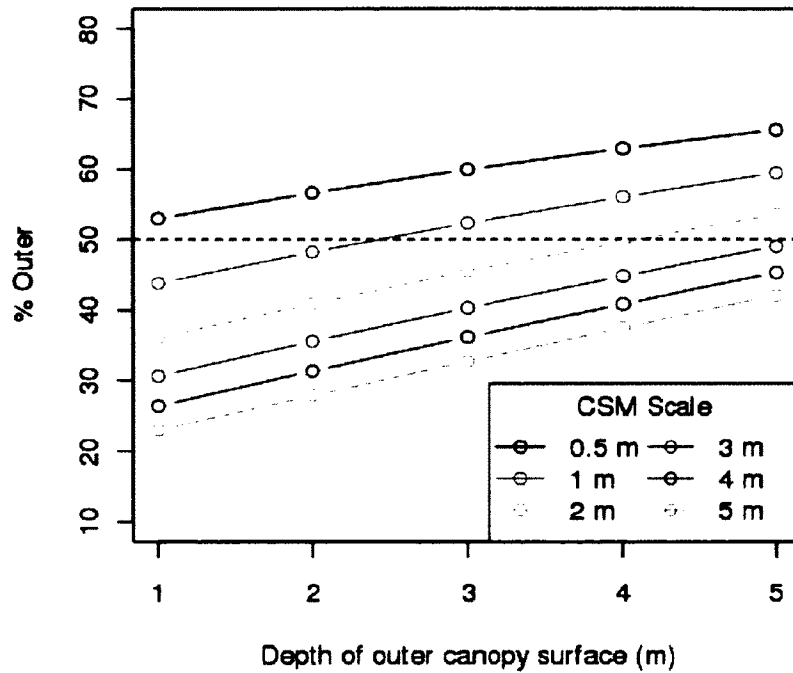


Figure 2.5 Percentage of returns in the outer canopy surface with depth of outer canopy surface for each of the six considered scales of the canopy surface model (CSM).

The percentage of returns in the outer-canopy-surface varied from 23 – 66% over the full range of depth and horizontal scales tested (Figure 2.5). The percentage of returns within the outer-canopy-surface is more dependent on the scale of the canopy surface model (CSM) than the depth of outer-canopy-surface considered. The highest percentage of outer-canopy-surface returns was found at the 0.5 m scale with a rapid decrease as the scale increased, likely due to decreased coverage. The height offset was also smallest at the 0.5 m scale. At this scale the height offset varied from 4.15 m – 4.37 m (Table 2.2). This gradually increased as the CSM was degraded; at the 5 m scale the height offset varied from 6.95 m – 8.06 m. At no scale was the height of returns from within the outer-canopy-surface representative of the mean height of the full set of returns. T-tests showed

significant difference ($p < 0.001$) in the mean heights for all cases considered. This is expected given the relatively low percentage of points within the outer-canopy-surface.

Table 2.2 Height offset and standard deviation with varying outer-canopy-surface depth (1 - 5 m) and canopy surface model scale (0.5 m to 5 m).

		Horizontal scale of CSM					
		0.5 x 0.5 m	1 x 1 m	2 x 2 m	3 x 3 m	4 x 4 m	5 x 5 m
Depth of outer-canopy-surface (m)	1 m	4.37 (1.54)	5.38 (1.47)	6.24 (1.73)	6.93 (1.97)	7.52 (2.18)	8.06 (2.38)
	2 m	4.33 (1.48)	5.25 (1.44)	6.08 (1.68)	6.74 (1.91)	7.32 (2.12)	7.85 (2.32)
	3 m	4.28 (1.44)	5.11 (1.43)	5.89 (1.66)	6.52 (1.88)	7.07 (2.09)	7.57 (2.28)
	4 m	4.22 (1.42)	4.96 (1.43)	5.69 (1.66)	6.28 (1.88)	6.80 (2.08)	7.26 (2.27)
	5 m	4.15 (1.42)	4.81 (1.46)	5.49 (1.67)	6.04 (1.88)	6.52 (2.08)	6.95 (2.28)

Given the high percentage of outer-canopy-surface returns and low height offset found for the 0.5 m horizontal scale, we checked for inter-leaf or inter-branch penetration.

Either type of penetration within individual canopies would cause an increase in outer-canopy-surface percentage and decrease in height offset. Though inter-leaf penetration is expected to occur only when outer-canopy leaves are smaller than the footprint size of lidar data, given the current data set there is no way to quantitatively describe the point at which inter-branch or inter-leaf penetration begins to occur, requiring visual inspection to rule out its occurrence. Regions were visually inspected in each of the three study regions and penetration within individual canopies was not found at the 0.5 m horizontal scale. Given the lack of within-canopy penetration in combination with the high percentage of returns within the outer-canopy-surface and low height offset, 0.5 m was chosen as the best horizontal scale for the available airborne lidar data set.

At the 0.5 m horizontal scale the height offset was smallest with a 5 m depth considered (4.15 m), increasing slightly to 4.37 m for a 1 m depth. As no significant difference was found between the height offset for 1 m depth and any other depth considered ($p>0.1$), there was no justification for using an outer-canopy-surface depth beyond the initial 1 m depth tested.

To display the effects of variation in scales, the outer canopy characteristics are shown for both the chosen scale and a larger horizontal scale and depth for a region of Tapajós National Forest (Figure 2.6). At the 0.5 m horizontal scale and 1 m outer-canopy-surface depth the variability of the outer-canopy-surface is captured without including points that appear to be inner canopy elements (Figure 2.6a). The overhead view mimics that of the canopy surface model itself (Figure 2.6b). When the 5 m scale CSM is used and depth is not increased the canopy surface is not well captured; crown curvature is not captured, nor are small openings or lower canopies. This scale more successfully separates individual emergent crowns, though it also captures low areas where no emergent crown is within 5 m. Increasing the depth improves the detection of the crown surface (Figure 2.6c) but excludes transition regions between crowns and continues to miss lower crowns and small openings to near the ground surface (Figure 2.6d). The issues in outer canopy delineation that occur in Figure 2.6 were previously presented in Figure 2.1. Specifically, the issues presented in Figure 2.1 panels (b) and (d) demonstrating potential problems when the horizontal scale is too wide or the vertical limit is too deep and the combination

of these issues demonstrated on the right-side of Figure 2.1c. At the 0.5 m horizontal scale and 1m depth none of the potential issues are present. Between-leaf penetration is not present leading to returns being marked as outer canopy that are beneath other canopies (Figure 2.1a), and outer canopy surfaces are well captured (left side of Figure 2.1c).

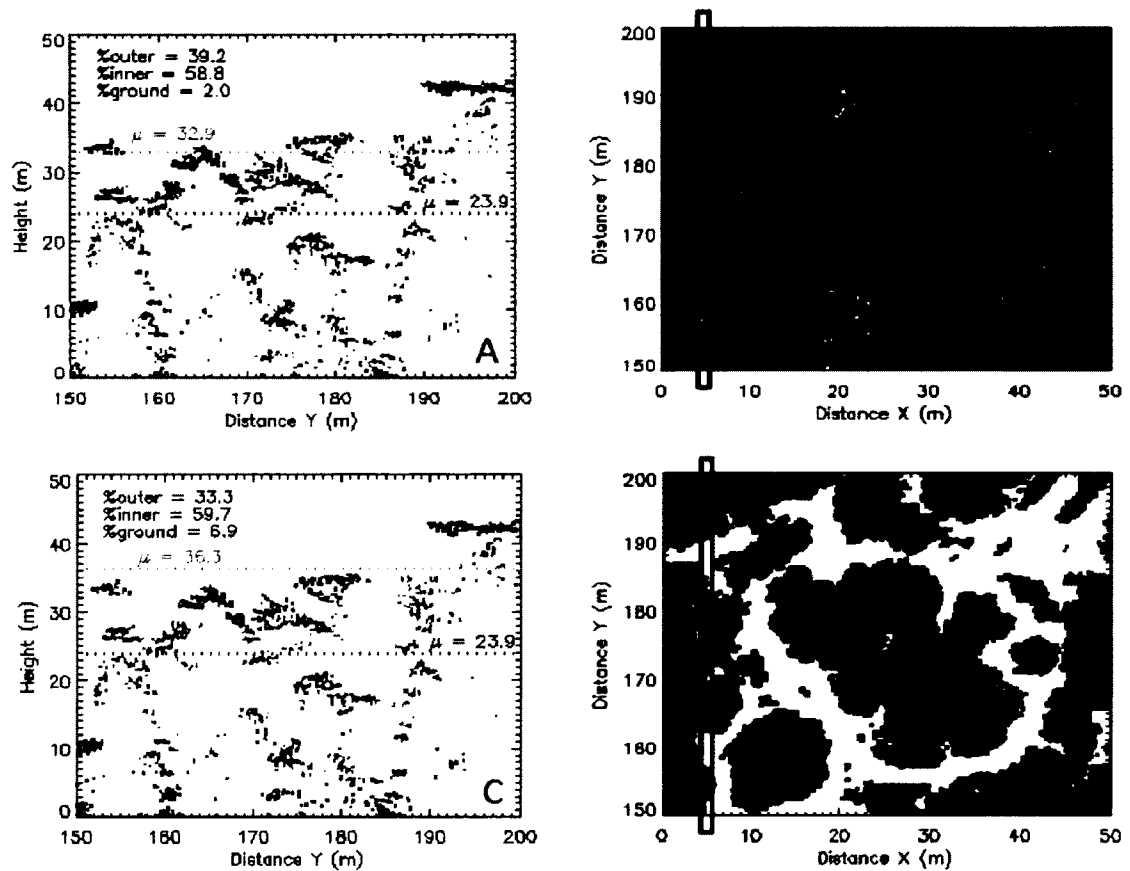


Figure 2.6 Comparison of horizontal and vertical scales used to define canopy layers. (a – b) CSM at 0.5 m scale and 1 m depth and (c – d) degraded CSM at 5 m scale and 5 m depth. Panels (a) and (c) display lidar point returns within a 1 m by 50 m swath at Tapajos National Forest, Brazil into outer canopy (red), inner canopy (yellow) and ground (green) components. Dashed lines show the mean height of the outer canopy surface (red) and all points (black); The percentage of returns in each canopy region is also reported. Panels (b) and (d) show an overhead view of lidar point returns within outer canopy surface. Color varies with height, and the bounding box delineates the 1 m x 50 m transect shown in panels (a) and (c) respectively.

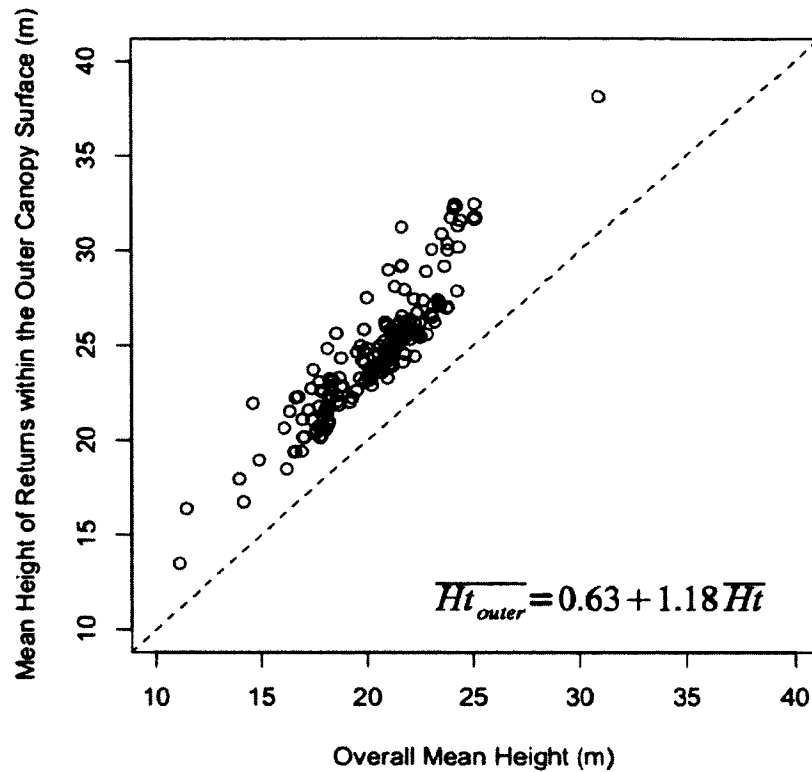


Figure 2.7 Mean height of returns within the outer-canopy-surface is consistently higher but correlated with the mean height of all returns. There is a significant linear correlation with a slope of 1.18 and an intercept of 0.63 m.

Using the 0.5 m scale CSM and 1 m outer canopy depth, variation between individual footprints was investigated. Mean height of returns within the outer canopy surface is consistently higher but correlated with the mean height of all returns (Figure 2.7). There is a significant linear correlation with a slope of 1.18 and an intercept of 0.63 m.

However, the coefficients of this relationship are expected to vary widely (i.e. depending on the forest type, disturbance pattern, etc.) and are therefore not likely to be applicable beyond this study. The height offset varied from 1.5 m - 9.6 m (mean 4.4 m) and is negatively correlated with the percentage of returns within the outer-canopy-surface ($R^2 = 0.65$; $p\text{-val} < 0.001$; Figure 2.8). The percentage within the outer canopy surface varied

from 37.6 – 65.4% and was not well correlated with mean height ($R^2 = 0.18$). This implies that canopy structures that influence the percentage of outer-canopy-surface returns are independent of mean height. This further strengthens the argument that while median height is a strong predictor of biomass and basal area, this is due to the importance of the tallest trees as opposed to the ability of this metric to represent overall canopy structures.

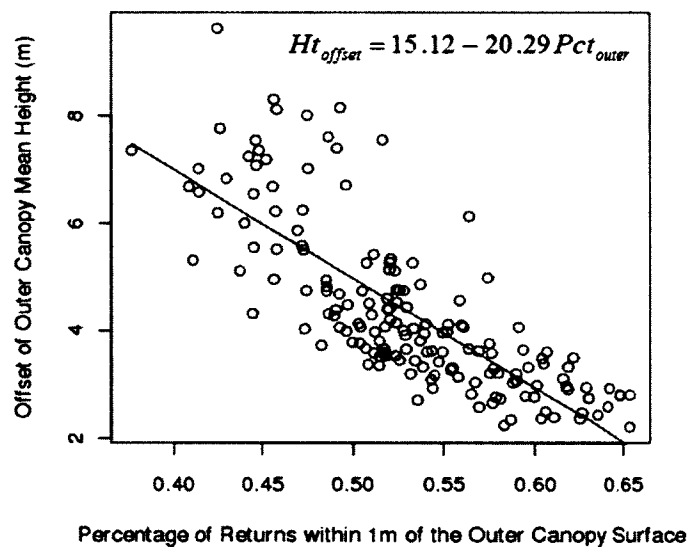


Figure 2.8 The percentage of returns within the outer canopy surface ranges from 37 - 65% when an outer-canopy-surface depth of 1 m is considered. It is also a strong indicator of the error in prediction of overall mean height from the outer-canopy-surface height. There is a significant linear correlation with a slope of -20.29 and an intercept of 15.12 m.

2.5 DISCUSSION

Synthetic Waveforms

The comparison of synthetic waveforms based on all returns and based on first returns to GLAS waveforms demonstrated significant differences in maximum height in both cases. Synthetic waveforms based on first returns also demonstrated significant differences in HOME as compared to GLAS waveforms whereas no significant difference was seen in this metric for synthetic waveforms based on all returns. The ratio of energy within 2 m of the ground was not significantly different between GLAS waveforms and either set of synthetic waveforms. Some of the structural differences may be due to temporal de-correlation as airborne lidar data was collected 239 - 1565 days after the GLAS waveforms. However, this is unlikely as results did not change when waveforms were filtered selecting those with a cross-correlation factor greater than 0.75. The cross-correlation factor serves as a proxy for filtering waveforms with large changes in canopy structure.

Two waveforms with varying maximum height and HOME are shown in Figure 2.9, allowing for a side by side comparison of GLAS and synthetic waveforms under different conditions. Given that calculated metrics are dependent on the gaussian decomposition of each waveform, this is shown with the initial waveform (black) and the cumulative distribution of power (dark grey). Figure 2.9A demonstrates a case where the gaussian

decomposition of the GLAS waveform is comprised of two peaks; a narrow peak that captures the initial strong return of power, and a wide peak that includes 3-4 small noisier features between 135 m and 165 m elevation. As the ground elevation is defined as the peak of the lowest gaussian, the ground elevation is approximately 161 m elevation. The fraction of power returned from less than 2 m above the ground is 0.35. The synthetic waveform based on all returns for the same location has a gaussian decomposition comprised of five narrow peaks. The lowest peak, that is used to calculate the ground elevation, is centered around 154 m. This is a difference of 7 m from the estimated ground elevation based on the gaussian decomposition of the GLAS waveform. The elevation corresponding to the HOME is approximately 167 m for the synthetic waveform and 169 m for the GLAS waveform and the elevations used to calculate maximum height are nearly identical. However, due to the large difference in estimated ground elevations, large differences are seen in HOME and maximum height as well. The synthetic waveform based on first returns is extremely similar to that based on all returns. When inspecting the three waveforms side by side it is apparent that the overall width is similar, as is the location of the dominant peak (near 174 m elevation). The second most dominant peak of the synthetic waveform coincides with a pulse of energy in the GLAS waveform (near 155 m elevation). The primary driver of differences between the GLAS and synthetic waveforms in this case is the difference in ground elevation.

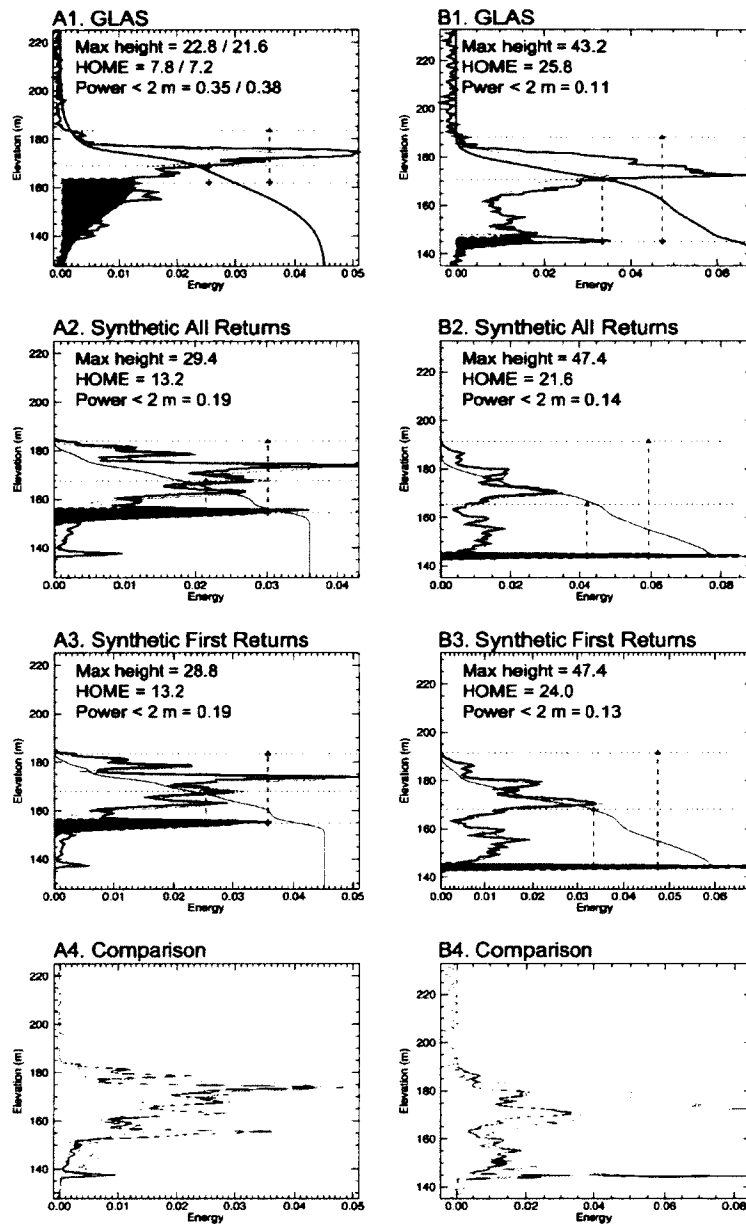


Figure 2.9 GLAS and synthetic waveforms compared for two waveforms within Site 15 (Tapajós National Forest). The cumulative energy distribution (dark grey) and the Gaussian decomposition of each waveform (light grey) are shown for each waveform. Lines display maximum height, height of median energy (HOME) and the estimated ground elevation. Power less than 2 m is displayed as the dark grey shaded region and values for all metrics are printed within each panel. The GLAS waveform (panel 1), the synthetic waveform constructed using all airborne lidar returns (panel 2) and the synthetic waveform constructed using first returns (panel 3) are compared in panel 4 in grey, black and red respectively.

In the second case study (Figure 2.9B) the GLAS waveform is best described by four gaussians of varying widths with the lowest peak at 145 m elevation defining the ground. The gaussians follow the shape of the waveform better than they capture the magnitude. The height of median energy is 25.8 m (terminating at an elevation of approximately 171 m) and the maximum height is 43.2 m (terminating at an elevation of approximately 188 m). The synthetic waveform based on all returns is best characterized by five gaussians, and the synthetic waveform based on first returns is best characterized by six, although both waveforms have similar shape and magnitude throughout. The ground elevation is approximately 145 m and the elevation of the first return (corresponding to maximum height) is at 191 m in both cases. The height of median energy varies minimally; terminating at elevations of 165 m for all returns and 167 m when only first returns are used. The ground elevation and overall signal width are similar between GLAS and synthetic waveforms. The greatest variation is seen in HOME which incorporates the magnitude of waveform features.

As is seen in these two examples, the statistics used for waveform description are reliant on the gaussian decomposition as well as the initial waveform. In both cases shown, synthetic waveforms based on all returns and based on first returns showed minimal differences. However, when all waveform pairs are taken into account significant differences are seen in the comparison with GLAS waveforms. Specifically, the difference in HOME between GLAS and synthetic waveforms based on first returns is significant, whereas it is not when the GLAS waveform is compared to the synthetic

waveform based on all returns. This is likely due in part to the effect of small differences in the synthetic waveforms on the gaussian decomposition from which metrics are calculated.

Lidar Penetration

Investigation of the penetration of airborne lidar through the canopy surface did not support the theory that the majority of reflected light comes from a shallow zone near the outer-canopy-surface (the hypsometric approach). A maximum of 66% of returns were found within the outer-canopy-surface at the highest resolution of canopy surface model and the most lenient definition of the outer-canopy-surface depth (within 5 m of the outer-canopy-surface). At this scale there remained a significant offset of 4.15 m between the mean height of the outer-canopy-surface returns and the mean height of all returns. This indicates that the power of the waveforms is not proportional to the area of tree crown at a given height which limits our ability to directly interpret the tree size distribution from lidar waveforms.

To determine the extent that observed waveforms diverged from the assumption that the majority of reflected light comes from a shallow zone near the outer-canopy-surface, the outer-canopy-surface must be defined on the basis of two spatial parameters: the depth of the zone considered and the width of the horizontal window (scale) used to determine the “local” maximum value. Six horizontal scales were tested, varying from 0.5 m to 5 m and

compared in terms of their ability to capture canopy variability. It is important that the optimal scale is able to capture variability such as the transition zones from tall emergent crowns to the ground surface (Figure 2.1). The 0.5 m horizontal scale showed the lowest height offset and the highest percentage of returns in the outer-canopy-surface of the scales tested without presenting inter-leaf or inter-branch penetration.

It is expected that a footprint size smaller than the average leaf size would allow for increased penetration within individual canopies. With 1 cm diameter footprints Parker and Russ (2004) showed penetration to the ground surface despite an instrument that was limited to first-returns. While the authors show a significant difference between ground estimates of mean foliage height and lidar-based estimates, it is not expected that these two estimates will ever be equivalent due to within canopy shading. However, it is expected that a canopy surface model with a horizontal scale near the scale of the individual footprint will yield an outer-canopy-surface that has the same mean height as the complete lidar data set.

As no significant differences were found in the height offset as the depth was increased we conclude that the additional returns included by increasing the outer-canopy-surface depth do not result in a significant change in mean height. Given that the coverage was also not significantly affected by increasing the depth of the outer canopy surface, it was determined that a 1 m depth was sufficient to capture the outer canopy surface.

Using the optimal scale determined for the outer canopy surface, we are able to determine the extent that waveforms deviate from the assumptions of the hypsometric interpretation of waveform power and the errors that are introduced when the hypsometric interpretation is applied. The extent of deviation is merely the percentage of returns coming from regions within the inner canopy and near the ground surface. A mean of 47% of returns came from these regions; 44.4% within the canopy and 2.7% within 1 m of the ground. However, this is widely variable depending on the individual GLAS footprint compared, ranging from 34.6 - 62.4%. Four footprints with varying levels of penetration into the inner canopy are shown in Figure 2.10. For each footprint the cumulative number of returns is displayed divided between the outer canopy surface (blue) and inner canopy and ground (green). The proportional number of tree crowns is also displayed based on average crown size by height class in 5 m increments (Keller, et al. *unpublished data*).

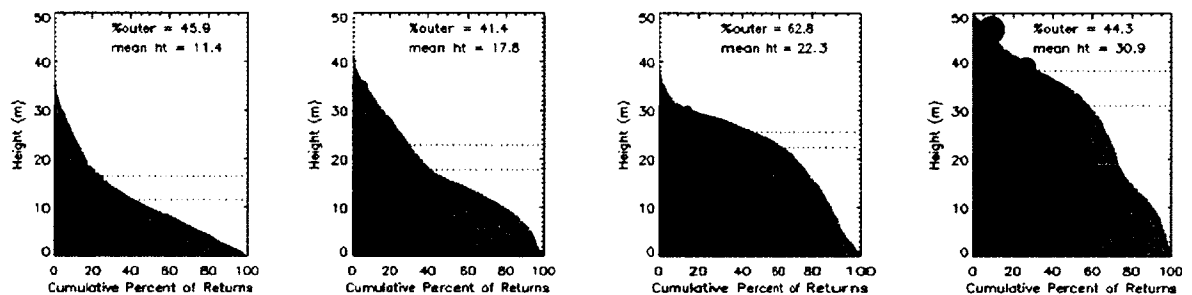


Figure 2.10 Cumulative percentage of returns in the outer (blue) and inner (green) canopy regions by height for four waveforms with increasing mean height and varying percentage of returns in the outer canopy surface. Points represent the proportional number of returns in each region (black in the outer canopy, and grey in the inner canopy) with size proportional to canopy size at a given height.

The first panel of Figure 2.10 (panel A) demonstrates a footprint with low overall height and mid-level penetration through the outer canopy surface. The number of returns within the outer-canopy-surface increase sharply from 0 – 9 m height and then gradually decrease in an approximately linear fashion to 40 m height. Returns within the inner canopy demonstrate a linear decrease from 0 – 20 m height with a minimal number of returns continuing until 34 m. In terms of the cumulative percentage of returns displayed, this equates to a sharp decrease in width of the blue region between 0 - 9 m followed by a linear decrease in this width above 9m. The number of returns in the smallest size class (height between 0 – 5 m) is over four times greater when returns from within the canopy are included. Under the assumptions of the hypsometric approach, all canopies in Figure 2.10 would be considered to be part of the outer-canopy-surface.

The second two panels of Figure 2.10 (panels B and C) have mean overall heights near 20 m, but demonstrate variability in the percentage of returns within the outer-canopy-surface as well as widely varying canopy structure. Returns within the outer canopy surface of panel B show a peak in the number of returns at 15 m, decreasing sharply on either side. From 18 – 35 m height the number of returns in the outer canopy is approximately linear near the half-max of the earlier peak and then decrease from 35 – 42 m. The outer canopy returns for panel C show a gradual increase from 0 – 20 m with an overall low number of returns in this region. A sharp peak in the number of returns occurs at 30 m, decreasing on either side to a maximum height of 40 m. The inner canopy

returns of panel B peak near 12 m, and those of panel C show two rounded peaks, one near 25 m and the other at approximately 3 m from the ground.

The fourth panel of Figure 2.10 (panel D) demonstrates a waveform region with high overall canopy height and high maximum canopy height. A minimal but non-zero number of outer canopy returns are present from 0 – 10 m; a low and relatively constant number of returns from 10 – 30 m; and a large number of returns from 33 – 50 m. The variability in the inner canopy returns is smaller, with returns present through the entire profile with two moderate peaks, one at approximately 35 m and the other near 15 m.

Of cases demonstrated, only panel D showed a nearly stable level of inner canopy returns through the height profile. In other cases the number of inner canopy returns was highly variable, and independent of the distribution of returns within the outer-canopy-surface. Cases that show a clumping of inner canopy returns near the ground result in an exaggeration of the number of small to medium statured trees in the outer canopy under the hypsometric assumption.

2.6 CONCLUSIONS

High density airborne lidar data is here compared with GLAS waveforms, potentially providing a possible method for forest structural attributes on a global scale. GLAS has been successfully used for estimation of biomass and basal area of tropical forests, but

analysis of size distributions and other complex structural characteristics has only begun recently (Palace et al. 2010). Derivation of size distributions from GLAS is dependent on the assumption that the power returned from a given height within the waveform is proportional to the surface area at that height within the canopy. This assumption has been tested and refuted.

We tested this assumption by evaluating the percentage of returns within GLAS footprints that come from the outer-canopy-surface. To do this, we determined the best scales for separating the canopy surface from all returns. At this scale (0.5 m CSM scale and 1 m depth), we found that 53% of returns came from within the outer canopy surface, 44% from the inner canopy and 3% from within 1 m of the ground. As the scale varied, the percentage of returns in the outer canopy surface increased as the depth considered outer canopy increased, and decreased as the resolution of the canopy surface model decreased showing overall variation of 23 - 66 percent. Additionally, we found that the percentage of returns in the outer canopy surface was not constant, but varied widely between individual footprints.

From these findings we conclude that without further modeling of light environments within the canopy calculations of forest structure variables, such as stem size distributions based on GLAS waveforms, are likely to include large errors.

Concluding Points:

1. Synthetic waveforms constructed using all returns are not significantly different from GLAS waveforms with regard to HOME or the percentage of returns from near the ground surface.
2. The horizontal and vertical scale used to define the outer canopy cause the percentage of returns within the outer-canopy-surface to vary significantly (23 - 66%)
3. The preferred scale chosen is 0.5 m horizontal scale and 1 m depth. At this scale, the outer canopy surface contains 53% of the total number of returns.
4. The percentage of returns in the outer-canopy-surface is highly variable between individual waveforms (i.e. there is no simple method to account for the penetration of lidar below the canopy surface).
5. The hypsometric approach to waveform analysis will induce large errors due to the relatively small percentage of returns in the outer-canopy-surface and the high variability between individual waveforms.

CHAPTER THREE

TREE HEIGHT AND TROPICAL FOREST BIOMASS ESTIMATION

Dissertation chapter published in Biogeosciences (www.biogeosciences.net/10/8385/2013/) in collaboration with D. Victoria, M. Keller, and D. Morton.

3.0 ABSTRACT

Tropical forests account for approximately half of above-ground carbon stored in global vegetation. However, uncertainties in tropical forest carbon stocks remain high because it is costly and laborious to quantify standing carbon stocks. Carbon stocks of tropical forests are determined using allometric relations between tree stem diameter and height and biomass. Previous work has shown that the inclusion of height in biomass allometries, compared to the sole use of diameter, significantly improves biomass estimation accuracy. Here, we evaluate the effect of height measurement error on biomass estimation and we evaluate the accuracy of recently published diameter:height allometries at four areas within the Brazilian Amazon. As no destructive sample of biomass was available at these sites, reference biomass values were based on allometries. We found that the precision of individual tree height measurements ranged from 3 to 20%

of total height. This imprecision resulted in a 5-6% uncertainty in biomass when scaled to 1 ha transects. Individual height measurement may be replaced with existing regional and global height allometries. However, we recommend caution when applying these relations. At Tapajos National Forest in the Brazilian state of Pará, using the pantropical and regional allometric relations for height resulted in site biomass 21% and 25% less than reference values. At the other three study sites, the pan-tropical equation resulted in errors of less than 2%, and the regional allometry produced errors of less than 12%. As an alternative to measuring all tree heights or to using regional and pantropical relations, we recommend measuring height for a well distributed sample of about 100 trees per site. Following this methodology, 95% confidence intervals of transect biomass were constrained to within 4.5% on average when compared to reference values.

3.1 INTRODUCTION

Tropical forests are an important component of global carbon stocks. They contribute an estimated 428 Pg (1 Pg = 10^{15} g) of carbon globally, divided approximately evenly between vegetation and soils (Watson 2000). This total is approximately one fifth of the global carbon stock, and the vegetation component is one half of the above ground carbon stored in vegetation of all biomes. However, there is a great deal of uncertainty in these numbers (Watson 2000). While some of this uncertainty is due to the unknown amount of deforestation and degradation in tropical forests, another large component is due to the uncertainties involved in estimating standing biomass in the field (Houghton

2005). This uncertainty is compounded when a limited area sampled is used to predict biomass over large tracts of forest.

Because of their high carbon density, tropical forests are increasingly viewed as an avenue for mitigation of climate change. In an effort to reduce deforestation and degradation by creating monetary value for the carbon in forests, the United Nations has developed REDD (Reducing Emissions from Degradation and Deforestation) (Gibbs et al. 2007). However, to implement this framework it is first necessary to quantify carbon stocks.

In an effort to create global biomass maps that can serve as REDD baseline carbon stock estimates, moderate and coarse resolution optical and microwave data from satellites has been combined with lidar remote sensing by ICESat to extrapolate field measured biomass over the global extent of tropical forest (Saatchi et al. 2011, Baccini et al. 2012). Recognizing the importance of biomass estimation the European Space Agency is scheduled to launch the BIOMASS radar satellite mission in 2020 in an effort to create three dimensional maps of the world's forests (Le Toan et al. 2011). NASA missions (such as the completed ICESat and the upcoming ICESat II lidar missions) have secondary goals of estimating forest biomass (Lefsky et al. 2007, Nelson 2010, Saatchi et al. 2011). However, neither existing nor planned remote sensing data sets directly measure biomass; they all rely on field data in combination with allometric estimations for calibration (see Clark and Kellner, 2012).

In most applications, estimation of tropical forest biomass is ultimately linked to the estimation of biomass of individual trees (although see Clark and Kellner 2012 who suggests an alternative approach). Individual tree biomass estimates depend upon allometric equations that are developed using a finite number of individuals from a limited region or a broader combination of sites (Chambers et al., 2001, and others). By necessity, these allometries are often applied beyond the region(s) for which they were developed, and often beyond the range of diameters sampled as well (Chave et al. 2003). Unfortunately, allometric equations do not transfer without error across all sites. For example, Vieira et al. (2008) applied allometric equations developed at sites in the central Amazon and Puerto Rico to Atlantic Forest trees and compared them with an allometry specific to the Brazilian Atlantic Forest. Equations developed at Puerto Rico and the central Amazon deviated by more than 36% and 68% respectively from the Atlantic forest values. Recently, broader analyses have been conducted that create regional and global allometric relations based on data from multiple sites (Chave et al. 2005, Feldpausch et al. 2012). These allometries are based on significantly larger sample sizes, and are assumed to be more robust for regions without site-specific equations. The Chave et al. (2005) allometry uses stem diameter and wood density, and optionally total tree height. Feldpausch et al (2011) have developed global and regional equations to relate height to diameter for sites where height measurements are lacking.

Studies in temperate and tropical regions have shown the advantages of species-specific biomass and volume allometries (Litton and Boone Kauffman 2008, Basuki et al. 2009). Given the variation in tree form and growth properties, species specific allometries are desirable. However, the species diversity present in tropical forests makes this prohibitively costly for most sites. For example, a study conducted near Manaus showed 280 - 285 species per hectare for three hectares sampled for trees greater than 10 cm diameter (De Oliveira and Mori 1999). Sites in the Brazilian Amazon typically have upwards of 100 tree species per hectare (Campbell et al. 1986), most of which do not have species specific allometries.

The inclusion of height in allometric equations greatly improves the accuracy of individual tree biomass estimation (Maia Araújo et al. 1999, Chave et al. 2005, Vieira et al. 2008, Feldpausch et al. 2012, Lima et al. 2012). Chave reported that the inclusion of height for stand level estimates of biomass reduced error from 19.5% to 12.8%, across all forms of tropical forests and across continents (Chave et al. 2005). At Brazilian sites specifically, the root mean squared error of individual tree biomass was reduced from 16% to 6%.

The accuracy of biomass estimation for individual trees and subsequently for plot scale biomass fundamentally depends on the accuracy of tree height measurements. Tree heights can be difficult to measure under the best conditions (Rennie 1979, Williams et al. 1994). Height measurements are dependent on forest conditions, observer experience,

and the equipment used. Tropical forests typically include significant obstacles for traditional field-based estimates of tree heights, including dense understory vegetation, tall canopies, and closed-canopy conditions that limit the line of sight. Tree height measurements in tropical forests are both labor intensive and have potentially large errors. Although researchers agree that height is a valuable addition when estimating biomass, the degree of acceptable error has been debated. Williams and Schreuder (2000) compared a diameter-only allometry to a diameter:height allometry and found that a height error of up to 40% was acceptable in temperate forests before the use of a diameter-only equation provided a better biomass estimate. Molto and colleagues (2013) showed that a height error of 2-5% can significantly influence estimates of above ground biomass for a tropical forest in French Guiana. We evaluate how tree height accuracy affects biomass estimation accuracy for moist tropical forests in Brazil by responding to a number of questions.

- How precise are ground-based tree height measurements using a hand-held clinometer and metric tape?
- How accurate are ground-based tree height measurements using the clinometer approach?
- What is the effect of tree-level uncertainty in height on the estimation of plot biomass?
- Are global and/or regional height-diameter relations adequate for accurate biomass estimation?

-How can field work be optimized to achieve acceptable accuracy in plot level biomass while limiting the number of tree height measurements used?

3.2 METHODS

Site Descriptions

Data from five sites in four regions of contrasting forest structure distributed across the Brazilian Amazon were used to answer the questions posed above (Table 3.1). The precision of ground-based tree height measurements was evaluated by comparing repeat measurements of height at one of the field sites, Tapajos km 67. The accuracy of height measurements was evaluated by comparing field and lidar data at two sites in the Tapajos National Forest and one at Reserva Ducke. The resulting estimates of accuracy were applied at Tapajos sites and at Reserva Ducke to answer the third question, and the remaining questions were addressed using field data from all sites.

Regional and pan-tropical height-diameter allometries published by Feldpausch et al. (2011) include local climate and structural parameters. Climate data for all sites was extracted from the WorldClim 2.5 minute resolution database (Hijmans et al. 2005) in order to conform to climatic data requirements proposed by Feldpausch et al. (2011) and is presented in Table 3.2. The precipitation variability was defined as the standard

deviation of monthly precipitation divided by the mean. Dry season length was defined as the number of months with less than 100 mm of precipitation.

Table 3.1 Data used to address each of the five questions posed by this research. Lidar data were available for three of the five sites.

Site	Reserva Ducke		Tapajos km 67		Tapajos km 83		Tanguro	Cauaxí
	Field	Lidar	Field	Lidar	Field	Lidar	Field	Field
Q1. Precision of ground-based height measurements			X					
Q2. Accuracy of ground-based height measurements	X	X	X	X	X	X		
Q3. Effect of height uncertainty on biomass prediction	X	X	X	X	X	X		
Q4. Use of global / regional diameter-height allometries	X	X	X	X	X	X	X	X
Q5. Optimization of field data collection	X	X	X	X	X	X	X	X

Table 3.2 Site locations and climatic characteristics. Climatic data are from the WorldClim 2.5 minute resolution database (Hijmans et al., 2005). The precipitation variability is defined as the standard deviation of monthly precipitation divided by the mean. Dry season length is defined as the number of months with precipitation less than 100 mm.

Site	Reserva Ducke	Tapajos km 67	Tapajos km 83	Tanguro	Cauaxí
Location	59°57'W 2°57'S	54°57'W 2°51'S	54°58'W 3°01'S	52°23'W 13°04'S	48°17'W 3°45'S
Mean annual temperature (C)	27	25	25	25	27
Average precipitation (mm)	2208	1909	1909	1740	2200
Precipitation variability (%)	33	45	45	79	85
Dry season length (months)	1	5	5	5	6

Forest structural characteristics including basal area, maximum diameter measured and mean canopy height all vary among sites and are presented in Table 3.3. The mean canopy height was calculated from field data as Lorey's height (basal area weighted mean height).

*Table 3.3 Details of field and lidar data collection. Lidar data were collected for three of the five sites: Reserva Ducke, Tapajos km 67 and Tapajos km 83. Lorey's height is the basal-area-weighted mean canopy height for all trees measured. *The nominal sample area of the field survey is reported at Tapajos and Reserva Ducke sites, as diameter-dependent line sampling was conducted.*

Site	Reserva Ducke	Tapajos km 67	Tapajos km 83	Tanguro	Cauaxí
Number of trees measured (N)	817	913	852	844	2171
Tree heights measured (N_{ht})	817	913	852	308	306
Area sampled (ha)*	3.0	5.1	5.1	6.7	14
Basal Area (m^2ha^{-1}) of trees ≥ 10 cm diameter	28.7	31	17.6	17.1	35.2
Diameter range measured (cm)	5 - 128	5 - 213	5 - 186	10 - 70	20 - 192
Lorey's height (m)	30	38	38	19	39
Date of field data collection	10/2009	06/2009	01/2010	11/2005	07/2000
Area of lidar data collected (ha)	1200	400	768	NA	NA
Mean CHM height (m)	25	34	34	NA	NA
Date of lidar data collection	06/2008	06/2008	06/2008	NA	NA

Reserva Adolpho Ducke

Reserva Adolpho Ducke (59°57'W 2°57'S) is a 10,000 ha forest preserve managed by the National Institute for Amazon Research (INPA) north of Manaus, Brazil. It is dominated by rolling terrain (30 - 120 m.a.s.l.) cut by small streams and covered by upland terra firme forest with a large number of palms present, especially in seasonally flooded valleys. The soils vary with topography with oxisols similar to those of Tapajos National Forest (see below) present on the upland plateaus, ultisols on the slopes and spodosols in the valleys (Chauvel et al. 1987). These soils are acidic and low in nutrients. Mean annual temperature is 27° C, and precipitation averages 2208 mm with a short dry season (1 - 3 months) during July - September (Table 3.2).

Tapajos National Forest- Tapajos km 67 and Tapajos km 83

The Tapajos National Forest (54°58'W, 2°51'S) is a 550,000 ha reserve situated south of Santarém, Brazil between the Tapajos River and the Cuiabá-Santarém Highway (BR-163). The reserve is dominated by upland forests on a nutrient-poor, clay oxisol plateau (Silver et al. 2000). The mean annual temperature and precipitation at Tapajos are 25° C and 1909 mm, respectively. The dry season generally lasts five months, from July-December (Vieira et al. 2004). Two field sites were installed within the Tapajos National Forest referred to by their entrance points along the BR-163 highway; an undisturbed forest site (Tapajos km 67) and a selectively-harvested site (Tapajos km 83).

Fazenda Tanguro

Fazenda Tanguro (52°23'W 13°4'S) is a private land holding of approximately 80,000 ha within the municipality of Querência, Mato Grosso. Located near the forest-cerrado transition, Fazenda Tanguro is classified as transitional forest characterized by comparatively low biomass and tree species diversity. Soils are oxisols throughout this generally flat region, with slopes less than 2 degrees (Balch et al. 2008). It has a mean temperature of 25° C, annual precipitation of approximately 1740 mm and a 5 - 6 month dry season lasting from May to September (Balch et al. 2010). Though the annual temperature and dry season length are similar to that of Tapajos, the variability in precipitation is much higher at Tanguro.

Fazenda Cauaxí

Fazenda Cauaxí is a mainly forested land holding in the municipality of Paragominas in eastern Pará state (48°17'W 3°45'S). The topography of this area is flat to mildly undulating and is characterized by tropical dense moist forest with a mean temperature of 27°C, annual precipitation averaging 2200 mm and a 5 - 6 month dry season from July through November (Pereira et al. 2002). The soils within the region are classified as dystrophic yellow latosols following the Brazilian system (Radambrasil 1983).

Field Inventory Measurements

Reserva Adolpho Ducke

Five 500 m transects were installed at Reserva Ducke in October of 2009. Diameter-dependent line sampling using a diameter factor of 10.0 (following Schreuder et al., 1987) was conducted along each 500 m transect including trees greater than 5 cm diameter. A total of 817 living trees were sampled at Reserva Ducke. The resulting average nominal plot size was approximately 0.6 ha, calculated as the average maximum distance from the transect times transect length.

Stems were mapped with respect to the transect, and geo-located using differential GNSS (Trimble GeoXH 6000 series receivers with estimated post-processed accuracy of < 0.5 m using Trimble Pathfinder Office V.5 software). Four differential GNSS (dGNSS) points were taken along each transect at roughly equal intervals. Individual tree positions were calculated using the two closest dGNSS points to any given stem.

For each stem, diameter at breast height (DBH), total height and crown extent were measured. Where buttresses or trunk deformities were present, diameter was measured above the deformation. Total height and bottom of canopy height were measured using a clinometer and tape-measure and calculated trigonometrically. The clinometer is used to measure the angle to the canopy top and bottom as well as the angle from the viewer to

the base of the trunk. All angles measured were under 50 degrees to minimize error within the trigonometric calculation. A tape-measure was used to measure the distance from the observer to the measurement point. In the case of measurements on sloped ground, the slope of the tape-measure was also measured and the distance corrected. Heights were calculated trigonometrically. All height measurements were taken by a single observer. Crown radius was measured in four cardinal directions with respect to the trunk. Notes were taken on the availability of light to the tree crown (full direct, partial direct, full indirect light) and the crown's position within the canopy (emergent, canopy or sub-canopy). Emergent trees were defined as those standing above the surrounding tree's canopies, not those taller than the dominant canopy height. While multiple life forms (including vines and palms) and standing dead were included in the field sampling, only the living trees were analyzed.

Tapajos National Forest- Tapajos km 67 and Tapajos km 83

A total of twelve 500 m transects were installed; six within the old-growth portion (Tapajos km 67) of Tapajos National Forest in June 2009, and another six in a selectively-logged portion (Tapajos km 83) in January 2010. The sampling method and measurements at the Tapajos sites were the same as at Reserva Ducke (see above). A total of 1765 living trees were sampled at Tapajos, with a resulting average nominal plot size of 0.85 ha.

Geolocation of individual stems at the Tapajos sites differed from the methods at Reserva Ducke. Stems were mapped with respect to the transect, and geo-located using differential GNSS (Trimble GeoXH 6000) in combination with data collected using hand-held GPS units (Garmin 76csx). Differential GNSS was used to collect a point at the start of each transect and hand-held GPS measurements taken at 50 m increments. Hand-held GPS points were used to determine the orientation of the transect. At two transects a greater density of differential GNSS was available (approximately six points spaced every 100 m along the transect) and transect and tree positions were compared to the single dGNSS point in combination with hand-held GPS data. Transect positions varied up to 19.2 meters and individual trees had a horizontal RMS error of 5.7 m.

During the survey of Tapajos km 67 a random subset of 20% of trees (174 individuals) were remeasured within a week of the initial survey. Diameter at breast height, bottom of canopy height, top of canopy height and light characteristics were all remeasured to assess the repeatability of field measurements. Remeasurement of all stems at this site occurred in July 2010.

Fazenda Tanguro

Eighteen 0.37 ha circular plots were installed in 2005, designed for correlation with satellite-based lidar footprints (ICESat-GLAS). Further sampling design information is available in Lefsky et al. (2005a). Total height, commercial height (height to lowest

branch) and longest crown dimension of all trees greater than 35 cm diameter were measured. Trees with 10 cm to 35 cm diameter were measured in a sub-plot of 0.075 ha with a random subset of 20% selected to measure canopy characteristics. Both total and commercial height were measured using a clinometer and tape measure.

Fazenda Cauaxí

Fourteen 1 ha plots (500 x 20 m transects) were surveyed at Fazenda Cauaxí in 2000 for trees greater than 20 cm diameter, totaling 2271 individuals (Asner and Keller 2002, Asner et al. 2012). Additional crown measurements were taken for a subset of 300 stems. These crown measurements included top of canopy height, commercial height and crown width along the estimated longest axis. See Asner, et al. (2002) for the complete methodology. Tree heights were estimated using a handheld laser range finder (Impulse-200LR, Laser Technology Inc., Englewood, CO), that measures distance using laser ranging and estimates height using a clinometer incorporated into the instrument.

Airborne Lidar Data

Airborne lidar was collected over Tapajos National Forest and Reserva Ducke between June 7 and July 3 2008 by Esteio, Ltda. (Curitiba, Parana, Brazil) using a Leica ALS-50 discrete-return lidar system capable of capturing four returns per outgoing pulse. Flights were conducted between 700 - 900 m above ground level, resulting in a footprint

diameter of 15 - 20 cm. The instrument was operated with a two sided scan angle of 30 degrees. Minimum pulse densities of 10 pulses m^{-2} were specified at Tapajos km 67 and Reserva Ducke and 3 pulses m^{-2} at Tapajos km 83. With up to 4 returns per outgoing pulse and flight line overlaps, mean return densities of 46.7 points m^{-2} for high density sites and 12.1 points m^{-2} for low density sites were observed. Position errors were tested using overlapping data from multiple flight lines. Features identifiable in both scenes, such as the crown edges of emergent trees were used to estimate position error. Mean differences did not exceed 70 cm vertical and 40 cm horizontal. This is an extremely conservative estimate of point accuracy as it includes both the geolocation error and error due to the likelihood of repeat sampling of the exact same point within the tree crown.

The lidar point cloud was summarized to create a Digital Terrain Model (DTM) and Canopy Height Model (CHM). The DTM was created by first separating ground returns following the algorithm of Zhang et al. (2003). The density of ground returns was 0.44 per m^2 at Tapajos km 67, 0.19 at Tapajos km 83 and 0.83 per m^2 at Reserva Ducke. Using a similarly high density of data collection and the same methods for constructing a DTM (1 m grid), a mean error of less than 10 cm was achieved (V. Leitold, personal communication). Delauney triangulation was used to create a triangular irregular network (TIN) of ground hits, and the TIN was then used to interpolate DTM elevations on a raster grid of 1 m spatial resolution. Additionally, the TIN was used to interpolate the elevation of every feature return in every grid cell, and feature heights were calculated as the difference from this elevation (Cook et al. 2013). The CHM was created by selecting

the greatest height of all non-ground return points within a given 1m grid cell (minimum of 3 returns per grid cell).

Lidar Estimation of Tree Heights

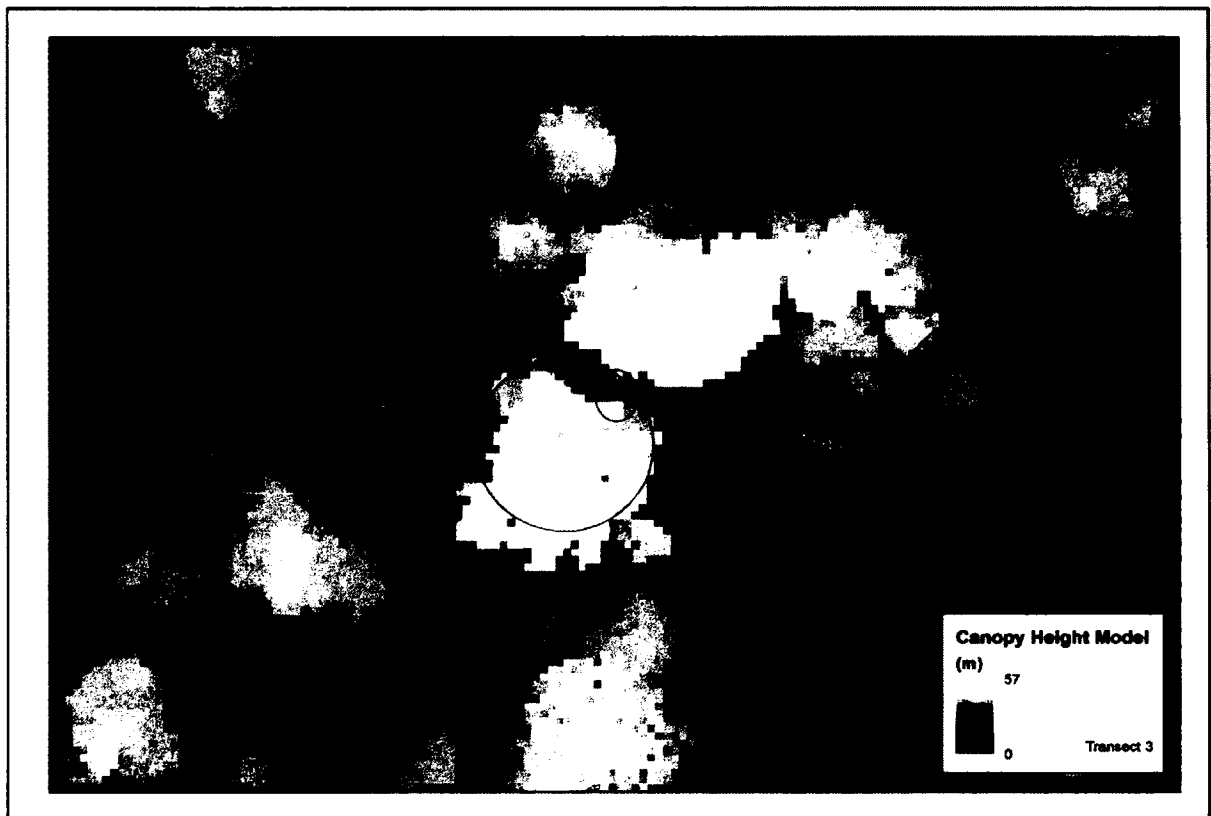


Figure 3.1 The canopy height model is shown for a region of Tapajos km 67, with darker shades of grey corresponding to lower canopy heights. Field data collected along a transect within this area include four measurements of crown radius and position. These field data were used to draw crown ellipses for emergent stems that are overlaid on the canopy height model.

Georeferenced crown locations were used to estimate tree heights from the lidar data at the Tapajos and Reserva Ducke sites. For each crown, an ellipse of crown inclusion was created based on four crown radii measured in the field in combination with the geo-

referenced trunk position (Figure 3.1). The 99th percentile height of the lidar data within each crown ellipse was defined as the lidar estimated maximum tree height.

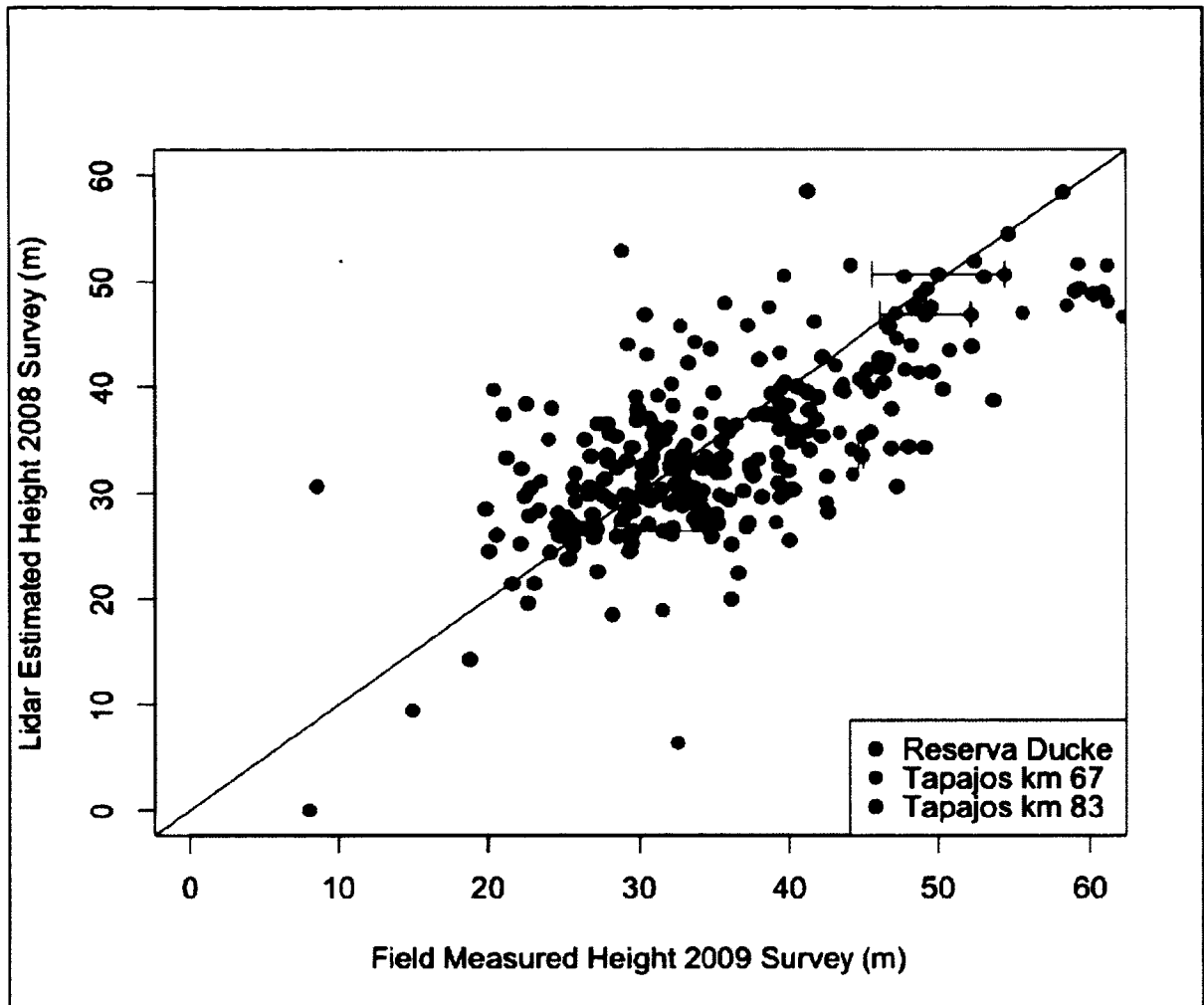


Figure 3.2 Comparison of field-measured height to that estimated using the lidar canopy height model (CHM) for stems with emergent crowns at Reserva Ducke and Tapajos sites (Tapajos km 67 and Tapajos km 83). RMSE of emergent crowns is 7.3 m. Where multiple field heights were taken for emergent stems, mean values are shown with error bar showing the range of repeated measurements.

The comparison of lidar height to field height measurements was limited to emergent stems, as they are expected to be visible in the lidar canopy height model (Figure 3.2).

Emergent stems were considered to be any tree whose canopy is above its immediate

neighbors. To assess the extent to which the time period between lidar and field data collections may affect our results, we compared field heights of emergent trees measured with a one year inter-sample period at Tapajos km 67.

Statistical Analysis and Simulation

To analyze the effect of the uncertainty in tree height on biomass estimates, a Monte Carlo analysis was conducted. Stems with multiple measurements at Tapajos km 67 (n=174) were split into four diameter classes with an equal number of stems: 5 - 7.3 cm, 7.4 - 13.7 cm, 13.8 - 33.4 cm, and greater than 33.5 cm. The standard deviation of the differences between initial and repeat height measurements was calculated for each class. Returning to the full data set, a series of random numbers normally distributed with a mean of zero, and a standard deviation matching that of the height difference within each diameter class was calculated. A random number from this distribution was added to each field height measurement and the Chave Model I (Chave et al. 2005) moist forest allometry was then used to re-calculate biomass for each stem, using a site average wood density of 0.64. The simulation was conducted 1000 times, and the resulting transect level biomass was reported.

To assess the necessity of time consuming height measurements at individual sites, site-specific diameter to height allometric relationships were compared with the best regional and pan-tropical allometries published by Feldpausch et al. (2011). Feldpausch et al.

(2011) found that environmental and structural parameters significantly improved diameter-height allometries. Both the regional and pan-tropical allometries include environmental (Table 3.2) and structural parameters (Table 3.3) that are site-dependent. Tapajos sites were combined because they have the same inherent structure, and the basal area of Tapajos km 67 was used to calculate regional and pan-tropical allometries as the basal area at Tapajos km 83 was reduced due to selective harvest. Site-specific allometries were fit to a log-log formulation following Feldpausch et al. (2011) using all field measurements of height. Individual stems were weighted evenly within each of four diameter classes, determined by the range of diameters sampled at a given site. The range of diameters used to determine the four diameter classes spans from the minimum to the 99th percentile of diameters measured. In order to divide the diameters into bins, the full range is further divided into fractional sub-ranges: 0 - 0.22, 0.22 - 0.35, 0.35 - 0.51, 0.51 - 1.0. Although these four diameter classes are weighted equally, the first three sub-ranges are divided in half to further distribute the sample.

At sites where heights were measured for all trees (Tapajos sites and Reserva Ducke), reference values for site and transect level biomass were calculated using field measured height. At Tanguro and Cauaxí reference values for biomass were calculated by applying the site-specific diameter:height allometries. To determine the approximate sample size of tree height necessary to estimate biomass within 5% of the value calculated based on all trees, bootstrap resampling was applied. For a given sample size, the entire data set was subset 1000 times (sampling without replacement within each subset) and allometries

were fit to each subset. The weighting scheme applied for the site specific fit was also applied to sample stems by diameter class. To determine the given allometry's accuracy in terms of biomass prediction, field data was regrouped to compare approximately 1 ha sized plots in all cases.

3.3 RESULTS

Precision of Ground-based Height Measurements

Remeasurement of 174 stems from the Tapajos km 67 field survey showed no significant difference from zero between the first and second measurements (t-test $p = 0.38$). The overall mean difference in height (first measurement minus second measurement) was 1.1 m, with a standard deviation of 4.7 m. There was a slight tendency toward lower remeasured heights (i.e. positive residuals) both overall and by diameter class (Figure 3.3). The difference between first and second measurements were an average of 16.57% of the mean height measured (median of 11.9%). Dividing the remeasured heights into four diameter classes with an equal number of samples, the standard deviation of height differences within individual size classes increases by a factor of eight from 1.09 m to 8.17 m. This represents an increase in relative terms as well as absolute terms and suggests that field measurements of tall trees are less precise than short trees.

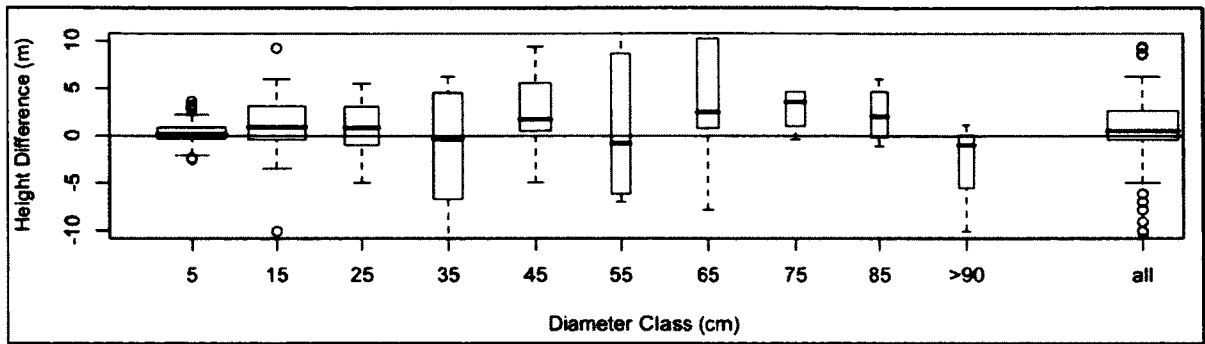


Figure 3.3 Height measurements were repeated for 174 trees during the 2009 field campaign at Tapajos km 67. Box width is proportional to the square root of the sample size. The mean height difference for all remeasured trees is 1.1 m, with a standard deviation of 4.7 m.

Accuracy of Field Measurements of Height Compared to Lidar

The height difference between emergent crowns measured in the field versus the height estimated using lidar was -1.4 m (lidar - field height). The mean residual of lidar minus field height was -1.3 m at Reserva Ducke (standard deviation of 6.4 m), -2.0 m at Tapajos km 67 (standard deviation of 8.9 m), and -0.9 m at Tapajos km 83 (standard deviation of 6.6 m). There are two possible explanations of these differences; One possibility is an overestimation of field height, the second possibility is an underestimation by lidar. A third possible explanation, that sampled trees grew during the time period between lidar and field data collections, was discarded. Comparing field heights of emergent trees measured at Tapajos km 67 with a one year inter-sample period showed no significant difference in mean heights (paired t-test $p=0.34$; mean of differences = -0.37 m and standard deviation = 3.6 m). Height residuals (lidar minus field height) show a slight positive trend when regressed against lidar height. This is consistent with the observation

that heights are increasingly difficult to measure above the dominant forest canopy (34 m at Tapajos and 25 m at Reserva Ducke). However, the uncertainty of field measurements is larger than the mean residual in all cases.

Effect of Height Error on Plot Level Biomass

At Tapajos the 95% confidence interval of transect-level biomass due to variability in field estimated heights ranged from 13 - 22 Mg ha⁻¹ with transect biomass estimates ranging from 147 to 398 Mg ha⁻¹ (Table 3.4). The mean biomass is lower and more variable at Tapajos km 83 (288 Mg ha⁻¹) as compared with the old-growth site Tapajos km 67 (325 Mg ha⁻¹). Typically, transects with higher biomass show a larger 95% confidence interval and smaller error in terms of percent biomass, although this is dependent on the size distribution of individual trees. The 95% confidence interval as a percentage of biomass ranged from 5.2% to 8.7% with a mean of 6.3%.

Although repeat field measurements were not available for Reserva Ducke, the height error estimated at Tapajos was applied to estimate variability due to the lack of precision of field measurements. The 95% confidence interval of transect biomass ranged from 17 to 21 Mg ha⁻¹ with biomass estimates ranging from 306 to 431 Mg ha⁻¹. Based on these calculations the lack of precision in height measurements results in a 95% confidence interval of 5.0% to 5.7% of biomass.

To test the effect of the potential bias towards over-estimating field height, the mean residual was subtracted from trees within 10 m of the mean canopy height and above. This shrank the height of canopy and emergent trees by 1.82 meters at Tapajos and 1.23 meters at Reserva Ducke resulting in an average decrease of 4.1% of transect level biomass at Reserva Ducke and an average decrease of 3.5% at Tapajos.

Table 3.4 Transect live biomass and 95% confidence interval due to height uncertainty as calculated using the Monte Carlo analysis described in section 2.2: Statistical Analysis and Simulation.

Site	Transect	Biomass (Mg ha ⁻¹)	95% confidence interval
Tapajos km 83	1	344	20
	2	310	18
	3	350	21
	4	314	17
	5	263	17
	6	146	13
Tapajos km 67	1	267	18
	2	365	22
	3	318	22
	4	267	17
	5	339	21
	6	398	21
Reserva Ducke	1	361	19
	2	306	17
	3	336	19
	4	431	21
	5	373	20

Height Prediction via Allometry

The variability in the diameter and height ranges between sites was large, with maximum heights varying between 39 and 66 m, and maximum diameters ranging from 70 to 213 cm. This variability is indicative of some of the variation in site specific diameter to height allometries. Two of the sites evaluated are within the eastern-central Amazon region: Tapajos and Reserva Ducke; whereas the Cauaxí and Tanguro sites are within the Brazilian Shield according to the classification of Feldpausch, et al. (2011).

Pan-tropical and regional allometries resulted in substantial differences in estimated heights and biomass at both the individual tree and transect scales (Figure 3.4). At all sites, heights calculated using generalized allometries were compared with heights modeled using site-specific allometries based on all field measured heights. At Tapajos the pan-tropical and regional allometries estimated tree heights as 22% and 27% less than the field height based model, with percentages calculated by evenly weighting across all diameter classes. Pan-tropical and regional allometries performed better at Reserva Ducke. There, the height estimate based on the pan-tropical equation was 1% higher than the field height based allometry whereas the regional equation resulted in height estimates 12% lower.

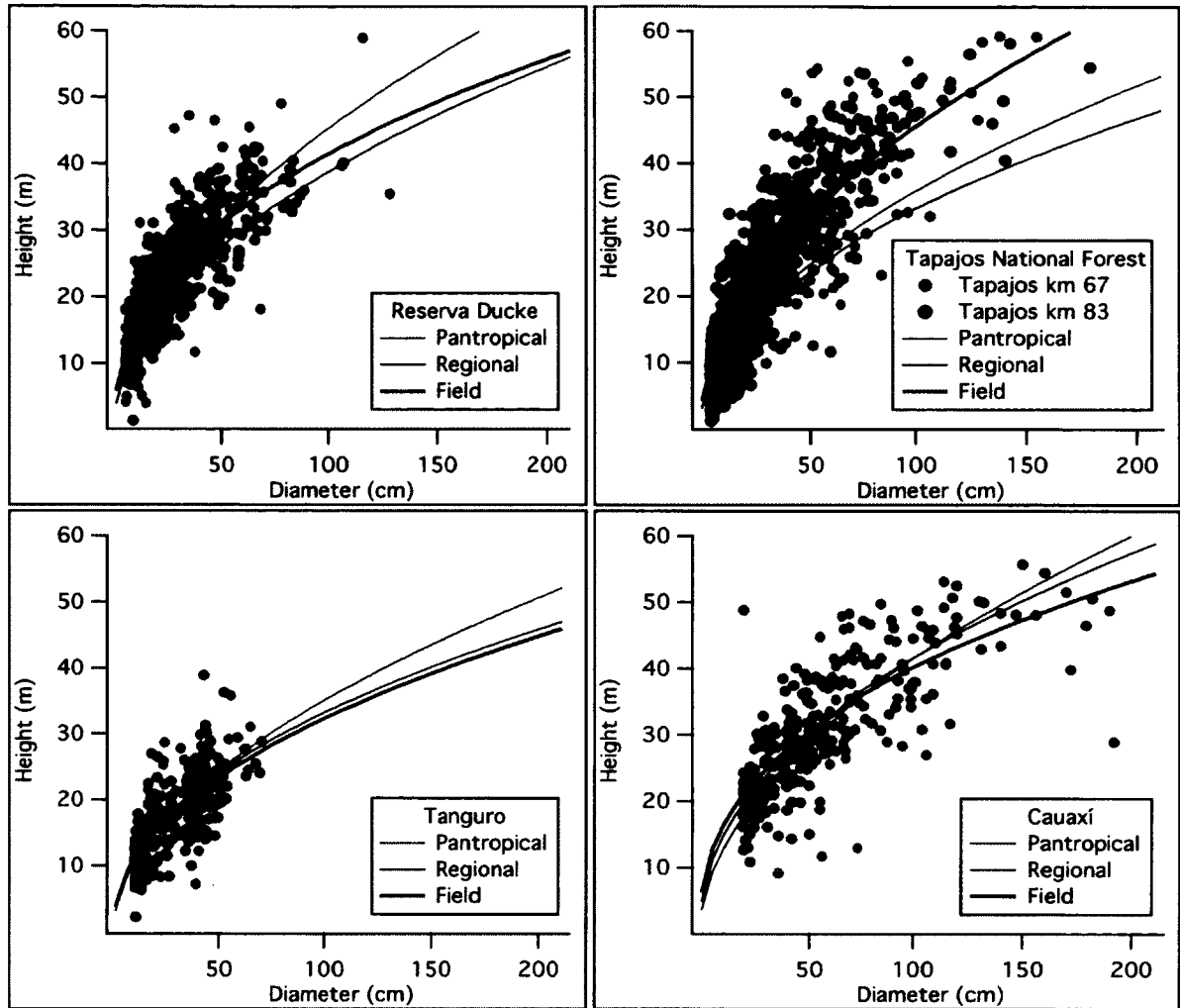


Figure 3.4 Comparison of allometric scaling relationships. Regional and pan-tropical allometries from Feldpausch et al. (2011) that include site-specific climatic and structural parameters (reported in Table 3.2 and Table 3.3, respectively) and a site-specific allometry (field) based on height and diameter measurements at all sites: Reserva Duce, Tapajos, Tanguro and Cauaxí.

At Tanguro and Cauaxí, both sites within the Brazilian shield, the generalized allometries performed well. At Tanguro, the pan-tropical equation fit the site extremely well, with an average height 0.3% higher than the field height based allometry. The regional equation also performed relatively well at this site, averaging a 4% over-estimation. At Cauaxí, the regional and pan-tropical equations also performed well, with heights 1% higher than the

field height based allometry using the regional equation and 1% lower when using the pan-tropical allometry.

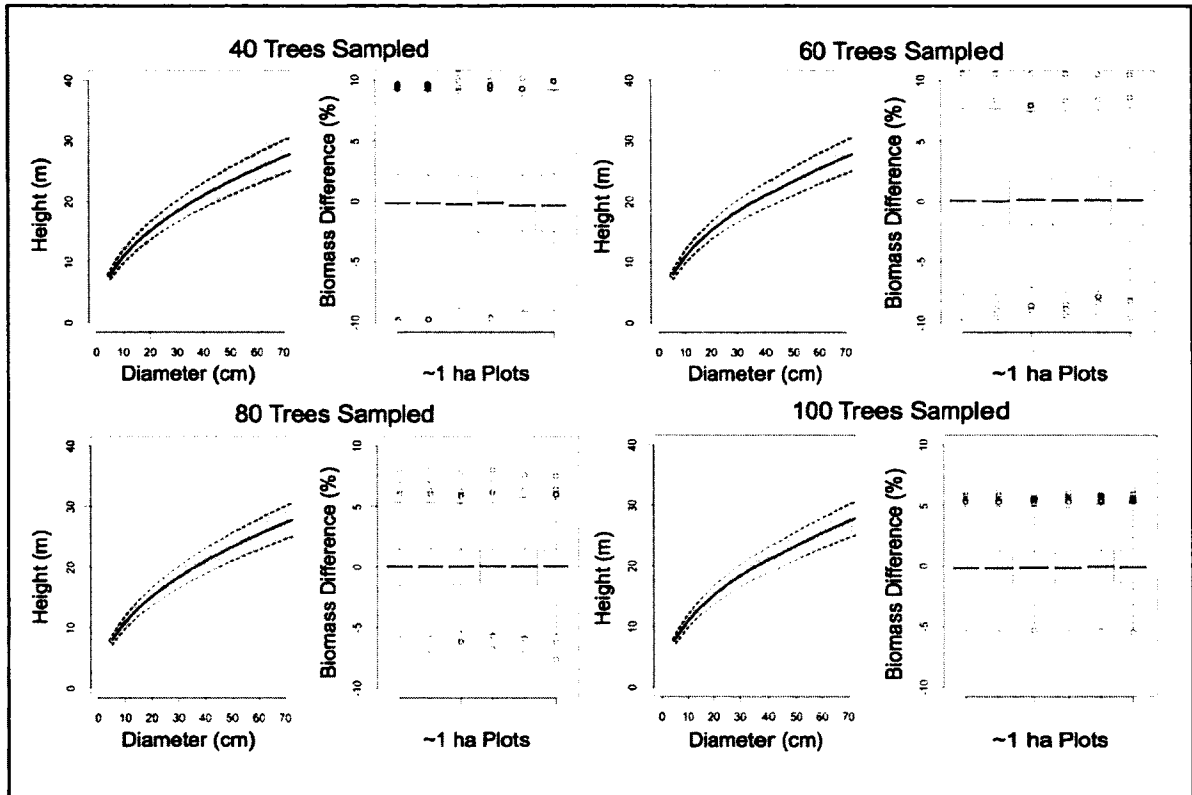


Figure 3.5 Effect of sample size on the resulting diameter-to-height allometric equation for Tanguro. Dashed lines represent a range of 10% difference in height. The grey area represents the range of bootstrap estimates. Boxplots show the variability in six 1 ha transect biomass estimates due to differences in the predicted tree height based on sample sizes of 40, 60, 80 and 100 stems.

Applying these height allometries to the estimation of biomass the regional Feldpausch allometry was 25% lower than the reference biomass at Tapajos and 12% lower at Reserva Ducke. The same allometry resulted in higher estimates of biomass at Tanguro (by 4%) and at Cauaxí (by 1%). The pan-tropical allometry resulted in lower estimates of biomass at Tapajos (by 21%), Reserva Ducke (by 1%) and Cauaxí (by 2%). This allometry yielded biomass estimates 1% above the reference value at Tanguro. Reference

biomass values were calculated using individual field measured tree heights at Tapajos and Reserva Ducke and site-specific allometries based on all field measured heights at Tanguro and Cauaxi (bold values in Table 3.3).

Optimization of Height Measurement for Biomass Prediction

We ask whether local measurements of height:diameter relationships are important to improve biomass estimates in tropical forests and if so, how much effort must be put into local estimation. Sample sizes of 40, 60, 80 and 100 trees were tested for each of the four sites. For each sample, an equal number of trees were chosen from each of four diameter classes (defined in section 3.2: Statistical Analysis and Simulations). A subset of 40 trees resulted in 95% confidence intervals of transect biomass of 7 - 10% across sites.

Increasing the sample to 100 trees decreased this variability to between 4 and 6% at all sites. As expected, as the sampled number of trees increased, the allometry became increasingly consistent with that found for all stems (Figure 3.5). Likewise, the variance in biomass estimates due to the differences in allometry converged.

3.4 DISCUSSION

We aimed to evaluate how precisely and how accurately we could measure tree height on the ground. We then evaluated how the uncertainty in tree height measurements translated into uncertainty in biomass estimates. Because height is important for biomass

estimation, we evaluated the accuracy of global or regional allometries. That evaluation suggests caution when employing those relations. We evaluated a labor-efficient alternative as we discuss below.

Height Measurement Precision

The variability in the field measured tree heights was significantly greater for trees above the mean canopy height. We note that the imprecision of height measurements causes a small error (5% to 9%, mean of 6%) in transect level biomass.

Most sources of height measurement error are pronounced for large trees. We recognize five sources of uncertainty that contribute to the precision of field height measurements. Issues in the field measurement of height are: offset between measured distance and crown top position, tree top occlusion, ground slope, obstacles for distance measurements, and clinometer operator error.

Differences between the distance measured and the true horizontal distance to the crown can cause an unbiased error in height measurement. It is equally likely that distances are overestimated as underestimated. In obvious cases, such as where the trunk was sloped, or the canopy was offset from the trunk location, we attempted to correct the distance measurement in the field. The uncertainty associated with displacement of crown tops

from trunk locations is most pronounced for the largest trees with large crowns (Andersen et al. 2006).

As the distance between the observer and the tree increases, visibility is reduced by surrounding vegetation resulting in tree top occlusion. This effect was most pronounced for large crowned trees with relatively flat crowns. For the ground-based observer, the flat-topped canopies of some broad leaf trees were indistinguishable from a more rounded shape, even at large distances without obstructions. The observer made assumptions about crown shape to approximate the total tree height. This error was reduced by increasing the distance from the tree and diminishing the extent that the view of the tallest crown point would be occluded by the crown itself.

Ground slope, if not properly accounted for, will cause a systematic overestimation of the distance between the observer and the stem measured. This overestimation of distance will result in an overestimate of height. This was only an issue for sites that were measured using a clinometer (Tapajos sites, Reserva Ducke, Tanguro). The laser range finder automatically corrects for slope when calculating horizontal distance. Of the four sites measured with a clinometer, only Reserva Ducke had notable slopes and for this site, the slope of the measurement tape was measured and the distance corrected.

The distance measurement is also affected by obstacles. When pulling a measuring tape through the forest it is necessary to weave through understory vegetation and other trees.

This will create a small bias towards over-estimating distance. Given that the individual making measurements must have a line of site with the trunk base, or a ground position directly beneath the canopy maximum, this line of site can also be used to pass the measuring tape. The measuring tape is always pulled taught and leveled before any reading is made to minimize the potential for overestimating distance.

Because of the perceived difficulty of measuring distance properly, many researchers prefer to use laser range finders or hypsometers (RAINFOR 2009, Chave 2005).

However, it is worthwhile to point out that replacement of the tape and clinometer with a laser range finder does not preclude two major sources of error, offset between measured distance and crown top position and tree top occlusion. Identifying the correct tree top position is the most difficult part of the measurement and the more sophisticated instrumentation does nothing to improve this situation. In addition, the laser range finder adds a source of error. Specifically, the presence of dense understory vegetation may lead to underestimation of the distance between the observer and the tree of interest because of intervening obstacles inadvertently hit by the laser beam (i.e. leaves, branches). This uncertainty led to our preference for direct measurement using a tape measure at the more recently studied sites.

As with any measurement, operator error may occur. The largest differences in repeat height measurement may have been cases of mistaken identity (the crown of one tree was thought to be another). In a comparison of multiple height measurement techniques,

Rennie (1979) showed that measurements made with clinometers were generally precise, but showed a slight underestimation bias for the tallest trees measured. However, when conducting a similar experiment Williams et al. (1994) showed a slight underestimation bias for small trees (less than 10 m) and an overestimation bias for tall trees (greater than 20 m). This overestimation bias was more pronounced for conifers than for all species, though the 95% confidence interval contained zero in all cases.

Recently, researchers have proposed an alternative method of height estimation ('the sine method') that does not require a horizontal distance measurement (Goodwin 2004). This measurement uses a single distance and angle measurement to the highest point on the tree crown using a laser range finder or hypsometer, and a second measurement of distance and angle to the tree base. The vertical component of each measurement can be calculated by the equipment used and added to yield the total tree height. Larjavaara and Muller-Landau (2013) compared this technique to the traditional tangent method used here and showed that the tangent method resulted in large errors, but unbiased results, consistent with results presented here. The sine method, however, resulted in underestimation of height by an average of 20%.

Height Measurement Accuracy

The errors that contribute to field height measurement precision likewise contributed to measurement accuracy. Errors due to slope and due to obstacles when measuring distance

will result in overestimation of the horizontal distance and lead to overestimation of tree height. Errors associated with the difficulty in seeing the tree top may result in underestimation or overestimation of tree height. To assess the accuracy of height measurement, field measured heights were compared with lidar estimated heights for emergent stems. Errors that contribute to lidar height error are: overtopping of canopy stems, geolocation error, and lidar measurement error (Popescu et al. 2002, Andersen et al. 2006, Ørka et al. 2010).

Overtopping of canopies will result in a positive bias for lidar heights. This bias is due to the use of the Canopy Height Model (CHM) for extracting lidar heights. In our study, this model filtered for the tallest returns within a given 1 m grid cell. By filtering for the highest points, only trees whose canopies are not over-topped by surrounding crowns or by taller vegetation are correctly measured (see Figure 3.1). This was taken into account when making comparison between lidar and field heights by only comparing emergent stems.

Error in lidar estimations of height are also expected due to error in crown position. Tree canopy positions were referenced to the trunk position, which was referenced to the transect. Transects were geolocated using a combination of differential GNSS and navigational GPS measurements. Errors are present in each of these components that may cancel or compound each other to affect canopy position. These errors will have the largest impact on the smallest crowns. Emergent crowns tend to have large canopies that

extend beyond the extent of location error. Emergent crowns average 6.2 m radius while the stem RMS error in horizontal position was about 5.7 m. This, in combination with the lack of local over-topping vegetation results in more accurate lidar heights for the tallest and largest canopies (i.e. emergent trees) compared to smaller, lower canopies.

The expected vertical uncertainty of the lidar instrument is 15 cm. The precision of field measurement was 3.8 m for trees within 10 m below the dominant canopy height, and greater than 8.2 m for trees above this height. Previous research has shown a consistent bias toward underestimation of height using lidar remote sensing in both broadleaf and coniferous trees. Gaveau and Hill (2003) showed an underestimation of 2.1 m for broadleaf trees, and Ronnholm et al. (2004) showed an underestimation of 0.7 - 1.4 m somewhat dependent on tree species (Gaveau and Hill 2003, Rönholm et al. 2004, Wang and Glenn 2008). Clark et al. (2004) found similar results for a tropical forest in Costa Rica. Gaveau and Hill (2003) showed that this underestimate of height is likely due to penetration of the lidar signal into the upper section of the canopy. However, this potential bias is small when compared to the uncertainty in field estimates of canopy tree height.

Our field heights were consistently higher than lidar heights for emergent trees. This is consistent with Williams (1994) results showing height measured with a clinometer to be biased about 1 m high on average for trees over 20 m, and in opposition to the results of Rennie (1979) showing a slight low bias. This result is also consistent with results

showing underestimation of height based on lidar CHMs due to penetration of the outer canopy surface (Gaveau and Hill 2003). Whether this difference is due to true overestimation of height in the field or due to lidar penetration is unclear. This 1-2 m potential bias represents a difference of less than 6% of the mean height of emergent trees.

The accuracy and precision of lidar and field measured heights further affects our ability to measure changes in height over short time spans. Where lidar data is available it provides a more accurate source of height information for canopy and emergent stems. This improved accuracy and precision reduce the variability in height measurement. Given that height growth in gaps is greater than 1 m y^{-1} (Fredericksen and Pariona 2002), significant changes in height should be distinguishable over shorter time spans using lidar as compared to field data once trees exceed a maximum height accessible by extensible measuring poles (10 to 15 m).

Biomass Precision

The effect of height imprecision on biomass is approximately 6% and the effect of potential inaccuracy on biomass is smaller (4.1% at Reserva Ducke and 3.5% at Tapajos) despite the large uncertainty in the height of tall trees (8 - 10.5 m for trees greater than 34 m). The uncertainty in biomass on the plot basis is less than the uncertainty of height in the largest trees partly because the measurement errors cancel each other out. More

importantly, the errors are greatest for the largest trees and most biomass was in medium-statured trees (canopy stratum) that had smaller relative error in height measurements.

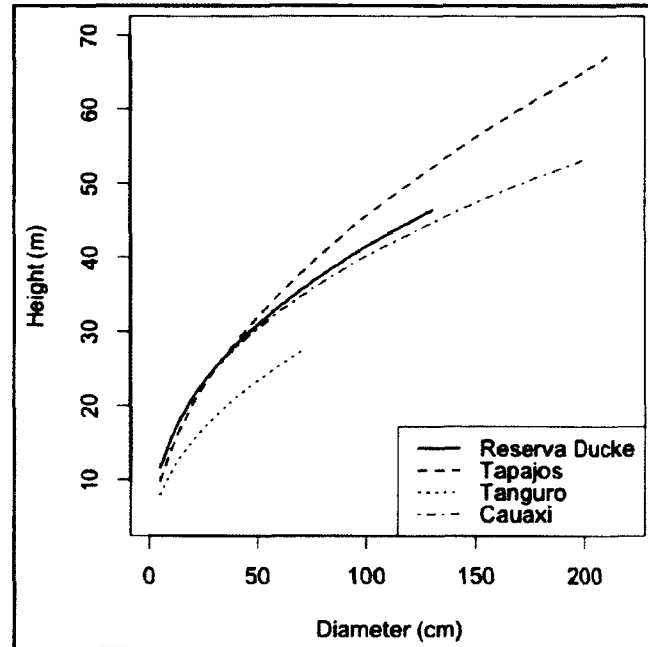


Figure 3.6 Comparison of site-specific diameter-height allometries for the four study areas.

Height has been repeatedly shown to improve biomass estimates as compared with diameter only in allometric relations for tropical forest trees (Maia Araújo et al. 1999, Chave et al. 2005, Vieira et al. 2008, Feldpausch et al. 2012, Lima et al. 2012). This result is obvious from inspection of height:diameter relations (Figure 3.6). All four areas studied here are moist tropical forests within the Brazilian Amazon but their diameter:height allometries vary significantly. Some of this variability in diameter-height allometries is believed to be due to climatic variability (Feldpausch et al., 2011). Tree architecture and variable species assemblages are also important drivers. Vieira et al. (2008) used two diameter-only allometries to estimate biomass in the Brazilian Atlantic

forest (Chave et al. 2005 and Chambers et al. 2001) and found overestimates of biomass by 52% and 68% respectively.

Table 3.5 Above-ground biomass estimate based on various allometries for the field sites detailed here. The two Tapajos sites (Tapajos km 67 and Tapajos km 83) are combined due to minimal difference in site-specific allometries. The biomass allometries applied are the Chave et al. (2005) Model I allometry including wood density, diameter and field measured tree height (“Field Ht”); the Chave et al. (2005) Model I allometry with site-specific model of diameter:height (“Modeled Ht”); the Chave et al. (2005) Model II equation without a height term (“Chave - D”); the Chambers et al. (2001) allometry based purely on diameter; the Chave et al. (2005) Model I allometry including height modeled using the Feldpausch et al. (2011) regional equation (“Regional”), and the Chave et al. (2005) Model I allometry including height modeled using the Feldpausch et al. (2011) pantropical height allometry (“Pantropic”). Percent difference from the field height value is shown for Reserva Ducke and Tapajos, and from the modeled height for Tanguro and Cauaxi. This is referred to as the reference case in the text and emboldened here.

Site	Field Ht	Modeled Ht	Chave - D	Chambers	Regional	Pantropic
Reserva Ducke	361	363 (+1%)	382 (+6%)	346 (-4%)	317 (-12%)	358 (-1%)
Tapajos	307	312 (+2%)	317 (+4%)	277 (-10%)	231 (-25%)	243 (-21%)
Tanguro	NA	121	170 (+40%)	184 (+52%)	126 (+4%)	122 (+1%)
Cauaxi	NA	328	360 (+10%)	261 (-21%)	331 (+1%)	322 (-2%)

We compared a number of approaches to biomass estimation using both height and diameter information for the four areas in our study (Table 3.5). Applying diameter only equations to estimate biomass led to variation of between 4% to 52% from our reference case (Table 3.3, bold values). The largest effect was found at Tanguro, which has the smaller stature of a transitional forest. Other areas generally showed differences of less

than 10%, though the Chambers et al. (2001) allometry performed significantly worse at Cauaxí.

Height Allometries

We evaluated the overall accuracy of the Feldpausch et al. (2011) regional and pan-tropical height allometries based on only four areas. In three cases the relations worked well but based on the substantial differences at one of the four areas we advise caution when applying generic diameter:height allometries. A sensitivity analysis conducted for Tapajos shows the inaccuracy in the diameter to height allometry is caused by variation in climatic variables, most importantly, dry season length. Applying the climatic variables specific to Manaus (which has a significantly shorter dry season) curiously yielded a better fit to the Tapajos data. This suggests that the inclusion of climatic parameters may not be universally advantageous.

The potential for inaccuracy of regional and pan-tropical allometries suggests that site-specific allometries are preferable for accurate estimates of biomass. When formulating site-specific allometries it is necessary to take into account the distribution of biomass at the site. The sampling scheme described in the methods section weighs diameter classes by their proportional biomass. The weighting scheme presented was applicable to all areas despite the variability in diameter ranges. Site-specific allometries estimate biomass

within 2% at Reserva Ducke and Tapajos compared to our reference case where all tree heights were measured.

Height Allometric Optimization

Given the potential for error using regional diameter:height allometries and the importance of height in estimating biomass it is advantageous to have site specific diameter:height allometries. Because height measurements are time consuming, it is important to minimize the number of height measurements necessary to define an allometry to within a target uncertainty. Sample sizes tested were limited by the small number of trees in the largest diameter classes. While allometries fit to Tapajos data were well constrained at the largest diameter sizes, allometries fit to data from Reserva Ducke were not. However, the variability in predicted height for the largest diameter stems made little difference in the predicted biomass at the transect scale due to the extremely small number of individuals in the largest classes. The RAINFOR network has recommended a stratified sample for measuring heights (RAINFOR, 2009) with height measurements for a total of 40 trees divided equally between four diameter classes: 10 - 20 cm, 20 - 30 cm, 30 - 50 cm, and > 50 cm. This smaller sample size would result in a 95% confidence intervals of transect level biomass approximately twice that of the 100 tree sample suggested here (see Figure 3.5).

3.5 CONCLUSIONS

We found that the precision of height measurements of individual trees ranged from 3 to 20% of total height, leading to a mean error of 16% in the estimate of individual tree biomass. When scaled to the plot level, this lack of precision of height measurements led to 5 - 6% uncertainty in overall plot biomass. Ground based measurements of height exceeded airborne lidar measurements of height by an average of 1.4 m. Whether this is due to overestimation of field height or underestimation by lidar, or a combination of these factors is unclear. If this represents a positive bias in field height, then overall plot-level biomass based on field measurements would be biased 4% high.

The use of diameter-based allometries, including pan-tropical and regional height-diameter relationships led to large biases for individual site biomass when compared to local field height measurements (Figure 3.4): -25% and -12% at Tapajos and Reserva Ducke respectively using the Feldpausch regional allometry. The pan-tropical allometry performed better at Reserva Ducke (-1%), but maintained a large bias at Tapajos (-21%). For other sites, the regional and pan-tropical allometries were within 4% of field-based height:diameter relationships. We recommend caution when employing regional and global relations and suggest that field work can be optimized by measuring the height of approximately 100 individuals to build a site specific height-diameter allometry. This approach reduced the potential uncertainty in the biomass of 1 ha plots due to the diameter:height allometry to an average of 4.5% for all sites studied (Figure 3.5).

Regional and global biomass estimates (e.g. Asner et al., 2011; Baccini et al., 2012; Saatchi et al., 2011) that use remote sensing and statistical algorithms for scaling ultimately depend upon the measurements of individual trees. Tree biomass estimates rely on field height measurements or estimates based on diameter-height allometries. Based on our work at sites in the Brazilian Amazon it is unclear whether heights of trees above mean canopy height were biased or merely imprecise. The majority of sources of field height error tend toward overestimation of height, whereas lidar has been shown to underestimate height. This potential bias in field height results in an overestimate of biomass by about 4%. This bias is small considering all of the uncertainties involved in field biomass estimates and is drawn from a limited set of measurements. However, given the availability of airborne lidar height estimates at an increasing number of tropical field sites, we recommend further investigation of this potential bias because of the important role of tropical forests in the global carbon cycle.

3.6 ACKNOWLEDGEMENTS

The authors would like to thank Ted Feldpausch and two anonymous reviewers for their help in improving this manuscript. This research was supported by NASA grants NNG06GE11A, NNX09AI33G, NNG04G073G and NNX06AH36G, NSF grant DEB0721140 and USAID Sustainable Landscapes.

3.7 AUTHOR CONTRIBUTIONS

Maria Hunter conceived of the research, conducted the field work at Tapajos and Reserva Ducke, completed the data analysis and was the primary author of all writing. Daniel Victoria contributed code that transformed calculated crown positions and extents into polygons and extracted lidar statistics for each polygon. Michael Keller helped develop the concept, design field work, and edit the manuscript. Douglas Morton helped develop the concept and edit the manuscript.

CHAPTER FOUR

STRUCTURAL DYNAMICS OF TROPICAL MOIST FOREST GAPS

Dissertation chapter accepted with minor revisions to PLoS ONE in collaboration with M. Keller, D.C. Morton, B. Cook, M. Lefsky, M.J. Ducey, S.R. Saleska, R.C. de Oliveira Jr., and J. Schiatti.

4.0 ABSTRACT

Gap phase dynamics are the dominant mode of forest turnover in tropical forests. However, gap processes are infrequently studied at the landscape scale. We used multi-temporal lidar data covering 1000 ha split between two sites, the Tapajos National Forest and Reserva Ducke in the Brazilian Amazon to study gap dynamics. We defined a gap as an area of significant growth, that corresponds to areas $> 10 \text{ m}^2$ with height less than 10 m. Applying this definition to repeated lidar acquisitions at two sites, we found over twice as much area in gap at Tapajos National Forest (4.8 %) as compared to Reserva Ducke (2.0 %). On average, gaps were smaller at Reserva Ducke, and closed slightly more rapidly, with estimated height gains of 1.2 m y^{-1} versus 1.1 m y^{-1} at Tapajos. Gap centers showed the same overall height change as all gap areas at Reserva Ducke, but show slight variation at Tapajos (1.3 m y^{-1} versus 1.1 m y^{-1}). These rates accounted for

the interplay between gap edge mortality, horizontal ingrowth and gap size at the two sites studied. We estimated that approximately 10% of gap area closed via horizontal ingrowth at Reserva Ducke as opposed to 6% at Tapajos National Forest. The comparative effects of height loss (interpreted as damage and/or mortality) and horizontal ingrowth into gaps were similar at Reserva Ducke, whereas height loss at gap edges had a comparatively stronger effect at Tapajos. Both sites demonstrate an increase in the likelihood of mortality in the immediate vicinity (~6 m) of existing gaps or gap contagiousness.

4.1 INTRODUCTION

Gaps are a prominent feature on the tropical forest landscape and key to the dynamics and species distribution of tropical forests (Brokaw 1985, Denslow 1987, Molino and Sabatier 2001). Gap phase dynamics maintain high light environments within closed forest canopies and promote natural regeneration and turnover (Bormann and Likens 1979, Oliver and Larson 1996). While the dynamic processes of regeneration and turnover of individuals and species are the ecological rationale for the study of gaps across the landscape, gaps are often treated as static environments defined in terms of light availability or vegetation height (Whitmore et al. 1993, van der Meer et al. 1994).

The majority of tropical forest turnover occurs via small to medium gaps caused by single trees or small groups of trees (Brokaw 1982). In the Brazilian Amazon, natural

catastrophic disturbances that destroy understory vegetation such as large-scale fire and wind-throw events are rare (Cochrane 2003, Espirito-Santo et al. 2010). One method of describing the structural development of forest regeneration following disturbance is that of Oliver and Larson (1996). Their methodology includes four stages: stand initiation from existing seed-banks or advanced regeneration, stem exclusion via density-dependent mortality, understory re-initiation and old-growth. Although this work was focused on temperate forests, processes described are similar in the tropics (Brokaw and Busing 2000). Stand establishment is typically most rapid when it is formed from advanced regeneration existing prior to the disturbance event (Franklin et al. 2002). The growth of advanced regeneration is one method of gap closure. However, small gaps may also close via horizontal ingrowth of surrounding vegetation.

Gaps are environments where high light conditions promote high growth. But gaps are not only changing environments themselves, but promote change in the surrounding forest. Ray and colleagues (Ray et al. 2005) showed that gaps change the microclimate of their immediate area as well as the surrounding forest. The change in the outer canopy surface also promotes the penetration of wind into the forest understory (Laurance et al. 1998). It has been hypothesized that this increased wind in combination with uneven growth of tree canopies may result in increased mortality of trees surrounding gaps, or gap contagiousness (Jansen et al. 2008).

For measurement purposes, gaps in the forest matrix must be defined by vertical and horizontal limits (van der Meer et al. 1994). The vertical limit is a maximum vegetation height, and the horizontal is the minimum gap size. The selection of these limits has usually been determined by feasibility of field measurements as opposed to the dynamics of forest structure. Considering the ecological importance of gaps, a gap definition should include areas of forest canopy below the dominant canopy height that receive abundant light to promote rapid growth.

Variability in gap definition leads to difficulty in comparing between gap studies, and calculated metrics (van der Meer et al. 1994). Two common gap definitions based on fieldwork are those proposed by Brokaw (1982) and Runkle (1981). Brokaw gaps are defined as openings in the forest canopy that extend to two meters above the ground (Brokaw 1982). The gap perimeter is defined by the innermost point reached by foliage at the two meter height, and is measured in at least eight directions. However, an opening can meet this definition despite a small tree or thin branch extending into the gap. Runkle (1981) defines a gap as an opening in the forest canopy that extends to the base of surrounding canopy trees. Canopy trees are typically classified as those above 20 m in height. This definition was designed to capture regions with expected changes in light environments, including areas directly and indirectly affected by the canopy opening. Independent of the definition used, field studies of gaps generally cover small areas and are unlikely to capture large, infrequent gaps.

Landscape scale studies typically use satellite-based remote sensing that cannot resolve small and medium sized gaps (Chambers et al. 2009, Negron-Juarez et al. 2011, Chambers et al. 2013). Studies using Landsat show limited success in estimating gap fraction at the pixel level (approximately 0.1 ha) but fail to capture gaps of the smallest sizes (Asner et al. 2002, Negron-Juarez et al. 2011). At higher resolution, passive optical images such as IKONOS are complicated by the presence of shadows (Asner 2003, Espirito-Santo et al. 2014b). Passive optical imagery also has to contend with the problems presented by clouds, which are prevalent in the humid tropics. At the other extreme, field plots rarely capture areas greater than 1 ha. The Center for Tropical Forest Science (CTFS) affiliated with the Smithsonian Institution operates a network of field plots, of which the largest are 50 ha (Hubbell and Foster 1986, Muller-Landau et al. 2006). Although these are significantly larger than the majority of field plots, they are still not large enough to capture landscape scale patterns of disturbance and recovery (Hubbell et al. 1999, Nath et al. 2006).

A promising method for analyzing both gap percentage and gap size distributions is high-resolution active remote sensing. Lidar (light detection and ranging or laser scanning) is an active remote sensing method that can collect multiple ranging measurements per square meter and provides highly accurate height information. It has been used to successfully describe surface canopy roughness and forest structure at varying scales (Drake et al. 2002a, Lefsky et al. 2002, Frazer et al. 2005). Recently, lidar has been used

for tropical gap studies, for example, to examine size frequency distributions over large areas (400 - 125000 ha) (Kellner et al. 2009, Asner et al. 2013, Lobo and Dalling 2014).

Using lidar data, height thresholds define gaps. For example, applying the Brokaw definition to lidar remote sensing classifies continuous regions of the canopy height model with height of less than 2 m (Kellner and Asner 2009, Boyd et al. 2013, Asner et al. 2013). It is not expected that this would yield similar results as field studies because it is not practicable to allow for exceptions such as small trees or thin branches. Also, the primary justification for using the Brokaw gap definition, its convenience for field application, is not applicable in the case of lidar remote sensing. We seek an alternative definition that accounts for the structural dynamics of the forest, and is easy to apply to multi-temporal lidar data.

To develop a gap definition based on structural dynamics it is important to understand patterns of growth. Limited information is available on the rate of height regrowth in tropical forests, especially in naturally formed gaps. Field studies that have been conducted typically focus on a few dominant or pioneer species as opposed to properties of the gap as a whole (Brokaw 1987, De Steven 1988, Whitmore and Brown 1996). An alternative to tracking individual tree growth is to estimate mean growth rates to predict gap closure over time. Lidar is particularly well suited to this task as it measures height accurately, and can cover large areas (Vepakomma et al. 2011). The high resolution of

airborne lidar allows for measurements of individual tree growth and mortality as well as generalized views of the forest structure.

Tapajos National Forest and Reserva Ducke are intensively studied field sites within the Brazilian Amazon (Chauvel et al. 1987, Keller et al. 2004, Vieira et al. 2004, de Castilho et al. 2006, Pyle et al. 2008). While no study of small gap dynamics has been conducted at Reserva Ducke, recently a paper was published using IKONOS imagery covering 167 ha of Tapajos National Forest (Espírito-Santo et al. 2014b). In 2008, airborne lidar was collected over both sites (Stark et al. 2012), with a second airborne lidar data collection approximately four years after the initial collection covering approximately 400 ha of Tapajos National Forest and 600 ha of Reserva Ducke. We apply this data to analyze gap presence, formation and closure at the landscape scale. Our goals are to define the rate of gap formation, the size frequency, distribution and regrowth rates of gaps at these two contrasting forest areas by asking the following questions:

- What is an ecologically appropriate definition for gaps at the two sites?
- What is the distribution of gap area and gap size at two sites in the Brazilian Amazon?
- What is the frequency of gap creation and how long do gaps persist within a landscape?
- How does the frequency of gap creation compare to field estimates of mortality?
- Are gaps contagious?

4.2 METHODS

Site Descriptions

We analyze data from two sites within the Brazilian Amazon to answer the questions posed above. These two sites have been frequently studied, but no comprehensive analysis of gap dynamics has been completed at these sites on a landscape scale.

Tapajos National Forest

The Tapajos National Forest (54°57'W 2°51'S) is a 550,000 ha reserve situated within the state of Pará, Brazil along the eastern shore of the Tapajos River. The reserve is primarily upland forest, and includes patches with canopy level palms. The dominant soils are nutrient-poor, clay, Oxisols (Silver et al. 2000). A pronounced dry season lasts approximately five months, from July - December (Vieira et al. 2004). Personal observations suggest that gap creation events occur more often during the wet season, consistent with other neotropical forests (Brokaw 1985). This is supported by the finding of Espirito-Santo (Espírito-Santo et al. 2014b) that showed the most frequent form of mortality is snapped trunks, associated with the high winds of the rainy season. However, inventories of coarse woody debris production did not show a strong seasonal pattern (Palace et al. 2007).

Reserva Ducke

Reserva Ducke (59°57'W 2°57'S) is a 10,000 ha forest preserve managed by the National Institute for Amazon Research (INPA) bordering the city of Manaus, in the state of Amazonas, Brazil. The reserve is covered by upland terra firme forest with a large number of understory palms and occasional canopy level palms, especially in seasonally waterlogged valleys. The soils vary with the rolling topography (30 - 120 m.a.s.l.) with Oxisols dominant in upland areas, Ultisols on the slopes and Spodosols in the valleys (Chauvel et al. 1987). These soils are acidic and low in nutrients. There is a short dry season, lasting 1 - 3 months, generally occurring from July through September. Standing death is the dominant form of mortality (54%) followed by snapping and uprooting (de Toledo et al. 2012).

Airborne Lidar Data

Airborne lidar data was collected in 2008 with a minimum required data density of 10 returns per m² and actual mean return densities at each site near 40 returns per m². A second airborne lidar data set was collected using a different lidar system in February 2012 at Reserva Ducke, and August 2012 at Tapajos National Forest (Tapajos) (Table 4.1) with a minimum required data density of 4 returns per m². The resulting time between sampling periods was 44 months at Reserva Ducke and 48 months at Tapajos. The total

area available for multi-temporal analysis was 398 ha at Tapajos and 603 ha at Reserva Duce.

Table 4.1 Details of airborne lidar data collections.

Data Characteristics	Initial Collection		Final Collection	
	Tapajos	Res. Duce	Tapajos	Res. Duce
Lidar System	Leica ALS50-II	Leica ALS50-II	ALTM 3100EA	ALTM 3100EA
Flight Altitude	700 - 900 m	700 - 900 m	600 m	600 m
Divergence	15 mrad	15 mrad	25 mrad	25 mrad
Footprint Size at nadir	10 cm	10 cm	15 cm	15 cm
Pulse Frequency	118 kHz	118 kHz	50 kHz	50 kHz
Acquisition Date	06-07/2008	06-07/2008	08/2012	02/2012
Minimum return density (m ⁻²)	10	10	4	4
Ground return density (m ⁻²)	0.44	0.83	0.49	0.19

Canopy height models (CHMs) and Digital Terrain Models (DTMs) were produced using the processing methods developed for NASA Goddard’s Lidar, Hyperspectral, and Thermal Airborne Imager (G-LiHT) (Zhang et al. 2003, Cook et al. 2013). This methodology separated vegetation and ground returns to develop a gridded representation of the ground surface (DTM) and height estimates of lidar returns from canopy and understory vegetation (CHM). Data for the Tapajos site were processed separately for each data collection. At Reserva Duce, we produced a unified DTM based on both year’s data (St-Onge and Vepakomma 2004, Vepakomma et al. 2011). This processing

approach provided the most robust estimate of ground topography from which to generate CHM data layers (1 m resolution) for each year. For Tapajos, the differences among years were trivial and it was not necessary to produce a unified DTM.

Field Surveys

Diameter-dependent line sampling was conducted along six 500 m transects at Tapajos National Forest and five transects at Reserva Ducke. Initial field surveys were conducted in June 2009 (Tapajos) and October 2009 (Reserva Ducke) and over 1000 trees were sampled at each location (Hunter et al. 2013). Permits for field work were obtained from the Instituto Chico Mendes (ICMBio) for work conducted at Tapajos National Forest and Instituto Nacional de Pesquisas da Amazônia (INPA) for work at Reserva Ducke. Live trees as well as standing dead greater than 5 cm diameter were included in each survey. For all living stems the crown radius was measured in each of four cardinal directions. The mean crown radius was calculated and a circular crown area estimated for each stem. The mean crown radius per site was calculated by multiplying each crown radius measurement by the numbers of trees per hectare that a given tree represents. Transects were resampled in July 2011 at Tapajos National Forest and October 2011 at Reserva Ducke. Percent mortality was estimated from trees that died between samples and corrected to an annual value. The fraction of fallen versus standing dead trees was estimated based on the height measurements for dead stems. A non-parametric bootstrap

analysis (Efron and Tibshirani 1994) was used to calculate 95% confidence intervals of annual mortality.

Height Structure

Distributions of canopy heights were compared for all sites and years. The height structure of the canopy was investigated using a random sub-sample of 1000 heights from each CHM, and comparisons between years were repeated 1000 times. Comparisons were also made between sites using the same technique. Sites and years were tested for significantly different height structures with a two-sided Kolmogorov-Smirnov test (R version 3.0.1). P-values reported are the average of 1000 tests.

Gap Definitions

We defined a gap using a dynamic measure of height change and a static minimum horizontal extent. We refer to this *dynamic gap* as a region characterized by significant vertical growth that accounts for the transient nature of gaps and the high light environment that exists at low canopy heights (see results). Expected vertical height change was determined by initial canopy height. To examine the height change at both sites while minimizing the effect of spatial autocorrelation we took a randomly distributed subset of 60 pixels from each initial integer height. At the most infrequent heights this is approximately a 1% sample. Tukey's HSD test was used to compare height

changes between initial height subsets. We compare this definition to the Brokaw (Brokaw 1982) definition, because the latter has been most commonly used.

The minimum horizontal gap area applied to both definitions was based on the average crown area of all trees greater than 5 cm diameter based on the living trees surveyed at both sites in 2009.

Distribution of Gap Areas

Both the Brokaw and dynamic gap definitions were applied to CHMs for each year and site. This was done by first classifying each CHM raster into gap and non-gap pixels. Gap pixels were then transformed into polygons, and those with areas of less than the minimum gap size were removed from analysis.

Gaps classified in each temporal acquisition were then used to calculate the size frequency distribution of gaps following a modified application of Clauset et al (2009). This technique fits gap size distributions to a power-law using a maximum likelihood estimator (Gloor et al. 2009, Chambers et al. 2009, Lloyd et al. 2009) and a fixed minimum gap size.

Gaps were also tested for the degree of spatial autocorrelation using Moran's I (Arc 10.1) an index that ranges from -1 (indicating perfect dispersion) to 1 (perfect correlation), with zero representing near perfect randomness.

Gap Creation and Lifetimes

New gap areas were analyzed in terms of their total area and the gap recurrence interval (t_{r1}) was calculated using Equation 4.1.

$$t_{r1} = t_s \frac{A_{undisturbed}}{A_{gap}} \quad \text{Eq 4.1}$$

$$t_{r2} = t_p \frac{A_{total}}{A_{gap}} \quad \text{Eq 4.2}$$

Equation 1 accounted for the non-gap area ($A_{undisturbed}$) that became gap (A_{gap}) over the sampling period (t_s). However, this excluded disturbances that could have both formed and closed between samples. We compared gap recurrence intervals calculated using equation 1 with recurrence intervals estimated using data from each of the individual time periods (t_{r2}) (Equation 4.2). In that case, the persistence time (t_p) was substituted for the sample period and the full acquisition (A_{total}) was used to calculate the ratio of sampled area to disturbed area.

Persistence time (t_p) was calculated as the gap height cutoff divided by the mean height change per year. The mean height change per year was calculated using all height change

measurements within gap areas (both height gain and height loss). Persistence times were calculated applying both the Brokaw (Brokaw 1982) gap definition and the dynamic gap definition.

In order to examine gap closure, the height change of each gap pixel between final and initial survey times was analyzed. To separate horizontal encroachment from vertical growth into gap areas on changing canopy height, the innermost section of gaps were separately classified for each site. The gap centers were defined as areas more than 5 m from the gap edge at Reserva Ducke where smaller gaps are prevalent and more than 10 m from the gap edge at Tapajos. These distances were more than twice the amount of lateral growth measured in temperate forests over a comparable time period (Runkle and Yetter 1987). Collecting these gap center pixels, the mean and standard deviation of height change were calculated. Maximum vertical growth was conservatively estimated as any change in height less than the mean plus three standard deviations. This captures 100% of the data at the gap center, and is consistent with the assumption that horizontal ingrowth was not possible at large distances from gap edges. Change in height that exceeded expected maximum vertical growth was assumed to be caused by horizontal ingrowth. Areas of height loss were excluded from this analysis, as these were considered evidence of repeated disturbance in gap areas. The proportion of area within each growth category (horizontal ingrowth, vertical growth and height loss) was compared with distance from gap edge and gap size.

Gap Contagiousness

We defined gap contagiousness following Jansen et al. (Jansen et al. 2008) as the increased risk of disturbance around existing gaps. Jansen et al. (2008) specifically hypothesized that: (1) Canopy disturbance risk decreases with increasing distance from gaps; (2) Canopy disturbance risk is elevated in the edge zone of existing gaps; and (3) Gap bordering trees have increased risk of mortality.

To assess whether canopy disturbance risk decreases with increasing distance from gaps or is elevated in the edge zone of existing gaps, we first calculated the minimum distance between all non-gap pixels and the nearest gap in the initial acquisition. We then separated the distances to pixels classified as gaps in the 2012 lidar data collections. The frequency of each distance was calculated, and the distribution of distances to new gap pixels was subtracted from the distribution of distances across the acquisition. A Kolmogorov-Smirnov test was applied to test the second hypothesis.

Jansen, et al. (2008) originally applied these three hypotheses to field data on 5660 trees greater than 10 cm diameter collected over a 12 ha area. Because we do not have field data for the full extent of the lidar data collection we applied a modified test for the third hypothesis. As opposed to testing the effect of gaps on all stems, we tested the effect of gaps on emergent stems (greater than 40 m tall) so that canopies and partial canopies that were present in 2008 but not in the second data collection were tallied. Canopies for

which any point was within 10 m of gaps in the 2008 data set were considered to be near gaps.

4.3 RESULTS

Variability of Forest Structure

The canopy surface (maximum vegetation height per pixel) at Reserva Ducke had a near Gaussian distribution with a mean canopy height of 26 m (Figure 4.1). In contrast, Tapajos National Forest had a skewed distribution of heights that was significantly different from the distribution of heights at Reserva Ducke (KS-test p-value $< 2.5e-12$). The dominant canopy at Tapajos National Forest was between 35 m and 40 m, but there was a sub-dominant layer that shows near equal frequency from 15 - 30 m (mean of 28 m). Both the mean canopy height and the 99th percentile canopy height were higher at Tapajos (99th percentile height of 54 m as opposed to 49 m). Canopy height distributions were not significantly different between time periods (KS-test p-values > 0.05 for both sites). The difference in canopy structure may reflect the difference in mortality rates between the two sites. Annual mortality at Tapajos was estimated from field surveys as 2.1% with a 95% confidence interval of 1.5% - 2.8%. At Reserva Ducke, annual mortality was 1.4%, with a 95% confidence interval of 0.8% - 2.2%.

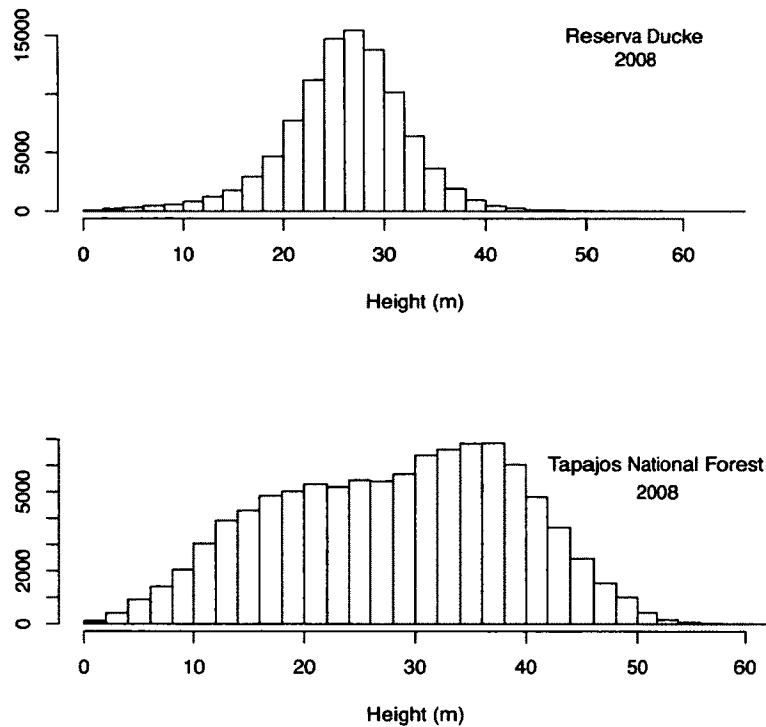


Figure 4.1 Distribution of canopy surface heights in 2008 airborne lidar acquisitions. Shown for (a) Reserva Ducke and (b) Tapajos National Forest.

Height Change

Height change between the initial and final lidar data collections varied with the initial vegetation height (Figure 4.2). The mean height change decreased exponentially with increasing initial height and became consistently less than zero above 20 m initial height at Tapajos National Forest and 18 m at Reserva Ducke.

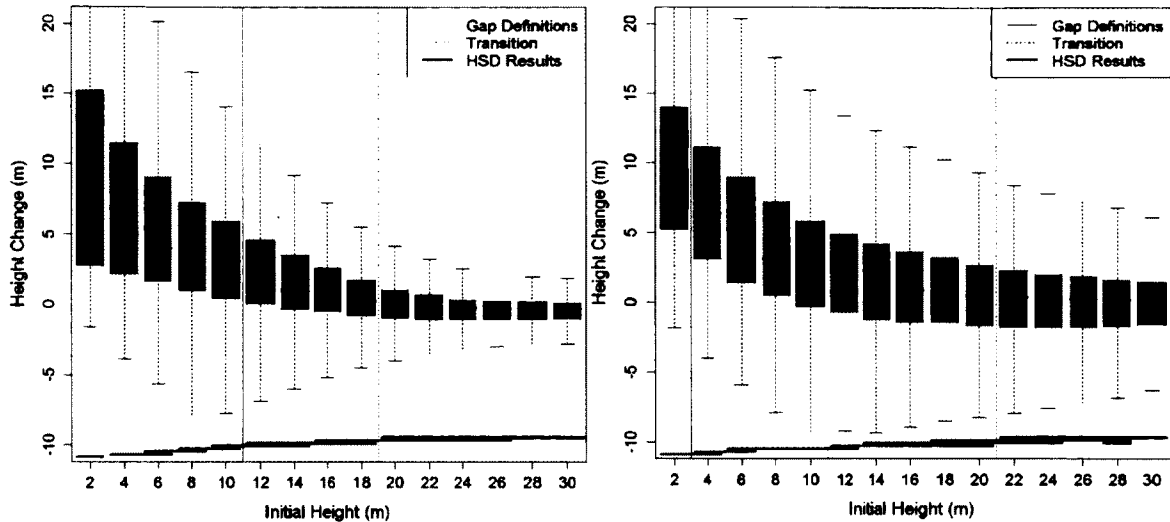


Figure 4.2 Mean and confidence interval of height change between initial and final lidar data acquisitions. Data collected at (a) Reserva Ducke and (b) Tapajos National Forest overlaid with the Brokaw (1982) and dynamic gap definitions' height cutoffs, and the transition height where height change is not significantly different from zero based on Tukey's HSD (horizontal segments at the base of the figure). Each horizontal line displaying Tukey's HSD results spans initial height bins for which there is no significant difference (p -value > 0.05).

Dynamic Gap Definition and Minimum Gap Size

Similar to traditional gap definitions, we used a height cutoff to determine gap areas.

Moving from the top of the canopy down, we examined the distribution of height change for each initial canopy height bin. The transition height was defined as the tallest initial height with a positive mean height change (20 m at Tapajos National Forest and 18 m at Reserva Ducke). We then compared the distribution of height change of all lower initial height bins with the transition height (Figure 4.2). We defined the height cutoff for our dynamic gap definition as the tallest initial height that showed significantly greater change in height than the transition class (Tukey's HSD p -value < 0.05). In other words,

these were the areas showing a statistically significant signal of height increase. This cutoff height was 10 m at both Tapajos National Forest and Reserva Ducke. *Gaps were defined as contiguous areas of the CHM with height less than 10 m at both sites.*

The minimum gap size (in m^2 of area) was defined as an approximation of the mean canopy area for trees greater than 5 cm diameter at breast height (DBH = 1.3 m). The calculation of mean canopy radius took into account the basal-area weighting of the initial sample. The mean radius length was 2.07 m for trees at Tapajos National Forest and Reserva Ducke, corresponding to an estimated crown area of 13.4 m^2 . This was approximated as 10 m^2 for ease of application and applied to both the Brokaw and dynamic gap definitions. *Thus our dynamic gap definition was defined as an area $> 10 \text{ m}^2$ where the lidar measured canopy height is always $< 10 \text{ m}$.*

Testing the effect of the minimum gap size using the 2008 data from Tapajos National Forest, we found that the proportion of area in gap decreased linearly from 4.6% with a 4 m^2 minimum gap size to 3.9% using a 20 m^2 minimum gap size, or less than 0.1% decrease per m^2 increase in minimum size. This change in the gap area resulted in an approximate 2-year increase in recurrence interval per m^2 increase in minimum size.

Gap Area

Tapajos showed a greater area in gap at both time periods using both definitions. Using the dynamic gap definition, Reserva Ducke had between 1.7 and 2.2% of area delineated as gap. This was below half of the 4.1 to 5.5% of area at Tapajos National Forest. Both sites showed a larger percentage gap during the second sampling (Table 4.2). Gaps at Tapajos showed no statistically significant spatial autocorrelation as analyzed using Moran's I suggesting near perfect randomness ($I = 0.004$; $p\text{-value}=0.5$). At Reserva Ducke, gaps showed a weak spatial autocorrelation ($I = 0.05$; $p\text{-value}<0.05$).

Not only was the total area different between sites, but the distribution of gap sizes at the two sites was also different (KS test $p\text{-value} < 0.01$). The mean gap size at Reserva Ducke was smaller than at Tapajos National Forest, as was the maximum gap size. The mean gap sizes were 35 m² and 68 m² respectively with a maximum gap size of 0.05 ha at Reserva Ducke and 0.9 ha at Tapajos. The exponent of the gap size power-law distributions averaged 2.16 at Reserva Ducke with 95% confidence intervals from 2.12 - 2.20. At Tapajos National Forest the exponent was 1.88 using the dynamic gap definition for both years (95% confidence interval of 1.84 - 1.90).

Applying the Brokaw definition while retaining the 10 m² area cutoff, we found that the proportion of area in gap was much lower, although the general comparison between sites was the same with a higher proportion in gap at Tapajos National Forest. The calculated

power law exponents were significantly higher (3.26 and 2.91 at Reserva Ducke for 2008 and 2011 respectively and approximately 2.86 at Tapajos National Forest for both years) and the overall number of gaps was low ($N_{\max}= 106$). Kolmogorov-Smirnov tests showed that gap size distributions did not differ between years (Table 4.2).

Table 4.2 Frequency of gap formation presented for both sites and gap definitions. The area covered by lidar at both time periods is reported with the percent initial gap area, percent final gap area, and the percent of the amount of final gap area newly formed between samples for both the dynamic gap definition (10 m height cutoff) and the Brokaw (1982) gap definition (2 m height cutoff) for a minimum gap area of 10 m². A Kolmogorov-Smirnov test was used to compare the distributions of gap sizes between years for each site by definition.

Site	Sample Area (ha)	Initial Gap Area (%)	Final Gap Area (%)	Percent New Gap (%)	KS-test p-value
Dynamic Gap					
Reserva Ducke	602	1.20	1.52	64.2	0.39
Tapajos	398	4.37	5.49	23.2	0.33
Brokaw (1982) Gap					
Reserva Ducke	602	0.01	0.04	98.9	0.78
Tapajos	398	0.03	0.11	98.8	0.95

Gap Creation and Lifetimes

Using the dynamic gap definition, approximately 65% of gap area at the second sampling was formed in the time between samplings at Reserva Ducke (3.67 years). At Tapajos National Forest 23% of gap area was formed between the samples, a period of 4 years.

Despite differences in the proportion of new gap area, the recurrence intervals are similar: 377 years at Reserva Ducke and 316 years at Tapajos National Forest.

To estimate recurrence intervals from a single acquisition requires an estimate of the amount of time that gaps are visible on the landscape (persistence time). The persistence time of gaps was calculated based on the height change observed over the sample period (Table 4.3). Height loss, which may represent repeat disturbance or decomposition following tree-fall events accounted for 13.4% of gap area at Reserva Ducke and 22.6% at Tapajos National Forest. Taking repeat disturbance into account resulted in estimated annual growth rates of 1.23 m y^{-1} at Reserva Ducke and 1.10 m y^{-1} at Tapajos National Forest.

Recurrence times calculated from a single acquisition were longer than those calculated based on new gap formation alone at Reserva Ducke and shorter at Tapajos National Forest. At Reserva Ducke the recurrence times were 675 years and 532 years for the initial and final acquisitions respectively. At Tapajos, recurrence times were 208 years and 165 years.

Using the Brokaw (1982) definition, almost 100% of the final gap area was new since the initial sample. Recurrence intervals were over ten times longer than those calculated at both sites using the dynamic gap definition, suggesting recurrence intervals calculated using the Brokaw gap definition are unrealistic. At Reserva Ducke the recurrence interval

was 9,009 years, longer than the estimated 3,725 years at Tapajos National Forest.

Growth was estimated as 2.36 m y⁻¹ at Reserva Ducke and 2.52 m y⁻¹ at Tapajos for initial heights less than 2 m. This rapid height change resulted in persistence times of less than a year at both sites. Recurrence intervals calculated for individual acquisitions were extremely variable.

Table 4.3 Gap recurrence frequencies based on persistence times calculated from the inter-sample growth period. Inter-sample period growth takes into account both height gain and height loss in gap areas. Three recurrence frequencies are presented: 'New Formation' takes into account only areas that were not gap at the time of the initial acquisition (Eq.1); 'Initial Acq.' and 'Final Acq.' recurrence frequencies are each calculated based on a single lidar data acquisition using Equation 4.2.

	Persistence Time y (t_p)	Recurrence Time y (t_r)		
		New Formation	Initial Acq.	Final Acq.
Dynamic Gap				
Reserva Ducke	8.1	371	675	532
Tapajos	9.1	301	208	165
Brokaw (1982) Gap				
Reserva Ducke	0.9	9009	7416	2122
Tapajos	0.8	3725	2367	732

The recurrence frequencies and persistence times presented are specific to the gap size and shape of each site at the time of sampling. For individual pixels, height changes over 40 m were observed over the inter-sample period at both sites and was attributed to horizontal growth of surrounding canopies. To gain a better understanding of methods of

gap closure, we estimated the extent to which horizontal ingrowth played a role at both sites. The mean positive height change per year at gap centers (assumed unaffected by horizontal ingrowth) was 1.2 m y^{-1} (sd = 0.9) at Reserva Ducke and 1.8 m y^{-1} (sd=0.7) at Tapajos National Forest. Maximum vertical growth was estimated to capture all gap center height changes (approximately 4 m per year at each site). All height changes greater than this were assumed to be horizontal ingrowth. We estimate that 9.8% of gap area at Reserva Ducke closed through horizontal ingrowth and 6.1% of gap area at Tapajos National Forest. Repeat disturbance (height loss) accounted for 13.4% of area at Reserva Ducke and 22.6% of area at Tapajos National Forest. When height loss was included, the average height change at gap centers was similar to the overall height change of gaps (1.1 m y^{-1} at Reserva Ducke and 1.3 m y^{-1} at Tapajos). However, this percentage varied when only the region within 5 m of gap edges was analyzed. In this region a higher percentage showed height loss at Tapajos National Forest (26.9%), but a lower percentage at Reserva Ducke (10.6%).

Gap Contagiousness

Canopy disturbance risk did not consistently increase with decreasing distance from gaps at either Reserva Ducke or Tapajos National Forest. At Reserva Ducke there was an increased risk of gap formation (compared to site mean) at distances of less than 10 m from existing gaps (Figure 4.3a). At Tapajos National Forest, this increased risk extended to 8 m from existing gaps (Figure 4.3b). Although there was not a consistent increase

with decreasing distance from gaps, there was an increased risk near to existing gaps (KS test $p\text{-val} < 0.01$). At both sites this zone of influence was strongest within 6 m of existing gaps.

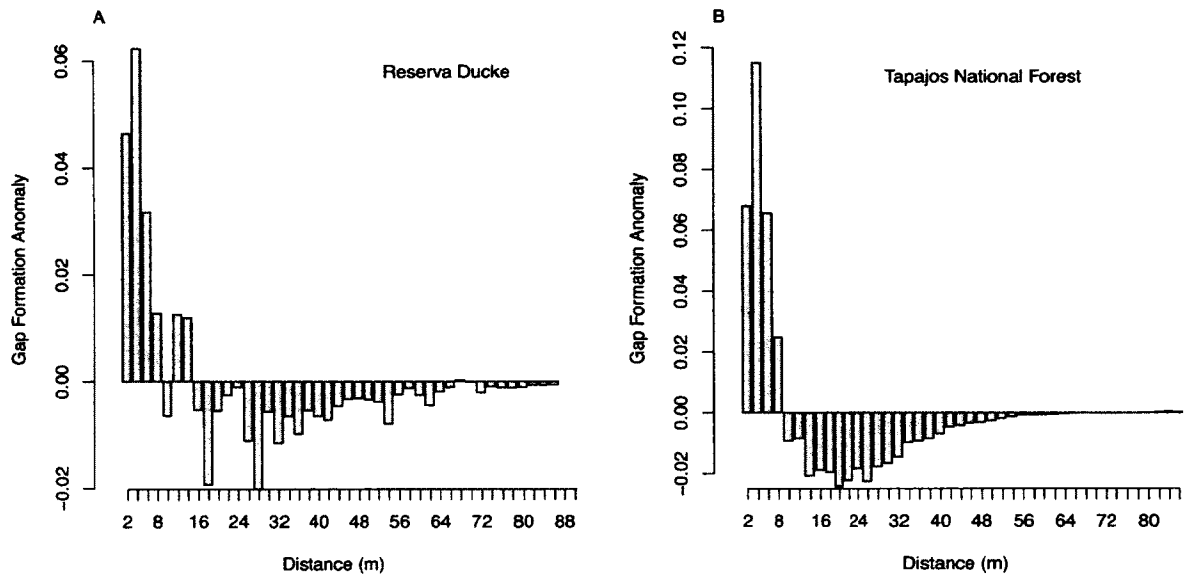


Figure 4.3 For each site, the average probability of gap formation between 2008 and 2012 was calculated. Next, the probability of gap formation was calculated based on distance from existing gaps. The average probability was subtracted from the probability based on distance from gaps in 2008 and the resulting difference (Gap Formation Anomaly) was plotted against distance for each site (a) Reserva Ducke and (b) Tapajos National Forest.

We looked for further evidence of gap contagiousness by counting mortality events for emergent trees. We found 177 full crown and a further 74 partial crown mortality events at Tapajos National Forest. Of these events, 49% were within 10 m of existing gaps, compared to 34% of the data that were within this same distance. The full crown mortality events represented 8.5% of counted emergent crowns in 2012, or 2.1% annual mortality of emergent crowns. At Reserva Ducke, we found 114 full crown mortality

events, and 34 partial crown events. The full crown events represented 7.2% of emergent crowns counted in 2011 (1.9% annual mortality). Annual mortality rates as estimated from lidar were not significantly different from field based measurements of emergents or the overall sample at Tapajos National Forest (Table 4.4).

Table 4.4 Estimates of annual mortality for all trees estimated from field sample as well as emergent trees (> 40 m) for both field and lidar samples. The number of newly dead trees (N_m), total sample size (N), percent annual mortality as well as the fraction fallen dead are presented. Fallen dead were considered those with height of less than 10 m in the 2011 survey.

	Reserva Ducke				Tapajos National Forest			
	N_m	N	% Ann. Mortality	% Fallen	N_m	N	% Ann. Mortality	% Fallen
All Field	23	899	1.4	53.0	49	1,137	2.1	59.1
Field Emergents	0	16	--	--	3	61	2.9	28.9
Lidar Emergents	114	1,583	1.9	--	177	2,082	2.1	--

At Reserva Ducke lidar based estimates of emergent tree mortality were not significantly different from overall site mortality. The distribution of mortality events is more similar to the distribution overall at Reserva Ducke; 20.3% of mortality events were within 10 m of gaps, and 16% of the area sampled. Mortality of the largest trees was consistent with the general trend of gap contagiousness. Observations showed higher than expected mortality near gaps at both sites with a 15% difference at Tapajos National Forest and a 4% difference at Reserva Ducke (observed - expected).

4.4 DISCUSSION

Gap Definition

We sought a functional gap definition based on light penetration through the canopy permitting high growth rates. It is not expected that a single set of horizontal or vertical limits will be appropriate for all sites due to different dynamics. The two sites studied show large variability in canopy structure, but analysis of canopy dynamics resulted in one consistent gap definition for both sites. This may be due in part to their similarities as moist tropical forests. Both the vertical and horizontal limits derived are within the ranges applied in previous studies. The height limit is close to those applied in the field by Young and Hubbell (1991) and to remote sensing data by Gaulton et al. (2010). We note that our quantitative dynamic gap definition can be calculated for any forest site where appropriate multitemporal data is available.

Comparing our dynamic gap definition to the fixed Brokaw definition, we find that application of the Brokaw definition to lidar data underestimated canopy openness and overestimated gap recurrence intervals. A previous remote sensing study on gap frequency in Peru does not present canopy openness or gap recurrence intervals, but tests the gap size distribution of the Brokaw and other gap definitions (Boyd et al. 2013). They showed no significant difference between the Brokaw gap definition and other height cutoffs when examining the gap size distribution in Peru (Boyd et al. 2013) whereas we

also observe significant differences in this variable. These differences may be due to the shape of gaps, annual variability, or the infrequency of newly formed gaps penetrating to within 2 m of the ground at our sites. Another important difference in our methods from those of Boyd et al. is the horizontal size limit applied. While Boyd et al. (2013) applied a 2 m² minimum gap size, we applied a 10 m² minimum gap size. Our larger minimum size reduced the total area of Brokaw gaps significantly (from 3824 m² with 1 m² minimum gap area to 709 m² at Reserva Ducke in 2008). However, when no minimum gap size is applied differences between the Brokaw and dynamic gap definitions remained significant (0.01% Brokaw gap versus 1.9% dynamic gap at Reserva Ducke).

As shown by Hubbell and Foster (1986), the death of canopy trees often does not indicate the death of all understory vegetation. They reported that small stems frequently remained in gaps up to 4 - 5 m in height. Lieberman et al. (1985) reported broken and damaged stems within a tree fall gap that were well above 2 m. Of the trees that were broken and died, they reported that all were less than 10 m tall (maximum 7 m). Of those that were broken and survived two were above the 10 m threshold applied here.

The minimum area of gaps delineated had a comparatively small affect on the gap characteristics presented here. Starting from a minimum area of 4 m² we found that a 1 m² increase in the minimum gap size results in a 0.1% decrease in total gap area and an approximate 2 year increase in recurrence interval. In contrast, the fractional area changes significantly when the height limit of the gap definition changes. Lobo and Dalling

(2014) also showed an exponential increase in the percent area in gap when the height limit is increased.

Gap Area

We measured about twice as much proportional area in gap at the Tapajos National Forest as compared to Reserva Ducke. The Tapajos National Forest distribution of gap sizes was weighted more strongly toward large gaps. Compared with other tropical sites, Tapajos National Forest has a more varied canopy structure, but the distribution of gap sizes is similar to previously published values (Kellner et al. 2009, Chambers et al. 2009, Boyd et al. 2013, Asner et al. 2013, Lobo and Dalling 2014). Unfortunately, the proportion of area in gap is not always reported in gap studies. Of sites with similar measurements, a study conducted at Tambopata (Boyd et al. 2013) that applies a minimum gap size of 2 m² reported proportion of area in gap and found that approximately 1.1% of the area studied was considered gap when applying the Brokaw gap definition, higher than at either of the sites considered here. In contrast, a study conducted in Panama using a 5 m² minimum gap size found 0.41% of area in gap when applying the Brokaw gap definition, and 6.04% of area in gap when applying a 10 m height cutoff (Lobo and Dalling 2014).

Gap Creation and Forest Turnover

Estimates of forest turnover by gap processes do not equate with field estimates of mortality (Lieberman et al. 1985, van der Meer et al. 1994). Not only do trees die without creating gaps, but single gaps may be formed by multiple trees (Putz et al. 1983, Gale and Barfod 1999, Gale and Hall 2001, Chao et al. 2009, Ferry et al. 2010). Espirito-Santo et al. (2013) found that gap formation resulted from about 30% of tree mortality events at the Tapajos National Forest. Therefore, we expect that remote sensing based estimates of gap recurrence intervals should be considerably longer than the recurrence intervals implied by mortality statistics. The extremely long recurrence intervals estimated based on a maximum height of 2 m and a minimum area of 10 m² (Brokaw gaps) is an artifact of the very small proportion of gap area when this definition is applied to lidar data.

The increased gap creation, faster dynamics and larger gap sizes of Tapajos National Forest should also be associated with faster regrowth within gaps. However, we observed slower average vertical growth in gaps at Tapajos National Forest compared to Reserva Ducke. Larger gap sizes at Tapajos National Forest are expected to result in higher light availability at Tapajos National Forest, resulting in faster growth (Stark et al. 2012). We attribute the lower observed average height change to the strong influence of repeat disturbance at gap edges, especially for gaps over 50 m². While Tapajos and Reserva Ducke show similar levels of repeat disturbance for gaps less than 50 m² (approximately 15%), gaps greater than 50 m² have higher repeat disturbance rates at Tapajos (28%

within 5 m of gap edges) and lower rates at Reserva Ducke (10% within 5 m of gap edges). Additionally, gaps are smaller at Reserva Ducke, and horizontal ingrowth has a stronger effect with a conservative estimate of 10% of gap area closing via horizontal ingrowth versus 6% at Tapajos National Forest. Furthermore, when only positive change data from gap centers were analyzed, maximum vertical growth rates are consistent with published values from other tropical forests (Brokaw 1987) and our result of larger average height change at Tapajos National Forest is consistent with the expectations of faster dynamics at this site (Stark et al. 2012).

The differences between turnover times as estimated from change between lidar data collections versus those based on single acquisitions highlights uncertainties due to the variability in persistence times. Given the variability in growth rates, persistence times are not well understood (Asner et al. 2004). Logging studies show canopy closure in terms of gap fraction as estimated from hemispherical photographs but rarely include information on understory height growth (Fredericksen and Pariona 2002, Pereira et al. 2002, Schulze and Zweede 2006). The increasing availability of repeat collections of lidar data in tropical as well as temperate ecosystems will improve our understanding of growth at the stand and landscape scales for gap and non-gap environments.

Gap Contagiousness

While gaps have clumped distributions (Poorter et al. 2009), it is debatable whether gaps influence the creation of other gaps (also known as gap contagiousness). Young and Hubbell (1991) surveyed large trees within Barro Colorado Island and hypothesized that gap contagiousness would occur over time due to observed canopy asymmetry. Jansen et al. (2008) tested four hypotheses related to canopy disturbance risk and the magnitude of canopy disturbances with relation to proximity to gaps and initial gap size within a 12 ha area of tropical forest in French Guiana. While new gaps formed more frequently close to existing gaps, the authors showed that this was due to the respective area at each distance from gaps within the landscape, and was not evidence for gap contagiousness. The authors concluded that in the forests of French Guiana surveyed newly formed gaps were consistent with previous theories of tropical rain forests as “patches with predictable regeneration cycles”.

Although gap contagiousness has not been conclusively shown, edge effects are a well known phenomena in fragmented landscapes. Laurance et al. (1998) showed increased mortality within 100 m of the forest edge, and suggested that this may be due to increased wind turbulence and changes in the local microclimate. While natural gaps within the forest matrix may not experience increased wind turbulence, changes in the local microclimate do occur (Ray et al. 2005).

Our results suggest that gap contagiousness does occur surrounding natural forest gaps but has an extremely small effective range. This was shown for all gaps and specifically in terms of the mortality of large trees. The small effective range (approximately 6 m at both sites) suggests that the gap definition used will have a strong effect on evidence for or against contagiousness. Jansen uses an expanded gap definition that is based on the Brokaw definition of a gap as a region where vegetation does not exceed 2 m height. The expanded gap definition, based on Runkle (1981) requires a central area of greater than or equal to 4 m² of less than 2 m height, but the gap edge is defined by the trunk locations of surrounding trees of at least 20 m in height. Young and Hubbell (1991) uses a different gap definition where gap areas were defined as areas greater than 25 m² with canopy height less than 10 m. Jansen and colleagues's gap definition will therefore include larger areas, but classify fewer gaps. This is apparent in their results that show mortality rates approximately twice as high within gaps as compared to the surrounding forest (Jansen et al. 2008).

4.5 CONCLUSIONS

We found that forest canopy structure is significantly different between the two sites studied in the Brazilian Amazon. Additionally, the growth rates within gaps were highly dependent on the initial height of vegetation examined. For vegetation less than 10 m in height, we observed average height changes of approximately 4.5 m at both sites. This equates to 1.2 m y⁻¹ at Reserva Ducke and 1.1 m y⁻¹ at Tapajos National Forest. With

regards to gaps, the gap size frequency was significantly different between the sites, as well as between gap definitions. The gap size frequency did not change between sample years, although the proportional area in gaps varied between years, suggesting that rates of canopy turnover are not constant through time. Both sites showed evidence of gap contagiousness, although the range of influence was extremely limited which may account for conflicting results in the literature.

4.6 AUTHOR CONTRIBUTIONS

Experiment concept and design were completed by MOH in collaboration with MK, MJD, ML, SRS and DCM. MOH, ML and JS contributed to raw data processing of the initial 2008 lidar data collection. MOH, MK, DCM and BC contributed to processing the 2012 lidar data. BC and DCM re-analyzed raw lidar data using the G-LiHT processing tools and created the merged DTM for Reserva Ducke. MOH collected field data at Reserva Ducke and Tapajos National Forest with logistical assistance from RCdO, JS and SRS.

CHAPTER FIVE

EFFECT OF LIGHT AVAILABILITY ON HEIGHT GROWTH IN TROPICAL FORESTS

5.1 INTRODUCTION

Variability in light is a key driver for forest growth and succession (Cannell and Grace 1993). Successional processes in tropical forests are typically driven by small gaps (Denslow 1987, Espírito-Santo et al. 2014a) that have been shown to have highly variable light environments. Variation has been shown both between gap sizes and gap geometries and well as within individual gaps, moving from gap centers to edges (Poulson and Platt 1989, Whitmore et al. 1993, Brown 1996).

Historically, estimation of light level within gaps depended on the use of forest structural models, canopy hemispherical photography or similar techniques including the LAI-2000 (Welles and Norman 1991). Whitmore et al. (1993) showed that canopy openness as predicted by hemispherical photographs was a strong indicator of local microclimate. Machado and Reich (1999) evaluated instantaneous light measurements' ability to predict transmitted light available during the growing season and found that hemispherical photography, LAI-2000 and instantaneous measurement of photosynthetic photon flux

density were well correlated with overall light availability. Additionally, they show that of tested techniques, hemispherical photographs had the lowest correlation with total light available (67%) whereas the LAI-2000 had the highest correlation (90%).

While previous research has shown the ability of instantaneous measurements to predict total light available for a given gap location, it is difficult to take the high degree of local variability into account in order to understand the influences of light in gaps across a broader landscape. Light patterns near the forest floor are influenced by complex interactions between all vegetation layers, and forest structural parameters such as basal area, mean tree height, mean crown area and stem density are not sufficient to predict light environments (Montgomery and Chazdon 2001). This suggests the difficulty of accurately estimating light environments without direct measurements or complex models. Even detailed forest inventory measurements are likely insufficient given the variability in tree architecture inherent in tropical forest ecosystems (however see Marthews et al. 2008).

Airborne lidar remote sensing provides detailed structural measurements of forest ecosystems (Lefsky et al. 2002, Lee and Lucas 2007, Vierling et al. 2008). Lidar sensors emit short duration laser pulses that are reflected by leaves, branches and the ground. The round trip time of the reflected pulse is recorded and converted to distance to the reflected surface. Discrete airborne lidar provides a three-dimensional cloud of points representing reflected surfaces. This data has been directly used to estimate understory

vegetation distribution (Martinuzzi et al. 2009) as well as estimate understory biomass based on height and fractional cover (Miura and Jones 2010, Morsdorf et al. 2010, Estornell et al. 2011). With limited assumptions about occlusion and signal die-off (e.g. Stark et al. 2012) it is possible to also use this data within a modeling framework to predict light environments.

High light environments have been shown to increase survivorship and growth of seedlings in tropical moist forests (Brokaw 1985, Denslow et al. 1990). The increased survival of seedlings in gap environments depends on light availability as well as a decrease in pathogens due to warmer temperatures, drier air and increased circulation. Though mortality is higher for saplings in gaps, growth is also generally higher. Welden et al. (1991) showed increased growth in gap environments for about half of species in a study on Barro Colorado Island, in Panama. This variability in response to gap environments is thought to be due to competition between saplings, as well as mortality of surrounding trees and branches (Hubbell and Foster 1986, Young and Hubbell 1991).

As trees grow taller, they are generally exposed to increasing light environments (Metcalf et al. 2009). This interdependence between light availability and tree height must be taken into account to accurately estimate growth. However, there are few studies that take into account tree size and light availability at the same time (Rüger et al. 2011b).

In this study, we aim to test the ability to predict height change in a tropical forest ecosystem based on a simple model that uses the spatial distribution of initial vegetation height in a canopy height model derived from lidar to predict solar radiation. Multi-temporal lidar data collected over a four year interval was used to estimate initial height and height change. Six 1 ha areas within the Tapajos National Forest, Pará, Brazil were used as test areas within the approximately 400 ha of overlapping lidar data between time periods. For these test areas, annual incident solar radiation was estimated for the canopy surface at a 1 m resolution. Predicted height changes based on initial height and solar radiation are compared to height change as measured by field inventory. Here we report on trends in field measurements of growth (diameter, height and crown radius increments) as a function of field assessments of light availability and crown position. We then present results of a simple model of solar radiation for areas with varying gap sizes and geometries, and compare trends in the prediction of height change from modeled light availability and initial height to field assessments.

5.2 METHODS

Site Description

Tapajos National Forest (54°58'W, 2°51'S) is a 550,000 ha forest reserve of tropical moist forest within the central Brazilian Amazon. The reserve contains upland forests on nutrient-poor, clay Oxisols (Silver et al. 2000) with limited topographic variability. Mean

annual temperature is 25°C and mean annual precipitation is 1909 mm (Hijmans et al. 2005). The dry season, defined by months with less than 100 mm rain, typically lasts from July through December (Vieira et al. 2004). We studied an undisturbed portion of the reserve although other regions of the reserve have been selectively-harvested.

Field Survey

Six transects of 500 m were installed within the study area in June 2009. Stems greater than 5 cm diameter were sampled using a diameter-dependent line sample using a diameter factor of 10.0 (Schreuder et al. 1987). We mapped stems with respect to the transects and geolocated the transects using a combination of differential GNSS and navigational GPS units. For each stem, we measured diameter, height and crown dimensions and noted canopy position and light availability. All stems were remeasured in July 2011. A total of 1193 stems were measured; 1137 stems were sampled in 2009 and 1142 in 2011. For further details of field sampling procedures see Hunter et al. (2013).

Airborne Lidar Data

Airborne lidar data was collected at the study site between June 7 and July 3 2008 and between 30-31 July 2012 and 3-4 September 2012. A digital terrain model (DTM) and canopy height model (CHM) was created for each lidar acquisition at a 1 m² resolution following Cook et al. (2013). Six 1 ha areas were selected for further analysis within the

400 ha covered by both data acquisitions. These areas include field-sampled transects and a wide variety of light environments.

Incoming Radiation

Incident photosynthetically active radiation (PAR) measurements taken on a canopy tower within the study area were used to estimate properties of incoming solar radiation. Incoming PAR was measured at 63.6 m elevation from January 3, 2002 to January 19, 2006 and reported as hourly means and standard deviations (Hutyra et al. 2007).

Tower data were analyzed to determine the maximum incident PAR and average PAR for sunny and cloudy conditions. The maximum incident PAR was defined as the 99th percentile of PAR measurements. Sunny conditions were defined as those with greater than 70% of the maximum PAR for a given month and hour. Cloudy conditions were defined as those with less than 70% of maximum PAR. The number of cloudy days per month was calculated as the number of cloudy measurements ($N_{shade(m)}$) divided by the total number of measurements ($N_{total(m)}$) in a given month (Eq 5.1).

$$f_c(m) = \frac{N_{shade(m)}}{N_{total(m)}} \quad \text{Eq 5.1}$$

Modeled Annual Solar Radiation

Annual incoming solar radiation was estimated for each of the six selected areas using the model of Rich et al. (Rich 1990, Rich et al. 1994) and further developed by Fu and Rich (Fu et al. 2000, Fu and Rich 2002). This model was developed to characterize the spatial and temporal variability of insolation across landscapes (Fu and Rich 2002) by simulating the influence of shadow patterns at discrete intervals through time. The variability in elevation, surface orientation and obstruction create strong local variability that cannot be modeled from simple interpolation of point measurements.

The area solar radiation calculation has been implemented in the spatial analysis package of ArcGIS (v9.2). We employed this function using the lidar CHMs as the only spatially explicit inputs. The model generates a hemispherical viewshed for each pixel within the raster, wherein the amount of sky visible is determined based on canopy topography. In our case the sky visibility was based on canopy surface topography at a 1 m resolution. The canopy height model for each area of interest was used as the spatially explicit input. The 'area solar radiation' tool also requests a slope input that can be determined either from the input raster or specified as a flat ground surface. Given that we are simulating the canopy surface as opposed to the ground surface this parameter was interpreted as the slope of the canopy surface elements. As leaf angle is highly variable, and likely not correlated to the slope of the outer canopy surface, we chose to specify a flat ground surface.

The ‘area solar radiation’ function calculates a *sunmap* that is a raster representation of the sun track over the sample period that we used to estimate direct radiation. Based on inputs including the year, time of year, day interval and time interval and center longitude and latitude from the input raster we estimated annual solar radiation for the 2009 calendar year, the first full year after initial lidar data collection. We modeled light conditions for one day per month at 2 hour intervals. The sunmap is overlaid with the viewshed previously calculated to model direct radiation. The calculation of direct solar radiation is completed according to equation 5.2.

$$Dir_{\theta,\alpha} = S_{Const} \cdot \beta^{m(\theta)} \cdot SunDur_{\theta,\alpha} \cdot SunGap_{\theta,\alpha} \quad \text{Eq 5.2}$$

This equation calculates direct solar radiation (*Dir*) as a function of constant solar flux outside of the atmosphere ($S_{const} = 1367 \text{ W m}^{-2}$), the transmissivity of the atmosphere (β) that is dependent on the relative optical path length (m), the time duration represented by a sky sector (*SunDur*) specific to the sunmap (generally the day interval multiplied by the hour interval), and the gap fraction for a sky sector (*SunGap*). Additional terms taking into account the interaction between solar angles and surface angles were not included as we specified a ‘flat ground surface’. The majority of these variables are dependent on the zenith angle (θ) and azimuth angle (α).

Table 5.1 Input parameters to ArcGIS 9.2 'Area Solar Radiation' tool.

Input Parameter	Value
Sky Area	200
Year	2009
Days	by month
Day Interval	7
Hour Interval	2
Slope Input	Flat Surface
Calculation Directions	32
Diffuse Fraction	monthly value
Transmission	0.5

The area solar radiation tool next generates a *skymap* that is used to estimate diffuse solar radiation. The skymap generated is a raster representation of the full sky hemisphere divided into a specified number of zenith and azimuth components. We employed the default calculation for 8 zenith divisions and 16 azimuth divisions. Diffuse radiation is estimated based on the direction of the centroid of each raster component. The skymap was overlaid with viewsheds previously calculated to determine the diffuse radiation component at each 1 m resolution pixel of the original input raster of the canopy height model. The diffuse solar radiation was calculated within the solar radiation tool based on Equation 5.3.

$$Difn_{\theta,\alpha} = R_{glb} \cdot P_{dif} \cdot Dur \cdot SkyGap_{\theta,\alpha} \cdot Weight_{\theta,\alpha} \quad \text{Eq 5.3}$$

This equation takes into account global normal radiation (R_{glb} calculated based on Eq 5.4), the proportion of global radiation flux that is diffused (P_{dif}), the time interval of the analysis (Dur), the proportion of visible sky for a given sky sector ($SkyGap$), and the proportion of diffuse radiation originating from a given sky sector ($Weight$). The global normal radiation (Eq 5.4) includes parameters previously defined for equation 5.2 including the constant solar flux outside of the atmosphere (S_{const}) and the transmissivity of the atmosphere (β) and the proportion of diffuse radiation (P_{dif}). The proportion of diffuse radiation in equations 5.3 and 5.4 was determined on a monthly basis following the equation published by Butt et al. (2010) that calculates the diffuse proportion based on the proportion of cloudy conditions calculated using equation 5.1. This equation was developed for Caxiuanã, Pará, a site within the eastern Amazon of Brazil.

$$R_{glb} = (S_{Const} \Sigma(\beta^{m(\theta)})) \div (1 - P_{dif}) \quad \text{Eq 5.4}$$

Simulations were run for each month using weekly time steps, and output on a monthly basis. Total solar radiation was calculated following equation 5.5.

$$SR = \Sigma_m[\Sigma(Difn_{\theta,\alpha}) + \Sigma(Dir_{\theta,\alpha})] \quad \text{Eq 5.5}$$

This equation sums diffuse and direct light summed over all zenith and azimuth angles for a given month and then sums over all months. Summed output values are in units of watt-hours per meter-squared ($Wh\ m^{-2}$).

Analysis

For each of the six scenes analyzed, initial canopy height and annual solar radiation were tested as predictors of canopy height change. Based on results presented in Hunter et al. (2014; Chapter 4) we separated lateral growth from trees surrounding gaps, mortality events including branch falls, and vertical growth within gaps. Based on this prior study, we modeled the influence of light on vertical growth only (positive height changes less than 3.9 m yr^{-1}) and on all height changes based on the full data set. We also investigated gap areas specifically both for all height changes and vertical growth only.

Six models were tested to predict height change, representing possible combinations of linear and natural log transformations (Table 5.2). Log transformation implies a saturation of the effect of a given term. Each model was fit using the generalized linear model function (R-Project v2.15) tested for all sites data together as well as each site individually. The best model was chosen based on the lowest AIC, with additional consideration of the adjusted correlation coefficient (R^2 value).

Table 5.2 Model forms tested to predict height change (HC) using initial height (Ht) and annual solar radiation (SR) as predictive variables.

M1	$HC = a + b \cdot Ht + c \cdot SR$
M2	$HC = a + c \cdot SR$
M3	$HC = a + b \cdot Ht$
M4	$HC = a + b \cdot \log(Ht) + c \cdot SR$
M5	$HC = a + b \cdot Ht + c \cdot \log(SR)$
M6	$HC = a + b \cdot \log(Ht) + c \cdot \log(SR)$

The comparative effect of solar radiation and initial height are initially compared using models 2 and 3, that each take into account a single parameter. To further test the effect of these individual components, a de-trending analysis was conducted. In this analysis, linear and log-linear relationships were first applied to initial height versus height change measured (HC_{meas}) using the generalized linear model function and parameters were fit (Eq. 5.6).

$$HC_{meas} = a + b Ht \quad or \quad HC_{meas} = a + b \ln(Ht) \quad Eq\ 5.6$$

Model parameters were then used to calculate a modeled value for height change (HC_{model}) based on initial height alone (Ht). The modeled value of height change was then removed from the measured value, resulting in a de-trended value for height change (HC_{det}). This value (HC_{det}) was then regressed against solar radiation (SR) testing both linear and natural logarithm formulations (Eq. 5.7).

$$HC_{det} = c + d SR \quad or \quad HC_{det} = c + d \ln(SR) \quad Eq\ 5.7$$

5.3 RESULTS

Field Surveys

Growth of individual trees was estimated over the two-year sample interval in terms of diameter, height, and crown radius increments. Data demonstrate increasing diameter

increment and crown radius increment with increased light availability. A weak positive signal for height increment is also shown, though errors in field measurements of height are large (Hunter et al. 2013). Similar patterns are shown when growth is separated by canopy position alone, with increasing mean growth shown as the canopy position changes from suppressed to emergent canopy positions. However, when height increment is regressed against initial measured height, a slight but significant negative correlation is found (intercept = 1.22, slope = -0.09, p-value < 0.001). This regression indicates that short vegetation had the greatest positive height change, and vegetation over 13.4 m showed a tendency toward decreasing height. Positive correlations are found for both crown radius and diameter increments.

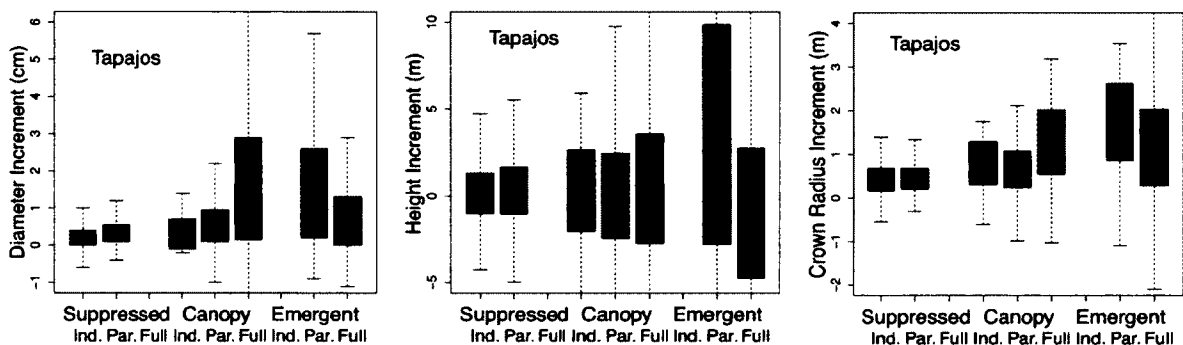


Figure 5.1 Field measured growth by canopy class and light availability class.

When field measurements of growth are divided into classes based on both canopy position and light availability, trends are more difficult to determine. This may in part be due to small sample sizes for some classes. Diameter increment increases most strongly within canopy position classes, with a slight trend visible for suppressed trees and no trend observable for emergents (Figure 5.1a). Diameter increment likewise increases for

indirectly illuminated and partially illuminated stems. There is no consistent trend for growth within canopy classes with regard to height or crown radius increment. For stems receiving indirect light there is an increasing trend of height increment, but this trend is not visible for partially or fully illuminated stems (Figure 5.1b). Crown radius likewise increases for both stems receiving indirect and partial sunlight (Figure 5.1c). No trend is visible for fully illuminated crowns for any metric.

Estimates of Incoming Radiation

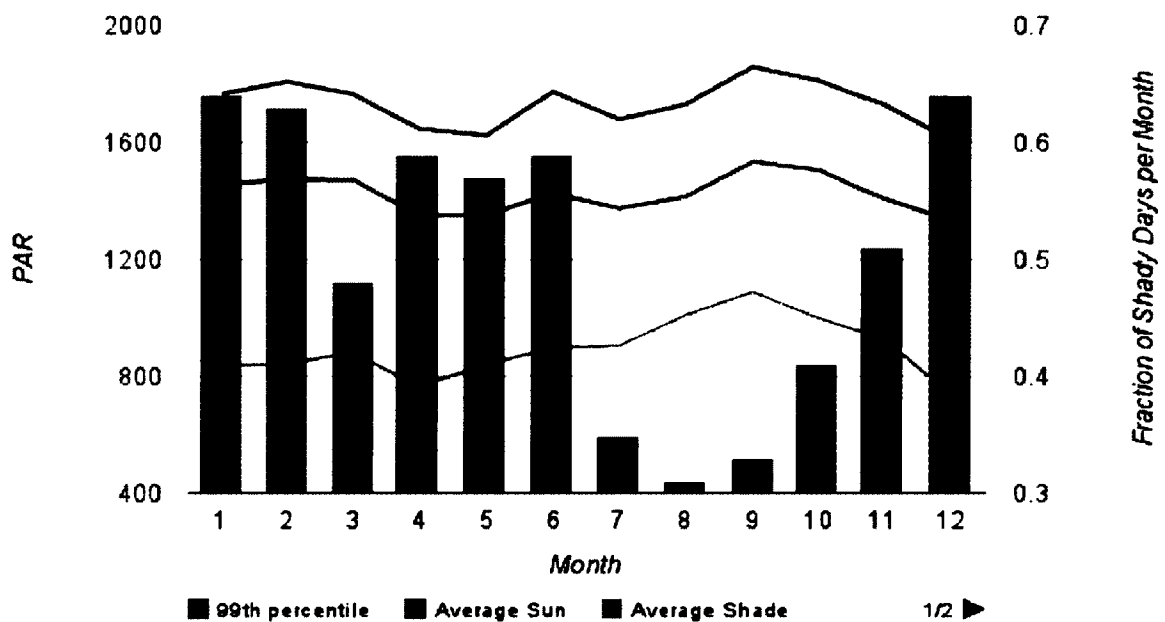


Figure 5.2 Incoming radiation in PAR wavelengths at Tapajos Tower and fraction of shady days. The 99th percentile of incoming PAR is shown for the 1600 - 1700 GMT hour (approximately 1230 local time) by month. Average sun PAR is estimated as the average PAR of periods with greater than 70% of max PAR. Average shade PAR is the average of the remaining measurements. The proportion of shade days per month was estimated as the number of shade measurements divided by the total number of measurements.

Modeled incoming radiation based on latitude and longitude varied with maximum values occurring during September. Maximum PAR as measured by the meteorological tower varied by hour, with mean values ranging from 1677 $\mu\text{mol m}^{-2}\text{s}^{-1}$ at 1230 and 457 $\mu\text{mol m}^{-2}\text{s}^{-1}$ at 1630 local time. However, no distinct seasonal pattern was observed. At 1230 local time the mean sunlit PAR was 1384 $\mu\text{mol m}^{-2}\text{s}^{-1}$ and the mean shade PAR was 848 $\mu\text{mol m}^{-2}\text{s}^{-1}$. Estimates of the proportion of cloudy days varied from 0.19 to 0.65 with fewer cloudy days during the five month dry season (July through November). This

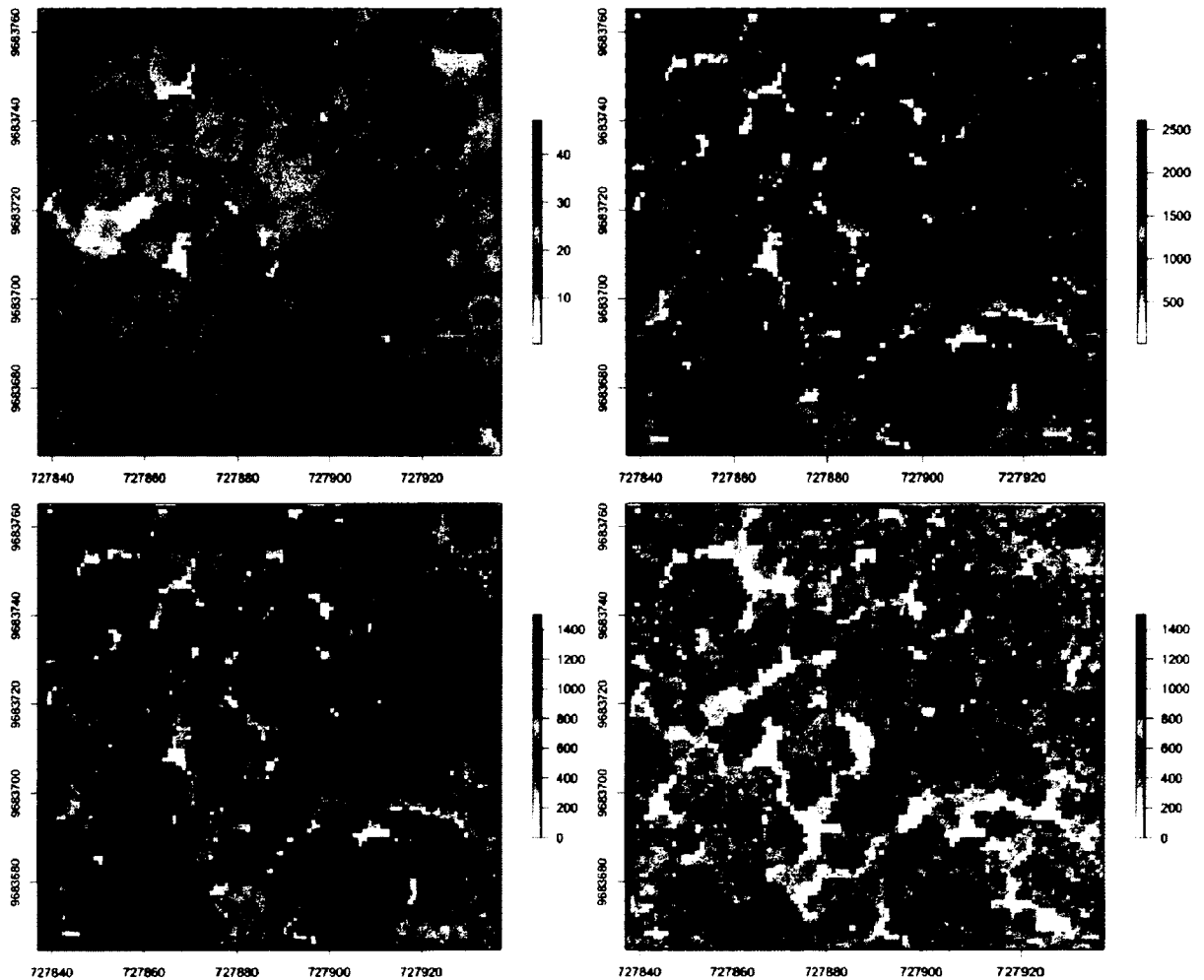


Figure 5.3 Area 6 canopy height (m; A) and estimated total annual solar radiation (kWh m^{-2} ; B) composed of direct radiation (C) and diffuse radiation (D) components.

proportion of cloudy days represented diffuse proportion ranging from 0.34 - 0.70 (Fig 5.2).

Modeled Annual Solar Radiation

Based on the raw direct and diffuse radiation output by the model, the maximum value of incident solar radiation is 2603 kWh m⁻². The maximum direct radiation is 1484 kWh m⁻² and the maximum diffuse is 1120 kWh m⁻².

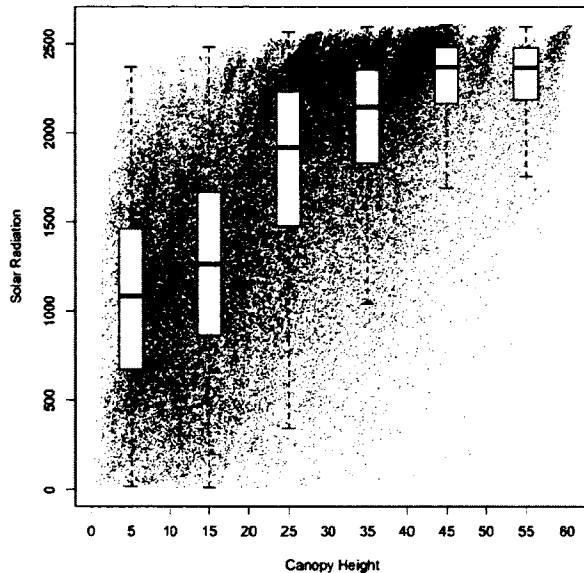


Figure 5.4 Relationship between initial canopy height (m) and estimated annual solar radiation (kWh m⁻²) for all areas of interest. Boxplot of data binned into 10 m canopy height classes is overlaid.

Estimated annual solar radiation varied from 9.18 to 2604 kWh m⁻² within the test scenes (example scene presented in Figure 5.3). Solar radiation was highly variable at the canopy surface with a mean of 1682 kWh m⁻² and a standard deviation of 636 kWh m⁻². In general, solar radiation was lower at lower initial canopy heights (slope = 33.1, R² = 0.44). However, there were a number of pixels where low canopy heights had high solar radiation and where tall canopy heights had low solar radiation (Figure 5.4).

The mean annual solar radiation varied between the studied areas, with low mean solar radiation generally correlated with high gap fraction (Table 5.3). When only areas in gap are considered, the opposite trend is observed with solar radiation increases with increasing gap fraction. However, there is significant variation in both leading to non-significant slopes when linear correlations were tested.

In general, annual solar radiation showed a slight negative correlation with height change over the four-year inter-sample period (slope = -0.003). This is the case when all solar radiation values are considered as well as only areas corresponding to vertical growth or gap areas.

Table 5.3 Details of study areas including gap fraction, mean and standard deviation of canopy height (m) and mean modeled solar radiation (kWh m⁻²) for the full scene as well as gap areas.

Site	Gap Fraction	Mean Canopy Height	Canopy Height (sd)	Mean Solar Radiation	Mean Solar Radiation in Gap
Area 1	3.86	27.45	9.80	1743	891
Area 2	15.15	22.86	11.88	1620	992
Area 3	23.25	21.10	11.49	1751	1283
Area 4	2.77	35.79	12.76	1747	487
Area 5	40.29	16.07	11.17	1507	1104
Area 6	4.65	25.50	9.29	1721	629

Effects of Light Availability on Growth

To separate the effects of solar radiation and initial canopy height on lidar measured height change, a series of models were tested that take both parameters into account. Results presented are for the prediction of vertical height change only. Initially testing models for all initial heights that include only solar radiation (M2) or initial height (M3) as predictors, we find that incident solar radiation is a stronger predictor of height change. While the AIC further declines and variance explained improves with the addition of the initial height parameter (M1), the difference is small.

Table 5.4 Parameters of models fit to vertical growth data within six areas of interest within Tapajos National Forest.

Model	a	b	c	R ²	AIC
M1	5.656	-0.018	-0.002	0.24	130655
M2	5.603		-0.002	0.24	130799
M3	4.330	-0.082		0.14	134178
M4	6.270	-0.353	-0.002	0.24	130630
M5	16.164	-0.032	-1.796	0.25	130529
M6	17.254	-0.544	-1.827	0.24	130593

Of models including all parameters, the variability in height change explained is not extremely variable with 24 - 25% explained in all cases. Model M5, which uses a linear relationship with initial canopy height and the log transformation of solar radiation,

showed the minimum AIC and maximum R^2 value with a total of 25% of variance explained (Table 5.4). Model 3, the only model tested that did not include the solar radiation term, had the highest AIC and explained the least variance overall (14%).

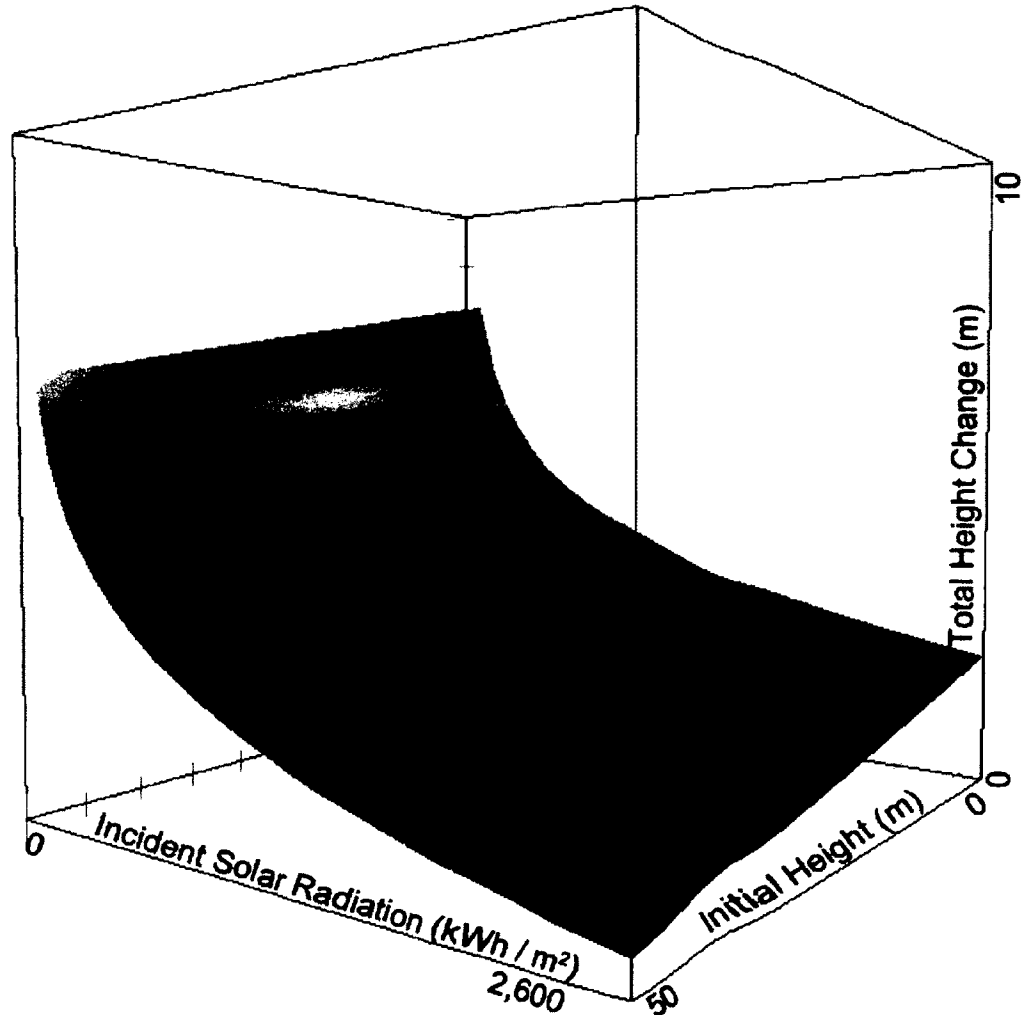


Figure 5.5 Modeled canopy height difference over the four year inter-sample period based on initial canopy height (x-axis) and annual solar radiation (y-axis).

When models were tested at individual areas, model M5 had the lowest AIC at four of the six areas, explaining between 25% and 31% of variance (Fig 5.5). The best fit model is of the form:

$$HC = 16.164 - 0.032 \cdot Ht - 1.796 \cdot \ln(SR) \quad \text{Eq 5.8}$$

At two of the individual areas (area 3 and area 5) M5 was not the best fit, but explained 28% and 13% of variance respectively. At area 3, M6 had the lowest AIC and explained the most variance (30%), whereas at area 5, M4 had the lowest AIC and explained the most variance (15%).

Table 5.5 Parameters of models fit to vertical growth data in gap areas (areas of less than 10 m initial height) within six areas of interest within Tapajos National Forest.

Model	a	b	c	R²	AIC
M1	6.231	-0.187	-0.001	0.05	27445
M2	5.094		-0.001	0.04	27520
M3	5.198	-0.222		0.02	27635
M4	6.864	-1.030	-0.001	0.05	27443
M5	12.132	-0.177	-1.069	0.06	27396
M6	12.654	-0.964	-1.058	0.06	27396

Testing the same models within gap areas (those with initial height less than 10 m) less variance is explained by all models (Table 5.5). Incident solar radiation remains a stronger predictor of height change than initial height. Of models including both parameters, between 5.4 and 6.3% of variance was explained and model 5 again showed the lowest AIC and highest variance explained. For gap areas the best fit model was of the form:

$$HC = 12.132 - 0.177 \cdot Ht - 1.069 \cdot \ln(SR) \quad \text{Eq 5.9}$$

All models tested showed a negative relationship between initial height and height change as well as between solar radiation and height change.

Detrending analysis also showed negative relationships between height change and both initial height and solar radiation. The linear regression between initial height and height change is presented as model 3 in Table 5.4 and explained 14% of variability. The natural log regression of these parameters explained slightly less variability and had a higher AIC (AIC=134399 as opposed to AIC=134178). Estimated solar radiation was then tested for linear and log-normal relationships with the de-trended value. The resulting linear relationship (intercept=1.73, slope=-0.0022) explained 24% of remaining variability. The log-normal relationship explained slightly less variability (23%) and had a higher AIC (AIC=135565 as opposed to AIC=135305).

5.4 DISCUSSION

Field Surveys

Increasing trends of growth are shown with increasing crown illumination and canopy class for diameter increment. However, trends are not visible within canopy classes when observing changes in height or crown radius despite strong correlation between crown radius and stem diameter. When we regressed diameter and crown radius increment against initial height, positive correlations were found, whereas a negative correlation

was found when height increment was regressed against initial height. The difference between results when observing canopy class versus initial height may be due to the large uncertainty in height measurements, especially of tall stems (Hunter et al. 2013). Trends are more visible within illumination classes for all metrics, suggesting that solar radiation may be a stronger driver of growth potential than initial height. This is consistent with results from Rüger et al. (2011b) showing stronger dependence on solar radiation than initial height. Additionally, our results showing increasing height growth for indirectly illuminated stems (primary understory stems) are consistent with the positive height increment demonstrated by Rüger et al. (2011b) and others.

It is important to remember that the field surveys include a large proportion of understory plants that are not accessible via remote sensing analysis. Canopy and emergent stems accounted for 54% of the 2009 field inventory. Of these, approximately 20% were classified as having crowns that were fully illuminated and 77% were classified as having partially illuminated crowns. Over 3% of stems were classified as receiving indirect light only despite being a part of the canopy layer. This may be due to patches of emergents strongly shading the dominant canopy layer.

Modeled Annual Solar Radiation

The solar radiation tool within ArcGIS provides significant improvements over previous studies that used shade indices as a proxy for measured light available. Estimates of solar

radiation produced by this tool were similar to those published for the Amazon (Butt et al. 2010). Rarely has light availability been measured in such a way that allows for individual trees exposure to be characterized, especially higher into the forest canopy. One recent example in the literature was published by Rüger et al. (2009), who developed a methodology applicable to high density forest inventory data that takes into account multiple layers of vegetation. They matched the probability distribution of this shade index with the probability distribution of 396 relative irradiance measurements at the near-ground level (Wirth et al. 2001). While this index showed correlation with growth for understory saplings, it could not be tested against light levels higher in the canopy.

While this solar radiation tool allows for distinct advantages, the simple framework may not be sufficient to accurately model solar radiation. A primary weakness of this model is the absence of transmitted radiation through the canopy surface. This is expected to cause significant variability in the amount of light available at lower canopy heights. Senna et al. (2005) reported that transmittance between the canopy top and 15 m at Tapajos National Forest varied from 20% - 70% throughout the year. A study completed in the Venezuelan Amazon (Anhuf and Rollenbeck, 2001) showed on average 80% of light was transmitted through the top 8 - 10 m of canopy with significant spatial variability. Both studies show large amounts of light transmitted through the canopy surface that are not accounted for in this model framework.

Effects of Light Availability on Growth

The model chosen explains 25% of variability in observed changes in height. This is similar to the variability explained when predicted biomass increment was compared with lidar metrics on the 1 ha scale (Stark et al. 2012), and significantly greater than variability explained by tree size and shade index (Rüger et al. 2011a). The approach used here is much simpler than these previous studies that use Bayesian techniques in combination with more complex models.

While tree height is an important parameter for forest yield modeling, it is most commonly modeled using diameter - height allometries or age - height allometries. Golser et al. (1997) presented a model of observed height increments for Austrian forests. This model includes species specific information on the potential height increment as well as multiple competition indices and an additional index taking edge effects into account (Golser and Hasenauer 1997). Many of these variables are directly associated with solar radiation, though they may also take into account nutrient limitation due to surrounding vegetation or crowding.

One study recently tests the effect of tree height and light availability on growth at Barro Colorado Island, Panama and showed that light availability had a stronger effect on diameter increment than initial height (Rüger et al. 2011b). However, this study used an adaptive shading index as opposed to a direct measurement of light availability. The

general result is consistent with our finding that light availability is a stronger predictor of height increment than initial height alone.

Overall, the best model shows a negative correlation with both increasing height and increasing light availability. While the negative correlation with height was expected because of slowing height change over time and is consistent with previously published results (Rüger et al. 2011b), a positive correlation with increasing light availability was expected based on previous studies. The two study areas where the overall best model did not perform as well as other models are the two areas with highest gap fraction (Table 5.2). In these two areas, high overall gap fraction is correlated with larger gap sizes. However, when gap areas were analyzed separately, the negative correlation between solar radiation and height change remained. These results suggest that physiological conditions present in large gaps other than increased light availability may drive observed growth or potential issues with the modeled solar radiation values themselves.

To further investigate this unexpected finding, we closely examined relationships between solar radiation and height change for individual height increments. We were particularly interested in vegetation classified as gaps in the 0 - 10 m height range. For all height classes, negative correlations between solar radiation and height change persisted with no discernible pattern for slope or intercept of linear regressions (Fig 5.6).

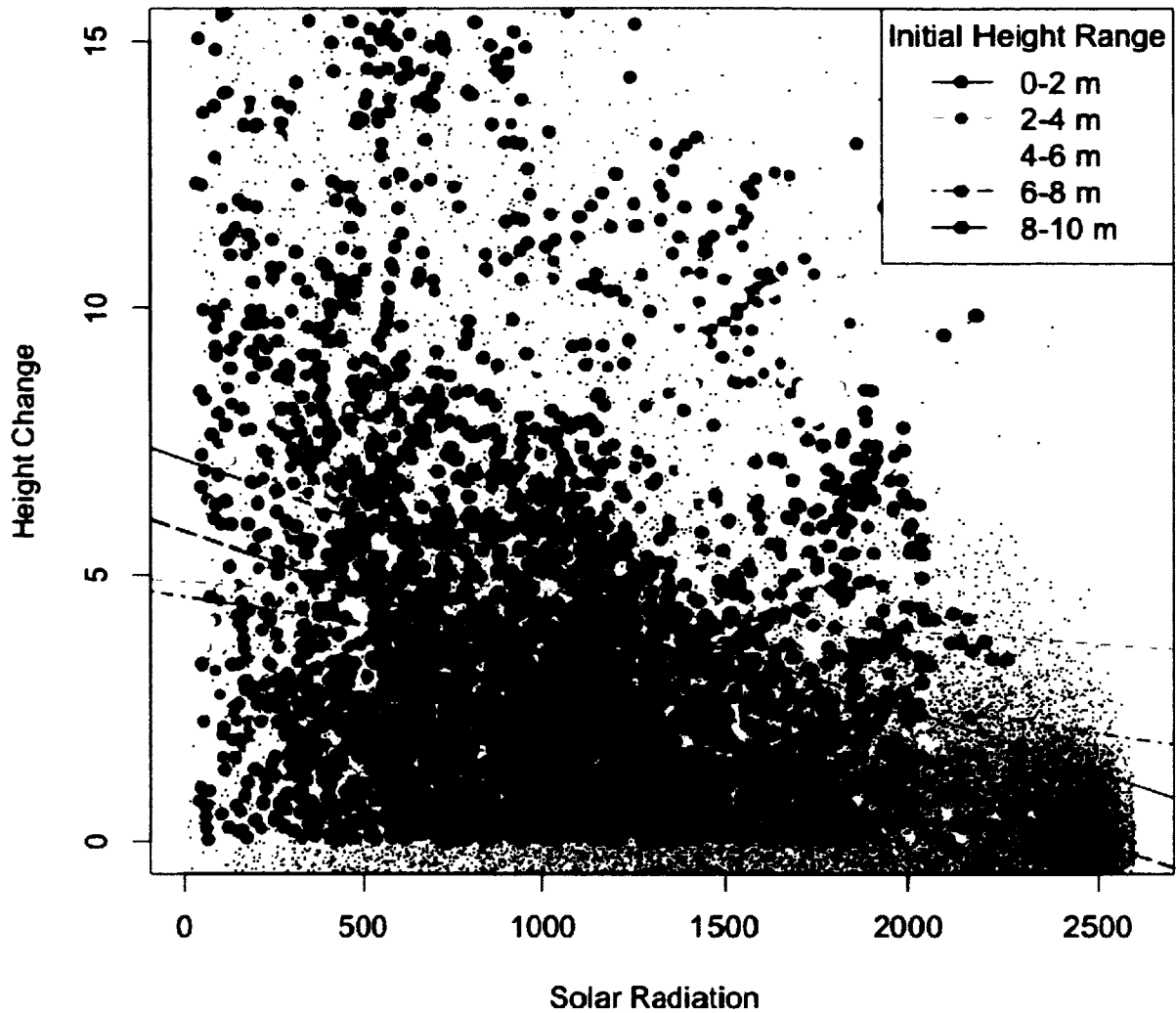


Figure 5.6 Correlation between incident solar radiation and height change for individual gap height bins of 2 m.

One potential explanation for this counter-intuitive result is the consideration of solar radiation at the pixel-scale. As individual crowns were not delineated, available solar radiation was not averaged to apply to the tree as a whole. This is expected to introduce an unknown error in the approximation of overall canopy illumination that would influence relationships between growth and light availability. Using area 6 as a test case, semi-variograms were run on the canopy height model and estimated solar radiation to look for differing scales of variability. The dominant scale of variation was significantly

longer for the canopy height model (25 m as opposed to 13 m) suggesting strong variability in light level within tree canopies.

The negative trend found between height increment and solar radiation is also not consistent with field data previously presented. Differences with presented field data may be partially methodological. In addition to the differences in scale mentioned above, the solar radiation model only takes into account stems reaching the outer canopy surface, therefore excluding suppressed vegetation subject to diffuse light only. In presenting results from our field inventory analysis, understory stems were considered alongside canopy and emergent trees. Stancioiu and O'Hara (2005) studied the effects of light availability on a fir-spruce forest in Romania and included overstory as well as understory vegetation. They showed that for silver fir the annual height increment decreases at high light levels as compared to moderate light. Given that the canopy surface is exposed to higher light environments, this may explain some pattern of decreasing height increment with increasing light.

Also, the effect of species level differences were not taken into account in this study. Responses to light variation have previously been shown to vary significantly dependent on both functional groupings and individual species without regard to function (Rüger et al. 2011b). In contrast, Coomes and Allen (2007) investigated a single species in New Zealand and found that competition for light had a strong influence on the growth of

small trees, but not larger stems whereas competition for nutrients affected trees of all sizes.

5.5 CONCLUSIONS

Field inventory measurements show increased diameter and crown radius increments with increased light availability, however, increases in height are not apparent. However, as positive diameter increment is correlated with positive height increment, we expect that height increment should also have a positive correlation with increased light availability. A potential cause for the lack of correlation in field measurements is the lower accuracy for measurements of height than diameter or crown radius.

Raw estimates of light availability are similar to expected values. Diffuse radiation accounts for a smaller portion than direct radiation at the canopy surface. Trends visible within the total solar radiation corresponded to expected differences. Low canopy height generally received lower solar radiation and small gaps showed lower incident radiation than large gaps.

Approximately 25% of the variability in vertical height change was explained by initial height and incident solar radiation. Solar radiation was a stronger predictor of height change than initial height. Height change showed a negative correlation with both initial height and solar radiation when modeled in a simplified framework. Though the negative

correlation was expected with regards to initial height, it was unexpected for solar radiation. These results may be due to the simplistic model treatment of light interaction with the canopy surface or bias in estimates of available solar radiation due to the absence of crown characterization. Other possibilities for this counter-intuitive result are the relative infrequency of extreme low light conditions that are common in the canopy understory most frequently studied in the field. Other possible explanations include the influence of species and physiological processes including nutrient competition and water availability that were not accounted for in this study.

CHAPTER SIX

CONCLUSION

PRIMARY RESULTS

The primary objective of this research was to quantify the effect of disturbance size and frequency on the rate and pattern of carbon cycling. Gap phase dynamics maintain high light environments within closed forest canopies and promote natural regeneration and turnover (Bormann and Likens 1979, Oliver and Larson 1996). The size of disturbance affects the degree to which light and nutrients are available (Denslow et al. 1990). Recent research has shown the particular importance of small and intermediate size gaps (less than 1 ha) at the landscape scale (Espirito-Santo et al. 2014b, Chambers et al. 2013).

Lidar is a remote sensing tool that is particularly well suited for ecological studies at the landscape scale as it can capture high density information on vegetation height and some stand structural characteristics. This information has been previously used to study variability in biomass, map gap size distributions and determine wildlife habitat (Drake et al. 2002b, Kellner et al. 2009, Vierling et al. 2008).

In chapter 2 I specifically addressed the consistency of lidar remote sensing, and variability of metrics as analysis scales changed. I found that certain metrics, including

the height of mean energy (HOME) and the percentage of returns near the ground surface were consistent between satellite and airborne platforms and across a multi-year time span. As lidar data is point based, maps of topography and forest structural characteristic are based on aggregations of the raw data at varying scales. Typically, a horizontal resolution is defined, and for some parameters (including height density) a vertical resolution as well, for summarizing the point data. I showed that the summary scale (both horizontal and vertical) led to significant variability in the outer canopy surface. Given the high degree of spatial variability, I concluded that small horizontal scales (0.5 - 1 m) were best for capturing canopy surface structure. I also addressed an assumption that has driven previous analysis of waveform lidar: self-similarity between the outer canopy surface (CHM) and the full patterns of returns. Independent of the summary scale applied, I concluded that canopy surface structure was not representative of the forest structure as a whole.

In chapter 3 I compared lidar and field measurements for estimation of total heights for canopy and emergent level trees. The difference between lidar and field estimates of height was small compared to the imprecision of field measurements of height (3 - 20%), resulting in an average uncertainty of 16% for individual stems. When scaled to the plot level, this lack of precision of height measurements led to 5 - 6% uncertainty in overall plot biomass. Despite uncertainties in height, carefully selected site-specific field measurements showed strong advantages over published regional and pan-tropical height allometries. In one case of four examined, the pan-tropical allometry led to an

underestimate of biomass by 25%. Measuring 100 stems in the field reduced plot-level variation in biomass to less than 5%. Using a combination of field and lidar measurements of height can likely reduce this error further.

While chapters 2 and 3 addressed specific issues with lidar remote sensing and biomass estimation, the remaining two chapters focused on patterns of disturbance and recovery and controls on these processes. In chapter 4, I quantified differences in canopy structure and gap size distribution and frequency between two well-studied sites in the Brazilian Amazon. I developed a gap definition that was based on measurable growth where gaps are defined as areas greater than 10 m² with vegetation < 10 m in height. Using this definition, I showed that average growth in gaps is similar at both sites despite the larger gap fraction at Tapajos National Forest, and faster turnover rate. By comparing gap centers to gap edges, I concluded that vertical growth was significantly higher at Tapajos National Forest as compared to Reserva Ducke but that the stronger signal of horizontal ingrowth at Reserva Ducke and more frequent repeat disturbance at Tapajos led to the similar numbers overall. With regard to controls over disturbance and recovery, in chapter 4 I further concluded that repeat disturbance within gap areas was frequent, accounting for 13% and 23% of gap area at Reserva Ducke and Tapajos National Forest respectively and that gap contagiousness occurred at both Tapajos National Forest and Reserva Ducke, but was limited to 6 - 8 m from gap edges.

In chapter 5, I investigated the extent to which variability in canopy height change is controlled by initial height and incident solar radiation. I modeled incident solar radiation using a detailed model of the canopy surface and I found that solar radiation was a much stronger predictor of height change than initial height, explaining 24% of variance compared to 13%. Gap size and initial canopy height controlled incident solar radiation, though significant variability was observed. Unexpectedly, initial height and solar radiation both showed negative correlations with height change. Whether this was driven by observations of the canopy surface as opposed to understory vegetation, or whether further parameters that were unaccounted for such as species variability with height or nutrient competition influenced observed patterns is an open question.

NEXT STEPS

This investigation led to advances in the understanding of forest structure and light controls on growth within the humid tropics. In chapter 4 I investigated gap creation and turnover at the landscape scale, and in chapter 5, addressed the importance of light to regrowth in local environments. In the future, I plan to scale-up analyses conducted as part of chapter 5 from individual 1 ha test areas to the landscape scale of the lidar data available (100s of ha). The additional information will help address how gap orientation and perimeter to area ratios effects light environments and subsequently, growth.

Additionally, I hope to continue to explore how forest structure and patterns of disturbance and growth translate into changes in above-ground biomass. This requires an understanding of patterns occurring throughout the matrix of forest vegetation, beyond surface processes. Further work to capitalize on the information available within airborne lidar beyond the simple use of canopy height models (CHMs) will be necessary.

Stark et al. (2012) published the results of a model that used lidar data to account for light availability throughout the vertical extent of the forest canopy at the 1 ha scale.

Interestingly, Stark's work explained a similar level of variability as the model used in chapter 5 that uses only the canopy surface. Stark's model integrated horizontally and this may result in a degradation of predictive ability. Perhaps light truly accounts for 25% of variability? Or perhaps an improved model of light availability that includes both horizontal and vertical variability will result in better predictions of growth?

One way to use a greater portion of the information provided by airborne lidar data is through synthesis with highly detailed models. The detailed radiative transfer model (DART) considers forest structure (Gastellu-Etchegorry 2008) based on a three-dimensional matrix of vegetation presence and absence. Lidar data may be used as inputs for this model (Morton et al. *in prep*). This model also allows for variability in cloud fraction throughout the day as well as the year, which may cause significant differences in light availability. While this model is specifically aimed to predicting light environment from scenes developed directly from airborne lidar or detailed field

measurements, other models that aim to predict carbon cycling may benefit from the detail of lidar generated scenes.

Recent work by Espírito-Santo et al. (2014a) shows that small gaps are the primary method of forest turnover in the Brazilian Amazon. Nearly 100% of biomass loss (99.98%) is due to disturbances less than 5 ha in size. Over 88% of mortality-induced biomass loss is due to gaps less than 0.1 ha. Chambers et al. (2013) further emphasizes the importance of small to intermediate gaps in forest turnover. They approximate 95% of disturbances consist of 15 or fewer trees, and nearly 99% of disturbances consisting of 82 trees or less (8 Landsat pixels or 0.7 ha). They further conclude that plots greater than 10 ha are necessary to determine temporal trends in biomass change within the Central Amazon.

Recent airborne sampling within the Brazilian Amazon as part of the Sustainable Landscapes project has collected data at several 1000 ha areas. Plots of 100 ha or greater can adequately characterize differences in small gap frequencies, as I showed in chapter 4. These landscape scale samples will allow for greater understanding of gap frequency and gap characteristic variability. By understanding disturbance patterns and regrowth at the landscape scale, as well as variability between landscapes, and the effect of these patterns on carbon stocks, regional and continental scales of carbon cycling can be better understood.

REFERENCES

- Andersen, H.-E., S. E. Reutebuch, and R. J. McGaughey. 2006. A rigorous assessment of tree height measurements obtained using airborne lidar and conventional field methods. *Canadian Journal of Remote Sensing* 32:355-366.
- Anhuf, D. and R. Rollenbeck. 2001. Canopy structure of the Rio Surumoni Rain Forest (Venezuela) and its influence on microclimate. *Ecotropica* 7:21-32.
- Asner, G. 2003. Canopy shadow in IKONOS satellite observations of tropical forests and savannas. *Remote Sensing of Environment* 87:521–533.
- Asner, G. P., and M. Keller. 2002. Estimating canopy structure in an Amazon forest from laser range finder and IKONOS satellite observations. *Biotropica* 34:483–492.
- Asner, G. P., J. Mascaro, H. C. Muller-Landau, G. Vieilledent, R. Vaudry, M. Rasamoelina, J. S. Hall, and M. V. Breugel. 2011. A universal airborne LiDAR approach for tropical forest carbon mapping. *Oecologia* 168:1147–1160.
- Asner, G. P., J. R. Kellner, T. Kennedy-Bowdoin, D. E. Knapp, C. Anderson, and R. E. Martin. 2013. Forest Canopy Gap Distributions in the Southern Peruvian Amazon. *PLoS ONE* 8:e60875.
- Asner, G., M. Palace, M. Keller, M. Pereira, J. Silva, and J. Zweede. 2012. LBA-ECO TG-07 Tree Geometry in an Undisturbed Forest in Cauaxi, Para, Brazil. Data set. Available on-line [<http://daac.ornl.gov>] from Oak Ridge National Laboratory Distributed Active Archive Center, Oak Ridge, Tennessee, U.S.A. <http://dx.doi.org/10.3334/ORNLDAAAC/1063>.
- Asner, G. P., M. Keller, R. Pereira, and J. Zweede. 2002. Remote sensing of selective logging in Amazonia-Assessing limitations based on detailed field observations, Landsat ETM+, and textural analysis. *Remote Sensing of Environment* 80:483–496.
- Asner, G. P., M. Keller, R. Pereira, J. Zweede, and J. N. M. Silva. 2004. Canopy damage and recovery after selective logging in Amazonia: field and satellite studies. *Ecological Applications* 14:S280–S298.

- Baccini, A., S. J. Goetz, W. S. Walker, N. T. Laporte, M. Sun, D. Sulla-Menashe, J. Hackler, P. Beck, R. Dubayah, and M. A. Friedl. 2012. Estimated carbon dioxide emissions from tropical deforestation improved by carbon-density maps. *Nature Climate Change* 2:182–185.
- Balch, J. K., D. C. Nepstad, and L. Curran. 2010. Size, species, and fire behavior predict tree and liana mortality from experimental burns in the Brazilian Amazon. *Forest Ecology and Management* 261:68–77.
- Balch, J. K., D. C. Nepstad, and P. M. Brando. 2008. Negative fire feedback in a transitional forest of southeastern Amazonia. *Global Change Biology* 14:2276–2287.
- Basuki, T. M., P. E. van Laake, A. K. Skidmore, and Y. A. Hussin. 2009. Allometric equations for estimating the above-ground biomass in tropical lowland Dipterocarp forests. *Forest Ecology and Management* 257:1684–1694.
- Blair, J., and M. Hofton. 1999. Modeling laser altimeter return waveforms over complex vegetation using high-resolution elevation data. *Geophysical Research Letters* 26:2509–2512.
- Bormann, F. H., and G. E. Likens. 1979. Catastrophic Disturbance and the Steady State in Northern Hardwood Forests: A new look at the role of disturbance in the development of forest ecosystems suggests important implications for land-use policies. *American Scientist* 67:660–669.
- Boyd, D. S., R. A. Hill, C. Hopkinson, and T. R. Baker. 2013. Landscape-scale forest disturbance regimes in southern Peruvian Amazonia. *Ecological Applications* 23:1588–1602.
- Brokaw, N. V. L. 1982. The Definition of Treefall Gap and Its Effect on Measures of Forest Dynamics. *Biotropica* 14:158–160.
- Brokaw, N. V. L. 1985. Gap-Phase Regeneration in a Tropical Forest. *Ecology* 66:682–687.
- Brokaw, N. V. L. 1987. Gap-phase Regeneration of Three Pioneer Tree Species in a Tropical Forest. *The Journal of Ecology* 75:9–19.
- Brokaw, N., and R. T. Busing. 2000. Niche versus chance and tree diversity in forest gaps. *Trends in Ecology & Evolution* 15:183–188.

- Brown, N. 1996. A gradient of seedling growth from the centre of a tropical rain forest canopy gap. *Forest Ecology and Management* 82:239–244.
- Butt, N., M. New, Y. Malhi, A. C. L. da Costa, P. Oliveira, and J. E. Silva-Espejo. 2010. Diffuse radiation and cloud fraction relationships in two contrasting Amazonian rainforest sites. *Agricultural and Forest Meteorology* 150:361–368.
- Campbell, D. G., D. C. Daly, G. T. Prance, and U. N. Maciel. 1986. Quantitative ecological inventory of terra firme and várzea tropical forest on the Rio Xingu, Brazilian Amazon. *Brittonia* 38:369–393.
- Canham, C. D., J. S. Denslow, W. J. Platt, J. R. Runkle, T. A. Spies, and P. S. White. 1990. Light regimes beneath closed canopies and tree-fall gaps in temperate and tropical forests. *Canadian Journal of Forest Research* 20:620–631.
- Cannell, M., and J. Grace. 1993. Competition for light: detection, measurement, and quantification - *Canadian Journal of Forest Research*. *Canadian Journal of Forest Research* 23:1969–1979.
- Chambers, J. Q., J. Santos, R. Ribeiro, and N. Higuchi. 2001. Tree damage, allometric relationships, and above-ground net primary production in central Amazon forest. *Forest Ecology and Management* 152:73–84.
- Chambers, J. Q., R. I. Negron-Juarez RI, G. C. Hurtt, D. M. Marra, and N. Higuchi. 2009. Lack of intermediate-scale disturbance data prevents robust extrapolation of plot-level tree mortality rates for old-growth tropical forests. *Ecology Letters* 12:E22–E25.
- Chambers, J. Q., R. I. Negrón Juárez, D. M. Marra, A. Di Vittorio, J. Tews, D. A. Roberts, G. H. P. M. Ribeiro, S. E. Trumbore, and N. Higuchi. 2013. The steady-state mosaic of disturbance and succession across an old-growth Central Amazon forest landscape. *Proceedings of the National Academy of Sciences* 110:3949–3954.
- Chao, K.-J., O. L. Phillips, A. Monteagudo, A. Torres Lezama, and R. Vásquez Martínez. 2009. How do trees die? Mode of death in northern Amazonia. *Journal of Vegetation Science* 20:260–268.
- Chasmer, L., C. Hopkinson, and P. Treitz. 2006. Investigating laser pulse penetration through a conifer canopy by integrating airborne and terrestrial lidar. *Canadian Journal of Remote Sensing* 32:116–125.
- Chauvel, A., Y. Lucas, and R. Boulet. 1987. On the genesis of the soil mantle of the region of Manaus, Central Amazonia, Brazil. *Experientia* 43:234–241.

- Chave, J. 2005. Measuring tree height for tropical forest trees: A field manual for the CTFS sites, www.ctfs.si.edu.
- Chave, J., C. Andalo, S. Brown, M. A. Cairns, J. Q. Chambers, D. Eamus, H. Fölster, F. Fromard, N. Higuchi, and T. Kira. 2005. Tree allometry and improved estimation of carbon stocks and balance in tropical forests. *Oecologia* 145:87–99.
- Chave, J., R. S. Condit, S. Lao, and J. Caspersen. 2003. Spatial and temporal variation of biomass in a tropical forest: results from a large census plot in Panama. *Journal of Ecology* 91:240–252.
- Chen, Q. 2007. Airborne lidar data processing and information extraction. *Photogrammetric Engineering and Remote Sensing* 73:109.
- Clark, D. B., and J. R. Kellner. 2012. Tropical forest biomass estimation and the fallacy of misplaced concreteness. *Journal of Vegetation Science* 23:1191–1196.
- Clark, M., D. Clark, and D. A. Roberts. 2004. Small-footprint lidar estimation of sub-canopy elevation and tree height in a tropical rain forest landscape. *Remote Sensing of Environment* 91:68-89.
- Clauset, A., C. Shalizi, and M. Newman. 2009. Power-law distributions in empirical data. *Society for Industrial and Applied Mathematics Review* 51:661–703.
- Cochrane, M. A. 2003. Fire science for rainforests. *Nature* 421:913–919.
- Cook, B., L. Corp, R. Nelson, E. Middleton, D. Morton, J. McCorkel, J. Masek, K. Ranson, V. Ly, and P. Montesano. 2013. NASA Goddard's LiDAR, Hyperspectral and Thermal (G-LiHT) Airborne Imager. *Remote Sensing* 5:4045–4066.
- Coomes, D. A., and R. B. Allen. 2007. Effects of size, competition and altitude on tree growth. *Journal of Ecology* 95:1084–1097.
- de Castilho, C. V., W. E. Magnusson, R. N. O. de Araújo, R. C. C. Luizão, F. J. Luizão, A. P. Lima, and N. Higuchi. 2006. Variation in aboveground tree live biomass in a central Amazonian Forest: Effects of soil and topography. *Forest Ecology and Management* 234:85–96.
- De Oliveira, A. A., and S. A. Mori. 1999. A central Amazonian terra firme forest. I. High tree species richness on poor soils. *Biodiversity and Conservation* 8:1219-1244.

- De Steven, D. 1988. Light Gaps and Long-Term Seedling Performance of a Neotropical Canopy Tree (*Dipteryx panamensis*, Leguminosae). *Journal of Tropical Ecology* 4:407–411.
- de Toledo, J. J., W. E. Magnusson, C. V. Castilho, and H. E. M. Nascimento. 2012. Tree mode of death in Central Amazonia: Effects of soil and topography on tree mortality associated with storm disturbances. *Forest Ecology and Management* 263:253–261.
- Denslow, J. S. 1987. Tropical rainforest gaps and tree species diversity. *Annual Review of Ecology and Systematics* 18:431–451.
- Denslow, J. S., A. M. Ellison, and R. E. Sanford. 1998. Treefall gap size effects on above- and below-ground processes in a tropical wet forest. *Journal of Ecology* 86:597–609.
- Denslow, J. S., J. C. Schultz, P. M. Vitousek, and B. R. Strain. 1990. Growth responses of tropical shrubs to treefall gap environments. *Ecology* 71:165–179.
- Duong, H., Lindenbergh, R., Pfeifer, N. and Vosselman, G. (2008). Single and two epoch analysis of ICESat full waveform data over forested areas. *International Journal of Remote Sensing*. 29:1453-1473.
- Drake, J., R. Dubayah, D. B. Clark, R. Knox, J. Blair, M. Hofton, R. Chazdon, J. Weishampel, and S. Prince. 2002a. Estimation of tropical forest structural characteristics using large-footprint lidar. *Remote Sensing of Environment* 79:305–319.
- Drake, J., R. Dubayah, R. Knox, D. B. Clark, and J. Blair. 2002b. Sensitivity of large-footprint lidar to canopy structure and biomass in a neotropical rainforest. *Remote Sensing of Environment* 81:378–392.
- Efron, B., and R. J. Tibshirani. 1994. *An Introduction to the Bootstrap*. First edition. Chapman and Hall/CRC, New York.
- Espirito-Santo, F., M. Keller, B. Braswell, B. W. Nelson, S. Frohling, and G. Vicente. 2010. Storm intensity and old-growth forest disturbances in the Amazon region. *Geophysical Research Letters* 37:L11403.
- Espirito-Santo, F. D. B., M. Gloor, M. Keller, Y. Malhi, S. Saatchi, B. Nelson, R. C. O. Junior, C. Pereira, J. Lloyd, S. Frohling, M. Palace, Y. E. Shimabukuro, V. Duarte, A. M. Mendoza, G. López-González, T. R. Baker, T. R. Feldpausch, R. J. W. Brienen, G. P. Asner, D. S. Boyd, and O. L. Phillips. 2014a. Size and frequency of

natural forest disturbances and the Amazon forest carbon balance. *Nature Communications* 5:1–6.

- Espírito-Santo, F. D. B., M. M. Keller, E. Linder, R. C. Oliveira Junior, C. Pereira, and C. G. Oliveira. 2014b. Gap formation and carbon cycling in the Brazilian Amazon: measurement using high-resolution optical remote sensing and studies in large forest plots. *Plant Ecology & Diversity* 7:305-318.
- Estornell, J., L. A. Ruiz, B. Velázquez-Martí, and A. Fernández-Sarría. 2011. Estimation of shrub biomass by airborne LiDAR data in small forest stands. *Forest Ecology and Management* 262:1697–1703.
- Feldpausch, T. R., J. Lloyd, S. L. Lewis, R. J. W. Brienen, M. Gloor, A. M. Mendoza, G. Lopez-Gonzalez, L. Banin, K. A. Salim, K. Affum-Baffoe, M. Alexiades, S. Almeida, I. Amaral, A. Andrade, L. E. O. C. Aragão, A. A. Murakami, E. J. M. M. Arets, L. Arroyo, G. A. A. C, T. R. Baker, O. S. Bánki, N. J. Berry, N. Cardozo, J. Chave, J. A. Comiskey, E. Alvarez, A. de Oliveira, A. Di Fiore, G. Djagbletey, T. F. Domingues, T. L. Erwin, P. M. Fearnside, M. B. França, M. A. Freitas, N. Higuchi, E. H. C, Y. Iida, E. Jiménez, A. R. Kassim, T. J. Killeen, W. F. Laurance, J. C. Lovett, Y. Malhi, B. S. Marimon, B. H. Marimon-Junior, E. Lenza, A. R. Marshall, C. Mendoza, D. J. Metcalfe, E. T. A. Mitchard, D. A. Neill, B. W. Nelson, R. Nilus, E. M. Nogueira, A. Parada, K. S. H. Peh, A. P. Cruz, M. C. Peñuela, N. C. A. Pitman, A. Prieto, C. A. Quesada, F. Ramírez, H. Ramírez-Angulo, J. M. Reitsma, A. Rudas, G. Saiz, R. P. Salomão, M. Schwarz, N. Silva, J. E. Silva-Espejo, M. Silveira, B. Sonke, J. Stropp, H. E. Taedoumg, S. Tan, H. ter Steege, J. Terborgh, M. Torello-Raventos, G. M. F. van der Heijden, R. Vásquez, E. Vilanova, V. A. Vos, L. White, S. Willcock, H. Woell, and O. L. Phillips. 2012. Tree height integrated into pantropical forest biomass estimates. *Biogeosciences* 9:3381-3403.
- Feldpausch, T. R., L. Banin, O. L. Phillips, T. R. Baker, S. L. Lewis, C. A. Quesada, K. Affum-Baffoe, E. J. M. M. Arets, N. J. Berry, M. Bird, E. S. Brondizio, P. B. de Camargo, J. Chave, G. Djagbletey, T. F. Domingues, M. Drescher, P. M. Fearnside, M. B. França, N. M. Fyllas, G. López-Gonzalez, A. Hladik, N. Higuchi, M. O. Hunter, Y. Iida, K. A. Salim, A. R. Kassim, M. Keller, J. Kemp, D. A. King, J. C. Lovett, B. S. Marimon, B. H. Marimon-Junior, E. Lenza, A. R. Marshall, D. J. Metcalfe, E. T. A. Mitchard, E. F. Moran, B. W. Nelson, R. Nilus, E. M. Nogueira, M. Palace, S. Patiño, K. S. H. Peh, M. T. Raventos, J. M. Reitsma, G. Saiz, F. Schrod, B. Sonké, H. E. Taedoumg, S. Tan, L. White, H. Wöll, and J. Lloyd. 2011. Height-diameter allometry of tropical forest trees. *Biogeosciences* 8:1081–1106.

- Ferry, B., F. Morneau, J.-D. Bontemps, L. Blanc, and V. Freycon. 2010. Higher treefall rates on slopes and waterlogged soils result in lower stand biomass and productivity in a tropical rain forest. *Journal of Ecology* 98:106–116.
- Forzieri, G., L. Guarnieri, E. Vivoni, F. Castelli, and F. Preti. 2009. Multiple attribute decision making for individual tree detection using high-resolution laser scanning. *Forest Ecology and Management* 258:2501–2510.
- Franklin, J. F., T. A. Spies, R. V. Pelt, A. B. Carey, D. A. Thornburgh, D. R. Berg, D. B. Lindenmayer, M. E. Harmon, W. S. Keeton, D. C. Shaw, K. Bible, and J. Chen. 2002. Disturbances and structural development of natural forest ecosystems with silvicultural implications, using Douglas-fir forests as an example. *Forest Ecology and Management* 155:399–423.
- Frazer, G., M. A. Wulder, and K. Niemann. 2005. Simulation and quantification of the fine-scale spatial pattern and heterogeneity of forest canopy structure: A lacunarity-based method designed for analysis of continuous canopy heights. *Forest Ecology and Management* 214:65–90.
- Fredericksen, T., and W. Pariona. 2002. Effect of skidder disturbance on commercial tree regeneration in logging gaps in a Bolivian tropical forest. *Forest Ecology and Management* 171:223–230.
- Fu, P., and P. M. Rich. 2002. A geometric solar radiation model with applications in agriculture and forestry. *Computers and Electronics in Agriculture* 37:25-35.
- Fu, P., P. M. Rich, and J. Wang. 2000. Integration of GIS with user models. *Proceedings of the Twentieth Annual ESRI User Conference* 1:1-6.
- Gale, N., and A. S. Barfod. 1999. Canopy tree mode of death in a western Ecuadorian rain forest. *Journal of Tropical Ecology* 15:415–436.
- Gale, N., and P. Hall. 2001. Factors determining the modes of tree death in three Bornean rain forests. *Journal of Vegetation Science* 12:337–348.
- Gastellu-Etchegorry, J. P. 2008. 3D modeling of satellite spectral images, radiation budget and energy budget of urban landscapes. *Meteorology and Atmospheric Physics* 102:187–207.
- Gaulton, R., and T. J. Malthus. 2010. LiDAR mapping of canopy gaps in continuous cover forests: A comparison of canopy height model and point cloud based techniques. *International Journal of Remote Sensing* 31:1193–1211.

- Gaveau, D., and R. A. Hill. 2003. Quantifying canopy height underestimation by laser pulse penetration in small-footprint airborne laser scanning data - Canadian Journal of Remote Sensing. *Canadian Journal of Remote Sensing* 29:650-657.
- Gibbs, H. K., S. Brown, J. O. Niles, and J. A. Foley. 2007. Monitoring and estimating tropical forest carbon stocks: making REDD a reality. *Environmental Research Letters* 2:045023.
- Gillespie, A., S. Brown, and A. Lugo. 1992. Tropical forest biomass estimation from truncated stand tables. *Forest Ecology and Management* 48:69–87.
- Gloor, E. U., O. L. Phillips, J. J. Lloyd, S. L. Lewis, Y. Malhi, T. R. Baker, G. López-Gonzalez, J. Peacock, S. Almeida, A. C. A. De Oliveira, E. Alvarez, I. Amaral, L. Arroyo, G. Aymard, O. Banki, L. Blanc, D. Bonal, P. M. Brando, K.-J. Chao, J. Chave, N. Dávila, T. Erwin, J. N. M. Silva, A. Di Fiore, T. R. Feldpausch, A. Freitas, R. Herrera, N. Higuchi, E. Honorio, E. Jiménez, T. Killeen, W. Laurance, C. Mendoza, A. Monteagudo, A. Andrade, D. Neill, D. C. Nepstad, P. N. Vargas, M. C. Peñuela, A. P. Cruz, A. Prieto, N. C. A. Pitman, C. Quesada, R. Salomão, M. Silveira, M. Schwarz, J. Stropp, F. Ramírez, H. Ramírez, A. Rudas, H. Ter Steege, N. Silva, A. Torres Lezama, J. Terborgh, R. Vasquez, and G. Van Der Heijden. 2009. Does the disturbance hypothesis explain the biomass increase in basin-wide Amazon forest plot data? *Global Change Biology* 15:2418–2430.
- Goetz, S., D. Steinberg, R. Dubayah, and J. Blair. 2007. Laser remote sensing of canopy habitat heterogeneity as a predictor of bird species richness in an eastern temperate forest, USA. *Remote Sensing of Environment* 108:254–263.
- Golser, M., and H. Hasenauer. 1997. Predicting juvenile tree height growth in uneven-aged mixed species stands in Austria. *Forest Ecology and Management* 97:133-146.
- Goodwin, A.N. 2004. Measuring Tall Tree Heights from the Ground. *Tasforests* 15: 85 - 97.
- Harding, D. J., and C. C. Carabajal. 2005. ICESat waveform measurements of within-footprint topographic relief and vegetation vertical structure. *Geophysical Research Letters* 32:L21S10.
- Harding, D. J., M. A. Lefsky, G. Parker, and J. Blair. 2001. Laser altimeter canopy height profiles: Methods and validation for closed-canopy, broadleaf forests. *Remote Sensing of Environment* 76:283–297.

- Hijmans, R. J., S. E. Cameron, J. L. Parra, P. G. Jones, and A. Jarvis. 2005. Very high resolution interpolated climate surfaces for global land areas. *International Journal of Climatology* 25:1965–1978.
- Hilker, T., M. Leeuwen, N. C. Coops, M. A. Wulder, G. J. Newnham, D. L. Jupp, and D. S. Culvenor. 2010. Comparing canopy metrics derived from terrestrial and airborne laser scanning in a Douglas-fir dominated forest stand. *Trees* 24:819–832.
- Houghton, R. A. 2005. Aboveground Forest Biomass and the Global Carbon Balance - Houghton. *Global Change Biology* 11:945-958.
- Huang, M., G. P. Asner, M. Keller, and J. A. Berry. 2008. An ecosystem model for tropical forest disturbance and selective logging. *Journal of Geophysical Research-Biogeosciences* 113:1–23.
- Hubbell, S. P., and R. B. Foster. 1986. Canopy Gaps and the Dynamics of a Neotropical Forest. Pages 77–96 in M. Crawley, editor. *Plant Ecology*. Blackwell Publishing Inc, Oxford, UK.
- Hubbell, S. P., R. B. Foster, S. T. O'Brien, K. E. Harms, R. S. Condit, B. Wechsler, S. J. Wright, and S. Loo de Lau. 1999. Light-Gap Disturbances, Recruitment Limitation, and Tree Diversity in a Neotropical Forest. *Science* 283:554–557.
- Hunter, M. O., M. Keller, D. Victoria, and D. C. Morton. 2013. Tree height and tropical forest biomass estimation. *Biogeosciences* 10:8385–8399.
- Hutyra, L. R., S. C. Wofsy, and S. R. Saleska. 2007. LBA-ECO CD-10 CO₂ and H₂O Eddy Flux Data at km 67 Tower Site, Tapajos National Forest. Oak Ridge National Laboratory Distributed Active Archive Center, Oak Ridge, TN, USA.
- Jansen, P. A., P. J. V. Meer, and F. Bongers. 2008. Spatial contagiousness of canopy disturbance in tropical rain forest: An individual-tree-based test. *Ecology* 89:3490–3502.
- Keller, M., A. Alencar, G. P. Asner, B. Braswell, M. M. C. Bustamante, E. Davidson, T. R. Feldpausch, E. C. Fernandes, M. Goulden, and P. Kabat. 2004. Ecological research in the large-scale biosphere-atmosphere experiment in Amazonia: early results. *Ecological Applications* 14:3–16.
- Keller, M., M. Palace, and G. C. Hurtt. 2001. Biomass estimation in the Tapajos National Forest, Brazil Examination of sampling and allometric uncertainties. *Forest Ecology and Management* 154:371–382.

- Kellner, J. R., and G. P. Asner. 2009. Convergent structural responses of tropical forests to diverse disturbance regimes. *Ecology Letters* 12:887–897.
- Kellner, J. R., D. B. Clark, and S. P. Hubbell. 2009. Pervasive canopy dynamics produce short-term stability in a tropical rain forest landscape. *Ecology Letters* 12:155–164.
- Larjavaara, M., and H. C. Muller-Landau. 2013. Measuring tree height: a quantitative comparison of two common field methods in a moist tropical forest. *Methods in Ecology and Evolution* 4:793–801.
- Laurance, W. F., L. V. Ferreira, J. M. R.-D. Merona, and S. G. Laurance. 1998. Rain Forest Fragmentation and the Dynamics of Amazonian Tree Communities. *Ecology* 79:2032–2040.
- Le Toan, T., S. Quegan, M. W. J. Davidson, H. Balzter, P. Paillou, K. Papathanassiou, S. Plummer, F. Rocca, S. S. Saatchi, H. Shugart, and L. Ulander. 2011. The BIOMASS mission: Mapping global forest biomass to better understand the terrestrial carbon cycle. *Remote Sensing of Environment* 115:2850–2860.
- Lee, A., and R. Lucas. 2007. A LiDAR-derived canopy density model for tree stem and crown mapping in Australian forests. *Remote Sensing of Environment* 111:493–518.
- Lefsky, M. A., D. J. Harding, M. Keller, W. B. Cohen, C. C. Carabajal, F. Del Bom Espirito-Santo, M. O. Hunter, and R. C. De Oliveira Jr. 2005a. Estimates of forest canopy height and aboveground biomass using ICESat. *Geophysical Research Letters* 32:1–4.
- Lefsky, M. A., D. J. Harding, W. B. Cohen, G. Parker, and H. H. Shugart. 1999a. Surface lidar remote sensing of basal area and biomass in deciduous forests of eastern Maryland, USA. *Remote Sensing of Environment* 67:83–98.
- Lefsky, M. A., D. Turner, M. Guzy, and W. B. Cohen. 2005b. Combining lidar estimates of aboveground biomass and Landsat estimates of stand age for spatially extensive validation of modeled forest productivity. *Remote Sensing of Environment* 95:549–558.
- Lefsky, M. A., M. Keller, Y. Pang, P. B. de Camargo, and M. O. Hunter. 2007. Revised method for forest canopy height estimation from Geoscience Laser Altimeter System waveforms. *Journal of Applied Remote Sensing* 1:013537.

- Lefsky, M. A., W. B. Cohen, G. Parker, and D. J. Harding. 2002. Lidar remote sensing for ecosystem studies. *BioScience* 52:19–30.
- Lefsky, M. A., W. B. Cohen, S. Acker, G. Parker, T. Spies, and D. J. Harding. 1999b. Lidar remote sensing of the canopy structure and biophysical properties of Douglas-fir western hemlock forests. *Remote Sensing of Environment* 70:339–361.
- Leitold, V. 2009. Canopy structure and function in the Tapajós National Forest in equatorial Amazonia, Brazil. Undergraduate Thesis. Harvard University.
- Lewis, S. L., J. J. Lloyd, S. Sitch, E. Mitchard, and W. Laurance. 2009. Changing ecology of tropical forests: evidence and drivers. *Annual review of ecology, evolution, and systematics* 40:529–549.
- Lieberman, D., M. Lieberman, R. Peralta, and G. S. Hartshorn. 1985. Mortality patterns and stand turnover rates in a wet tropical forest in Costa Rica. *The Journal of Ecology* 73:915–924.
- Lima, A., R. Suwa, and G. de Mello Ribeiro. 2012. Allometric models for estimating above- and below-ground biomass in Amazonian forests at São Gabriel da Cachoeira in the upper Rio Negro, Brazil. *Forest Ecology and Management* 277:163–172.
- Litton, C. M., and J. Boone Kauffman. 2008. Allometric Models for Predicting Aboveground Biomass in Two Widespread Woody Plants in Hawaii. *Biotropica* 40:313–320.
- Lloyd, J. J., E. U. Gloor, and S. L. Lewis. 2009. Are the dynamics of tropical forests dominated by large and rare disturbance events? *Ecology Letters* 12:E19–E21.
- Lobo, E., and J. W. Dalling. 2014. Spatial scale and sampling resolution affect measures of gap disturbance in a lowland tropical forest: implications for understanding forest regeneration and carbon storage. *Proceedings of the Royal Society B: Biological Sciences* 281:20133218–20133218.
- Lovell, J., D. L. Jupp, D. Culvenor, and N. C. Coops. 2003. Using airborne and ground-based ranging lidar to measure canopy structure in Australian forests. *Canadian Journal of Remote Sensing* 29:607–622.
- MacArthur, R.H. and Horn, H.S. (1969). Foliage profile by vertical measurements. *Ecology*. 50:802-804.

- Machado, J.-L., and P. B. Reich. 1999. Evaluation of several measures of canopy openness as predictors of photosynthetic photon flux density in deeply shaded conifer-dominated forest understory. *Canadian Journal of Forest Research* 29:1438–1444.
- Maia Araújo, T., N. Higuchi, and J. Andrade de Carvalho Júnior. 1999. Comparison of formulae for biomass content determination in a tropical rain forest site in the state of Pará, Brazil. *Forest Ecology and Management* 117:43–52.
- Marthews, T., D. Burslem, R. Phillips, and C. Mullins. 2008. Modelling Direct Radiation and Canopy Gap Regimes in Tropical Forests. *Biotropica* 40:676–685.
- Martinuzzi, S., L. A. Vierling, and W. A. Gould. 2009. Mapping snags and understory shrubs for a LiDAR-based assessment of wildlife habitat suitability. *Remote Sensing of Environment* 113:2533-2546.
- Metcalf, C. J. E., C. C. Horvitz, S. Tuljapurkar, and D. A. Clark. 2009. A time to grow and a time to die: a new way to analyze the dynamics of size, light, age, and death of tropical trees. *Ecology* 90:2766–2778.
- Miura, N., and S. D. Jones. 2010. Characterizing forest ecological structure using pulse types and heights of airborne laser scanning. *Remote Sensing of Environment* 114:1069–1076.
- Molino, J.-F., and D. Sabatier. 2001. Tree diversity in tropical rain forests: a validation of the intermediate disturbance hypothesis. *Science* 294:1702–1704.
- Molto, Q., V. Rossi, and L. Blanc. 2013. Error propagation in biomass estimation in tropical forests. *Methods in Ecology and Evolution* 4:175-183.
- Montgomery, R. A., and R. L. Chazdon. 2001. Forest structure, canopy architecture, and light transmittance in tropical wet forests. *Ecology* 82:2707–2718.
- Morsdorf, F., A. Márell, B. Koetz, N. Cassagne, F. Pimont, E. Rigolot, and B. Allgöwer. 2010. Discrimination of vegetation strata in a multi-layered Mediterranean forest ecosystem using height and intensity information derived from airborne laser scanning. *Remote Sensing of Environment* 114:1403-1415.
- Muller-Landau, H. C., R. S. Condit, J. Chave, S. C. Thomas, S. Bohlman, S. Bunyavejchewin, S. J. Davies, R. Foster, S. Gunatilleke, and N. Gunatilleke. 2006. Testing metabolic ecology theory for allometric scaling of tree size, growth and mortality in tropical forests. *Ecology Letters* 9:575–588.

- Naesset, E., and T. Okland. 2002. Estimating tree height and tree crown properties using airborne scanning laser in a boreal nature reserve. *Remote Sensing of Environment* 79:105–115.
- Nath, C., H. S. Dattaraja, H. S. Suresh, N. Joshi, and R. Sukumar. 2006. Patterns of tree growth in relation to environmental variability in the tropical dry deciduous forest at Mudumalai, southern India. *Journal of Biosciences* 31:651–669.
- Negron-Juarez RI, R. I., J. Q. Chambers, D. M. Marra, G. H. P. M. Ribeiro, S. W. Rifai, N. Higuchi, and D. A. Roberts. 2011. Detection of subpixel treefall gaps with Landsat imagery in Central Amazon forests. *Remote Sensing of Environment* 115:3322–3328.
- Nelson, R. 2010. Model effects on GLAS-based regional estimates of forest biomass and carbon. *International Journal of Remote Sensing* 31:1359–1372.
- Nelson, R., W. Krabill, and J. Tonelli. 1988. Estimating forest biomass and volume using airborne laser data. *Remote Sensing of Environment* 24:247–267.
- Neuenschwander, A.L., Urban, T.J., Gutierrez, R. and Schutz, B.E. 2008. Characterization of ICESat/GLAS waveforms over terrestrial ecosystems: Implications for vegetation mapping, *Journal of Geophysical Research*. 113:G02S03.
- Oliver, C. D., and B. C. Larson. 1996. *Forest stand dynamics*. John Wiley and Sons, New York.
- Ørka, H. O., E. Næsset, and O. M. Bollandsås. 2010. Effects of different sensors and leaf-on and leaf-off canopy conditions on echo distributions and individual tree properties derived from airborne laser scanning. *Remote Sensing of Environment* 114:1445–1461.
- Palace, M.W., Hagen, S.C., Bustamante, M., Ferreira, L.G. and Miranda, S. (2010). Fusing Radar, Lidar and High Resolution Optical Remotely Sensed Data to Estimate Vegetation Structure in the Brazilian Cerrado. *EOS Transactions AGU Meeting of the Americas Supplement*. 91:B21A-08 Poster.
- Palace, M., M. Keller, G. P. Asner, J. N. M. Silva, and C. Passos. 2007. Necromass in undisturbed and logged forests in the Brazilian Amazon. *Forest Ecology and Management* 238:309–318.
- Pang, Y., M. Lefsky, H. Andersen, M. E. Miller, and K. R. Sherrill. 2008. Validation of the ICESat vegetation product using crown-area-weighted mean height derived

- using crown delineation with discrete return lidar data. *Canadian Journal of Remote Sensing* 34:471–484.
- Parker, G., and M. Russ. 2004. The canopy surface and stand development: assessing forest canopy structure and complexity with near-surface altimetry. *Forest Ecology and Management* 189:307–315.
- Parker, G., M. A. Lefsky, and D. J. Harding. 2001. Light transmittance in forest canopies determined using airborne laser altimetry and in-canopy quantum measurements. *Remote Sensing of Environment* 76:298–309.
- Pereira, R., J. Zweede, G. P. Asner, and M. Keller. 2002. Forest canopy damage and recovery in reduced-impact and conventional selective logging in eastern Para, Brazil. *Forest Ecology and Management* 168:77–89.
- Pesonen, A., M. Maltamo, and A. Kangas. 2010. The comparison of airborne laser scanning-based probability layers as auxiliary information for assessing coarse woody debris. *International Journal of Remote Sensing* 31:1245–1259.
- Phillips, O. L., Y. Malhi, N. Higuchi, W. Laurance, P. Núñez, R. Vasquez, S. Laurance, L. Ferreira, M. Stern, and S. Brown. 1998. Changes in the carbon balance of tropical forests: evidence from long-term plots. *Science* 282:439-442.
- Poorter, L., L. Jans, F. Bongers, and R. S. A. R. Van Rompaey. 2009. Spatial distribution of gaps along three catenas in the moist forest of Taï National Park, Ivory Coast. *Journal of Tropical Ecology* 10:385-398.
- Popescu, S., R. Wynne, and R. Nelson. 2002. Estimating plot-level tree heights with lidar: local filtering with a canopy-height based variable window size. *Computers and Electronics in Agriculture* 37:71–95.
- Poulson, T., and W. Platt. 1989. Gap light regimes influence canopy tree diversity. *Ecology* 70:553–555.
- Putz, F. E., P. D. Coley, K. Lu, A. Montalvo, and A. Aiello. 1983. Uprooting and snapping of trees: structural determinants and ecological consequences. *Canadian Journal of Forest Research* 13:1011–1020.
- Pyle, E. H., G. W. Santoni, H. E. M. Nascimento, L. R. Huttyra, S. Vieira, D. J. Curran, J. van Haren, S. R. Saleska, V. Y. Chow, P. B. Carmago, W. F. Laurance, and S. C. Wofsy. 2008. Dynamics of carbon, biomass, and structure in two Amazonian forests. *Journal of Geophysical Research-Biogeosciences* 113:G00B08.

- Radambrasil. 1983. Levantamento de Recursos Naturais. Rio de Janeiro/Vitória: geologia, geomorfologia, pedologia, vegetação e uso potencial da terra. Ministério de Minas e Energia, folhas SF.
- RAINFOR. 2009. Field Manual for Plot Establishment and Remeasurement. www.rainfor.org.
- Ray, D., D. Nepstad, and P. Moutinho. 2005. Micrometeorological and canopy controls of fire susceptibility in a forested Amazon landscape. *Ecological Applications* 15:1664–1678.
- Rennie, J. C. 1979. Comparison of Height-Measurement Techniques in a Dense Loblolly Pine Plantation. *Southern Journal of Applied Forestry* 3:146–148.
- Rich, P. M. 1990. Characterizing plant canopies with hemispherical photographs. *Remote Sensing Reviews* 5:13–29.
- Rich, P. M., R. Dubayah, W. A. Hetrick, and S. C. Saving. 1994. Using viewshed models to calculate intercepted solar radiation: applications in ecology. *American Society for Photogrammetry and Remote Sensing Technical Papers* pp.524–529.
- Rönholm, P., J. Hyypä, H. Hyypä, H. Haggren, X. Yu, and H. Kaartinen. 2004. Calibration of laser-derived tree height estimates by means of photogrammetric techniques. *Scandinavian Journal of Forest Research* 19:524–528.
- Runkle, J. 1981. Gap regeneration in some old-growth forests of the eastern United States. *Ecology* 62:1041–1051.
- Runkle, J. R., and T. C. Yetter. 1987. Treefalls revisited: Gap Dynamics in the Southern Appalachians. *Ecology* 68:417–424.
- Rüger, N., A. Huth, S. P. Hubbell, and R. S. Condit. 2011a. Determinants of mortality across a tropical lowland rainforest community. *Oikos* 120:1047–1056.
- Rüger, N., U. Berger, S. P. Hubbell, G. Vieilledent, and R. Condit. 2011b. Growth Strategies of Tropical Tree Species: Disentangling Light and Size Effects. *PLoS ONE* 6:e25330.
- Saatchi, S. S., R. Houghton, R. Dos Santos Alvala, J. V. Soares, and Y. Yu. 2007. Distribution of aboveground live biomass in the Amazon basin. *Global Change Biology* 13:816–837.
- Saatchi, S. S., undefined author, S. Brown, M. Lefsky, E. T. A. Mitchard, W. A. Salas, B. R. Zutta, W. Buermann, S. L. Lewis, undefined author, undefined author, L.

- White, M. Silman, and undefined author. 2011. Benchmark map of forest carbon stocks in tropical regions across three continents. *Proceedings of the National Academy of Sciences* 108:9899–9904.
- Schreuder, H. T., S. G. Banyard, and G. E. Brink. 1987. Comparison of three sampling methods in estimating stand parameters for a tropical forest. *Forest Ecology and Management* 21:119–127.
- Schulze, M. D., and J. Zweede. 2006. Canopy dynamics in unlogged and logged forest stands in the eastern Amazon. *Forest Ecology and Management* 236:56–64.
- Senna, M.A.C, M.H. Costa and Y.E. Shimabukuro. 2005. Fraction of photosynthetically active radiation absorbed by Amazon tropical forest: A comparison of field measurements, modeling and remote sensing. *Journal of Geophysical Research - Biogeosciences* 110: G01008.
- Silver, W. L., J. Neff, M. Mcgroddy, E. Veldkamp, M. Keller, and R. Cosme. 2000. Effects of Soil Texture on Belowground Carbon and Nutrient Storage in a Lowland Amazonian Forest Ecosystem. *Ecosystems* 3:193–209.
- Spies, T. 1998. Forest structure: a key to the ecosystem. *Northwest science* 72:34–36.
- Stancioiu, P. T., and K. L. O’Hara. 2005. Regeneration growth in different light environments of mixed species, multiaged, mountainous forests of Romania. *European Journal of Forest Research* 125:151–162.
- St-Onge, B., and U. Vepakomma. 2004. Assessing forest gap dynamics and growth using multi-temporal laser-scanner data. *Power* 140:200uJ.
- Stark, S. C., V. Leitold, J. L. Wu, M. O. Hunter, C. V. de Castilho, F. R. C. Costa, S. M. McMahon, G. G. Parker, M. T. Shimabukuro, M. A. Lefsky, M. Keller, L. F. Alves, J. Schiatti, Y. E. Shimabukuro, D. O. Brandão, T. K. Woodcock, N. Higuchi, P. B. de Camargo, R. C. de Oliveira, and S. R. Saleska. 2012. Amazon forest carbon dynamics predicted by profiles of canopy leaf area and light environment. *Ecology Letters* 15:1406–1414.
- Steege, Ter, H., N. C. A. Pitman, O. L. Phillips, J. Chave, D. Sabatier, A. Duque, J.-F. Molino, M.-F. Prévost, R. Spichiger, H. Castellanos, P. Von Hildebrand, and R. Vasquez. 2006. Continental-scale patterns of canopy tree composition and function across Amazonia. *Nature* 443:444–447.

- Tabarelli, M., and W. Mantovani. 2000. Gap-phase regeneration in a tropical montane forest: the effects of gap structure and bamboo species. *Plant Ecology* 148:149–155.
- Thomas, R. Q., G. C. Hurtt, R. Dubayah, and M. H. Schilz. 2008. Using lidar data and a height-structured ecosystem model to estimate forest carbon stocks and fluxes over mountainous terrain. *Canadian Journal of Remote Sensing* 34:S351–S363.
- van der Meer, P. J., F. Bongers, L. Chatrou, and B. Riéra. 1994. Defining canopy gaps in a tropical rain forest: effects on gap size and turnover time. *Acta oecologica* 15:701–714.
- Vepakomma, U., B. St-Onge, and D. Kneeshaw. 2011. Response of a boreal forest to canopy opening: assessing vertical and lateral tree growth with multi-temporal lidar data. *Ecological Applications* 21:99–121.
- Vieira, S. A., L. F. Alves, M. Aidar, L. S. Araujo, T. R. Baker, J. L. F. Batista, M. C. Campos, P. B. de Camargo, J. Chave, and W. B. C. Delitti. 2008. Estimation of biomass and carbon stocks: the case of the Atlantic Forest. *Biota Neotropica* 8:21-29.
- Vieira, S., P. B. de Camargo, D. Selhorst, R. Silva, L. R. Hutyrá, J. Q. Chambers, I. Brown, N. Higuchi, J. Santos, S. C. Wofsy, S. Trumbore, and L. A. Martinelli. 2004. Forest structure and carbon dynamics in Amazonian tropical rain forests. *Oecologia* 140:1–12.
- Vierling, K. T., L. A. Vierling, W. A. Gould, S. Martinuzzi, and R. M. Clawges. 2008. Lidar: shedding new light on habitat characterization and modeling. *Frontiers in Ecology and the Environment* 6:90–98.
- Wang, C., and N. F. Glenn. 2008. A linear regression method for tree canopy height estimation using airborne lidar data. *Canadian Journal of Remote Sensing* 34:S217–S227.
- Wang, C., J. Qi, and M. A. Cochrane. 2005. Assessment of tropical forest degradation with canopy fractional cover from Landsat ETM+ and IKONOS imagery. *Earth Interactions* 9:1–18.
- Watson, R. T. 2000. *Land Use, Land-Use Change, and Forestry*. (R. T. Watson, I. R. Noble, B. Bolin, N. H. Ravindranath, D. J. Verardo, and D. J. Dokken, Eds.). Cambridge Univ Press, Cambridge.

- Weishampel, J., J. Blair, R. Knox, R. Dubayah, and D. B. Clark. 2000. Volumetric lidar return patterns from an old-growth tropical rainforest canopy. *International Journal of Remote Sensing* 21:409–415.
- Welden, C. W., S. W. Hewett, S. P. Hubbell, and R. B. Foster. 1991. Sapling Survival, Growth, and Recruitment: Relationship to Canopy Height in a Neotropical Forest. *Ecology* 72:35–50.
- Welles, J. M., and J. M. Norman. 1991. Instrument for indirect measurement of canopy architecture. *Agronomy journal* 83:818–825.
- Whitmore, T. C., and N. D. Brown. 1996. Dipterocarp Seedling Growth in Rain Forest Canopy Gaps during Six and a Half Years. *Philos T R Soc Lond B* 351:1195–1203.
- Whitmore, T. C., N. D. Brown, M. D. Swaine, D. Kennedy, C. I. Goodwin-Bailey, and W. K. Gong. 1993. Use of Hemispherical Photographs in Forest Ecology: Measurement of Gap Size and Radiation Totals in a Bornean Tropical Rain Forest. *Journal of Tropical Ecology* 9:131–151.
- Williams, M. S., and H. T. Schreuder. 2000. Guidelines for choosing volume equations in the presence of measurement error in height. *Canadian Journal of Forest Research* 30:306–310.
- Williams, M. S., W. A. Bechtold, and V. J. LaBau. 1994. Five instruments for measuring tree height: An evaluation. *Southern Journal of Applied Forestry* 18:76–82.
- Wirth, R., B. Weber, and R. J. Ryel. 2001. Spatial and temporal variability of canopy structure in a tropical moist forest. *Acta oecologica* 22:235-244.
- Young, T., and S. P. Hubbell. 1991. Crown asymmetry, treefalls, and repeat disturbance of broad-leaved forest gaps. *Ecology* 72:1464–1471.
- Zhang, K., S. Chen, D. Whitman, M. Shyu, J. Yan, and C. Zhang. 2003. A progressive morphological filter for removing nonground measurements from airborne LIDAR data. *IEEE Transactions on Geoscience and Remote Sensing* 41:872–882.
- Zimble, D. A., D. L. Evans, G. C. Carlson, R. C. Parker, S. C. Grado, and P. D. Gerard. 2003. Characterizing vertical forest structure using small-footprint airborne LiDAR. *Remote Sensing of Environment* 87:171–182.